Anatomical and functional mapping of striatal circuits controlling licking

Sevinç Mutlu

Dissertation presented to obtain the Ph.D degree in Biology/Neuroscience

Instituto de Tecnologia Química e Biológica António Xavier | Universidade Nova de Lisboa

Research work coordinated by:

FCT Fundação para a Ciência e a Tecnologia
MINISTÉRIO DA CIÊNCIA, TECNOLOGIA E ENSINO SUPERIOR

FUNDAÇÃO CALOUSTE GULBENKIAN
Instituto Gulbenkian de Ciência

neuron
Network of European Funding for Neuroscience Research

Champalimaud Foundation

hhmi
Howard Hughes Medical Institute

SEVENTH FRAMEWORK PROGRAMME

Oeiras, December, 2016

UNIVERSIDADE NOVA DE LISBOA

TABLE OF CONTENTS

ACKNOWLEDGEMENTS

In neuroscience, different levels of specific functional questions are generally studied separately. The anatomy of a circuit and its function has been generally studied separately. However, it is important to bring together different levels of knowledge to fully understand a functional question. Thanks to my amazing collaborators, I was able to study a functional question at anatomical, functional and behavioral level.

I would like to thank my supervisor Dr. Rui M. Costa for accepting me into his team, for giving me the opportunity to learn and perform great research, and for his supervision during my PhD. I feel lucky that I had the opportunity to meet him, learn about neuroscience and the scientific process from him and his team.

To my colleagues in the Neurobiology of Action Laboratory, for teaching me amazing hands on neuroscience techniques, for great discussions, and for the friendly environment.

Especially to Dr. Fatuel Tecuapetla, for teaching me the basics of behavioral training and optogenetics, and the basics of basal ganglia research, Dr. Catia Feliciano for teaching me molecular cloning techniques, Dr. Eran Lottem for great discussions and his enthusiasm, Dr. Joaquim Silva for his everyday collaboration and fruitful discussions during my PhD., Dr. Ana Machado, Dr.

Megan Carey, Dr. Eran Lottem and Dr. Zach Mainen for collaborating with us and bringing our research into a more interesting, exciting level together, and to Ivo Marcelo and Dr. Jonathan Tang for their valuable feedback on the thesis.

To our support staff Ricardo Riberio, Carlos Mao de Ferro, Artur Silva, Filipe Carvalho, Ana Cunha, Sergio Casimiro and Susana Dias for their help.
To my thesis committee Luisa Vasconcelos and Joe Paton, and to my thesis examners Eric Burgueire, Ana Joao Rodrigues and Maria Armenia Carrondo for their time evaluating our work and their valuable comments.
Last but not least, I would like to thank to Fabian and my family for their patience and support during my PhD.

SUMMARY

The basal ganglia receive information about sensory-motor state, internal state, the recent history of actions and their outcomes. They integrate information in order to select the optimal action in the right sensory environment, to receive or avoid the predicted outcome based on the recent history. Eventhough models, such as reinforcement learning, reward prediction error, direct and indirect pathway antagonism, linking cognitive-behavioral phenomenon with neural data are widely agreed upon, they are not sufficient to explain a vast amount of experimental data. Therefore the roles of basal ganglia structures in action selection are yet to be understood.

Striatum is considered to be the main basal ganglia structure that receives input from the whole cortex, many thalamic nuclei and midbrain dopaminergic cells and integrates these inputs and projects onto basal ganglia output structures. Therefore, striatum could be the key structure involved in optimal action selection by integrating information from different brain structures, together with dopaminergic input and where the decision for optimal action is made. Therefore understanding the role of striatum in action selection could be the key step in understanding basal ganglia functioning. Different striatal populations were shown to project onto different regions of GPe and SNr. However, the rules of these projections were not described in detail. Therefore, we first mapped projection patterns of striatonigral and striatopallidal pathways onto their output nuclei. We observed that striatonigral projections kept their striatal mediolateral position, but inverted their dorsoventral position onto SNr. Striatopallidal projections directly translated their striatal

position onto GPe. Dorsomedial and dorsolateral striatum were shown to be involved in goal directed and habitual behaviors, respectively. We observed that dorsomedial and dorsolateral striatum project onto different parts of target regions, GPe and SNr, in line with studies suggesting that they could be components of different basal ganglia loops. We also showed that direct pathway ventrolateral striatal cells projects on the "core" region of SNr, while indirect pathway ventrolateral striatal cells projects on ventrolateral GPe. Core region of SNr was suggested to be involved in orofacial motor control. We showed that ventrolateral striatum receives input from orofacial areas of motor cortices, and is involved in the control of orofacial movements in different conditions. We developed a head fixed-olfactory guided operant task and investigated the role of ventrolateral striatum striatonigral and striatopallidal populations in orofacial motor control. We trained mice to respond to different olfactory cues by licking to receive water reward, not licking to avoid punishment, and withholding licking to receive a delayed water reward. Striatonigral ventrolateral striatum stimulations induced licking, and suggested a context-dependent involvement in control of licking. Indirect pathway ventrolateral striatum stimulations stopped licking for all conditions. Population calcium imaging of striatonigral and striatopallidal pathway aVLS cells suggested that both pathways were active during initiation of instrumental licking, and striatopallidal pathway was also active during different stages of instrumental licking. These results support the previous observations that activity of both pathways might be involved in initiation of

instrumental actions, and also suggest that these pathways are involved differently in different aspects of instrumental actions. In summary, in this thesis, we mapped inputs to and outputs from different striatal domains, and uncovered a striatal circuit in ventrolateral striatum that specifically controls licking, which could serve as a novel model to accurately study the role of basal ganglia structures in action selection and performance.

RESUMO

Os gânglios da base recebem a informação sobre o estado sensitivo e motor, o estado interno e a história recente das ações e os seus resultados. São os gânglios da base que integram esta informação por forma a selecionar a ação mais apropriada num dado ambiente sensorial, permitindo ou evitando um determinado resultado com base na história recente de ações. Os mecanismos através dos quais é feita essa seleção de ação complexa são ainda desconhecidos. O estriado é a principal estrutura de entrada de informação dos gânglios da base, onde a entrada de informação cortical, talâmica e dopaminérgica é integrada. Assim, o estriado pode ser visto como a estrutura-chave para a compreensão do mecanismo através do qual os gânglios da base estão envolvidos na seleção de uma ação. Começámos por mapear os padrões de projeção das vias estriado-nigral e estriado-palidal até aos núcleos de saída. Observámos que as projeções estriado-nigrais mantiveram a sua posição medio-lateral relativa, mas inverteram sua posição dorso-ventral no SNr. Além disso, verificámos que as projeções estriado-palidais traduziram diretamente sua posição striatal no GPe.

Observámos ainda que, o estriado dorso-medial e dorso-lateral, que se sabe estarem envolvidos, respectivamente, em comportamentos dirigidos e hábitos, projetavam para diferentes partes das regiões alvo, GPe e SNr, sugerindo que estes constituíam componentes de diferentes ‘loops’ dos gânglios da base.

Mostrámos ainda que as células ventro-laterais da via direta projetam para a região central do SNr, enquanto que as células ventro-laterais indiretas projetam sobre o GPe ventrolateral.

Em seguida revelámos que o estriado ventrolateral anterior recebe entrada de áreas orofaciais dos córtices motores e está envolvido no controlo de movimentos orofaciais em ratinhos e treinados e sem serem treinados. Para investigar o papel dos neurónios estriado-nigrais e estriado-palidais do estriado ventrolateral anterior no controle orofacial desenvolvemos uma tarefa operante de cabeça fixa, dependente do olfacto. Treinámos os ratinhos para lamberem de modo a receberem uma recompensa de água, a pararem de lamber para evitarem uma punição e a deixarem de lamber para receberem uma recompensa de água mais tarde.

Estimulações da via estriado-nigral do estriado ventro-lateral anterior induziram os animais a lamberem, de forma dependente do contexto. As estimulações da via indireta levaram os animais a pararem de lamber durante todas as condições. 'Calcium imaging' da população de células VLS estriado-nigrais e estriado-palidais sugeriu que ambas as vias estavam ativas durante o início da lambidela, e que a via estriatopalidal também estava ativa durante a execução das lambidelas. Esses resultados corroboram as observações de que a atividade de ambas as vias é necessária para a iniciação de ações instrumentais, mas sugerem um papel diferencial para essas vias na execução de ações instrumentais.

Em resumo, nesta tese, mapeámos entradas e saídas de diferentes domínios estriatais e descobrimos um circuito estriatal no estriado ventrolateral anterior que controla especificamente os movimentos orofaciais e lambidelas tanto expontâneas como instrumentais.

ABREVIATION LIST

MSN	Medium spiny neurons
aVLS	Anterior ventrolateral striatum
aDLS	Anterior dorsolateral striatum
aNacc	Anterior Nucleus Accumbens
DMS	Dorsomedial striatum
DLS	Dorsolateral striatum
VLS	Ventrolateral striatum
aDMS	Anterior dorsomedial striatum
mDMS	Mid dorsomedial striatum
pDMS	Posterior dorsomedial striatum
aDLS	Anaterior dorsolateral striatum
mDLS	Mid dorsolateral striatum
pDLS	Posterior dorsolateral striatum
aVLS	Anterior ventrolateral striatum
mVLS	Mid ventrolateral striatum
pVLS	Posterior ventrolateral striatum
GPe	Globus Pallidus external segment
aGPe	Anterior Globus Pallidus external segment
mGPe	Mid Globus Pallidus external segment
pGPe	Posterior Globus Pallidus external segment
GPi	Globus Pallidus internal segment
SNr	Substantia Nigra Reticulata
SNc	Substantia Nigra Compacta
STN	Subthalamic nucleus

PPN	Peduncular pontine nucleus
SC	Superior Colliculus
LTP	Long term potentiation
LTD	Long term depression
PcRT	Parvicellular reticular nucleus
IRT	Intermediate reticular nucleus
Gi	Gigantocellular reticular nucleus

CHAPTER 1| INTRODUCTION

INTRODUCTION

Basal ganglia diseases such as Parkinson's disease, Huntington's disease, Hemibalism, obsessive-compulsive spectrum disorders and many others, disrupt one's ability to transform decision to actions. In Parkinson's, Huntington's and Hemibalism this disruption appears in the form of difficulties in controlling unwanted movements. Patients with obsessive-compulsive spectrum disorders on the other hand, seem to overly perform actions independent of their consequences. Therefore one's ability to evaluate consequences of actions seems to be disrupted. Therefore basal ganglia are thought to be the set of subcortical structures that together are the key involved in the transformation of decisions to actions (Smith et al., 2014).

In everyday life, we either perform actions that are exploratory (spontaneous), or actions that we do in order to receive or avoid their expected outcomes. We repeat some of these actions so many times that their outcomes become predictable and we reduce attention to their execution. However, some actions that we repeat less frequently require more attention, show variability in their execution, and they can be disrupted easily by unexpected sensory events. The basal ganglia are a set of subcortical nuclei that are thought to be composed of the critical circuits involved in action selection, action-outcome associations, and stimulus response associations.

The basal ganglia receive information about sensory-motor state, internal state, recent history of actions and their outcomes. They integrate this information in order to select the next action in the right sensory environment to receive or avoid the predicted outcome, based

on the recent history. The mechanisms via which such complex action selection might be implemented are not clear.

The striatum is the largest basal ganglia nucleus that receives input from most of the cortex, many different thalamic nuclei, amygdala, hippocampus, dorsal raphe and peduncular pontine nucleus (Graybiel, 1998, Silberberg et al., 2015). The main modulator of striatal activity is dopamine (Surmeier et al., 2007, Gerfen et al., 2011). The sources of the striatal dopamine are SNc and VTA dopaminergic cells projecting onto striatum, spanning the whole structure (Gerfen et al., 2011). Around 90% of the cells in striatum are spiny GABAergic projection neurons that express either D1 or D2 dopamine receptors (and rarely both receptors) (Gerfen et al., 1990, Gerfen, 1992, Gerfen et al., 2011). Although cells of these two populations are similar in soma size and spacial distribution in striatum, they express different dopamine receptors and project onto different structures (Gerfen, 1992, Silberberg et al., 2015). D1 dopamine receptor expressing cells project to internal segment of Globus Pallidus (GPi) and Substantia Nigra (SN) and are therefore called striatonigral pathway. D2 dopamine receptor expressing cells, project to GPe and are called striatopallidal pathway (Gerfen et al., 1990, Gerfen, 1992). D1 receptor depolarizes and D2 receptor hyperpolarizes the MSN's in response to dopamine agonist binding (Gerfen et al., 1990). Although both MSN types show LTP and LTD, D1 receptor activation promotes expression of LTP and D2 receptor activation promotes expression of LDT (Shen, et al., 2008).

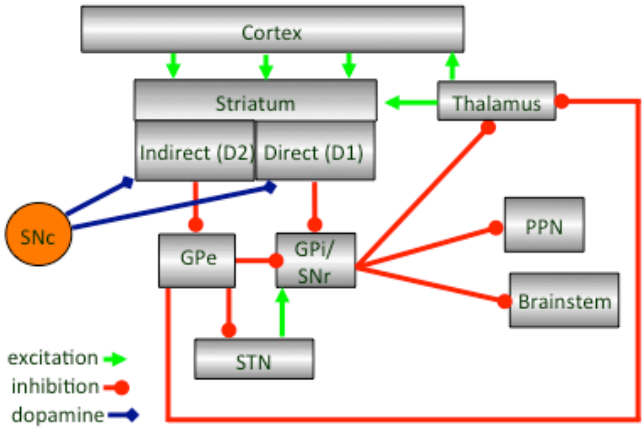

Figure 1.1| Main input and output connections of basal ganglia structures.

Disinhibition within basal ganglia

Disinhibition is thought to be the main mechanism via which basal ganglia allows movement to be executed. SNr activity was shown to decrease during movement (Chevalier et al., 1985, Deniau et al., 1985, Chevalier et al., 1990). Striatonigral cells project onto SNr directly, inhibiting it, while striatopallidal cells disinhibit SNr (Chevalier et al., 1985, Deniau et al., 1985, Chevalier et al., 1990). Striatopallidal cells project onto GPe, which projects onto either SNr or STN, and both of these structures disinhibit SNr in response to striatopallidal pathway activation (Chevalier et al., 1985, Deniau et al., 1985, Chevalier et al., 1990, Gerfen et al., 1990). Striatonigral and striatopallidal pathways are thought to work antagonistically to control movement; the striatonigral pathway facilitates movement and the striatopallidal pathway suppresses it (Albin, et al., 1989, Alexander, et al., 1990, DeLong et al, 1990, Gerfen et al., 1990).

Disinhibition of SNr is thought to increase the inhibition onto premotor regions, increasing the threshold for movement, while decrease of disinhibition on SNr would have the opposite effect and reduce the threshold for movement (Chevalier et al., 1985, Deniau et al., 1985, Albin et al., 1989, Chevalier et al., 1990). While the main effect of striatal stimulation on SNr was suggested to be inhibitory, 20-25 % of SNr cells projecting to SC and thalamus showed excitation (Chevalier et al., 1985, Deniau et al., 1985). Therefore, when animals are immobile, striatum is silent and STN might be keeping SNr under high level of inhibition, and when animals are moving striatal direct and indirect pathways modulate SNr activity to allow movement to be performed (Chevalier et al., 1985, Deniau et al., 1985).

However, the number of circuits involved in disinhibition of SNr to allow movement to be performed are much complex than simple striatonigral pathway mediated inhibition, and striatopallidal mediated disinhibition model. Multiple new functional connections were described between basal ganglia nuclei that contribute to either inhibition or disinhibition of SNr; intrastriatal connectivity mostly from striatopallidal onto striatonigral cells (Tecuapetla et al, 2009), intrastriatal inhibitory neurons inhibiting striatopallidal and striatonigral cells (reviewed in Smith et al., 1998, Kreitzer, 2009), arkypallidal cells projecting from GPe back to striatum inhibiting it (Mallet et al., 2012, Mallet et al., 2016), GABAergic GPe projections directly to cortex (Saunders et al., 2015), and cholinergic Projections to striatum (Dautan et al., 2014). Therefore, intra-basal ganglia circuits seems to be more complex than initially proposed, with

implications for new roles of direct and indirect pathway in movement and action selection.

Still, models of inhibition and disinhibition have been useful to understand the basal ganglia disorders, where imbalance between direct and indirect pathways may play a role (Albin, et al., 1989, Alexander, et al., 1990). In Parkinson's disease loss of dopamine cells, was reported to cause spine loss and increased firing rates in high affinity D2 dopamine receptor expressing population (Day et al., 2006, Mallet et al., 2006). In early and middle stages of Huntington's disease degeneration of striatopallidal population was more prominent than degeneration of striatonigral population (Reiner et al., 1988). It is possible that striatonigral and striatopallidal pathway cells are affected differently by perturbations in disease states.

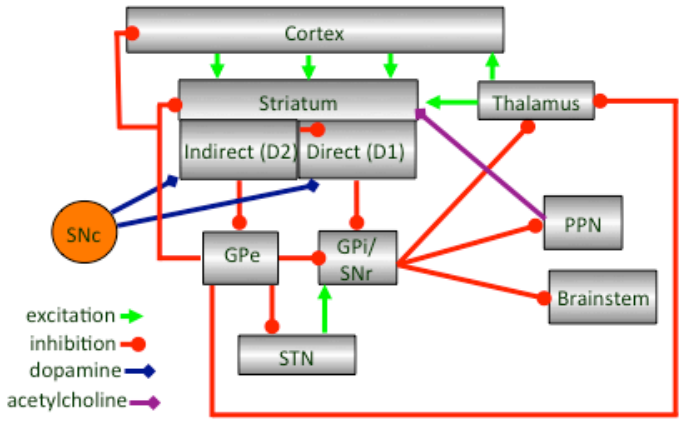

Figure 1.2| Updated scheme of main input and output connections of basal ganglia.

D2 receptor expressing striatopallidal population has higher affinity for dopamine, is more excitable than striatonigral population and could inhibit striatonigral activity via intra-striatal lateral inhibition (Tecuapetla et al, 2009), projects back to striatum (Mallet et al., 2012), frontal cortex (Saunders et al., 2015), and thalamus which projects back to striatum or cortex (Gerfen et al., 1990, Mastro et al. 2014, Gittis et al., 2014). On the other hand striatonigral cells project directly onto SNr to inhibit it and allow movement (Gerfen et al., 1990, Chevalier et al., 1990). Considering the complexity of the circuitry and the divergence of indirect pathway output it is possible that indirect pathways might be involved in multiple different aspects of actions selection showing richer functional heterogeneity compared to direct pathway (Tecuapetla, et al., 2016).

Recent optogenetic manipulations suggested that striatonigral pathway activation promoted locomotion while striatopallidal pathway activation stopped it (Kravitz et al., 2010). However, population calcium imaging and recordings from optogeneticly identified striatonigral and striatopallidal populations suggested that both populations were simultaneously active preceding initiation of an instrumental action (Jin et al., 2010, Cui, et al, 2013, Jin, et al., 2014). Both striatonigral and striatopallidal populations were also simultaneously active preceding initiation of spontaneous locomotion (not associated with a particular outcome) (Tecuapetla et al., 2014). However, the cells of both pathways that showed activity preceding initiation were suggested to be sub-populations and both pathways showed heterogeneous activity during performance of an instrumental action (Jin et al., 2014). Subpopulations from both pathways showed

execution related inhibited, sustained (more striatonigral cells showed sustained activity and more striatopallidal cells showed cells of inhibited activity) or stop related activity (Jin et al., 2014). Following these findings, optogenetic manipulations of both pathway populations before initiation and during execution showed that balanced activity of both pathways were necessary for proper initiation and execution of instrumental actions and striatonigral pathway might be facilitating action initiation and performance and indirect pathway might be inhibiting competing actions (Mink, 1996, Hikosaka et al., 2000, Tecuapetla et al., 2016).

Corticostriatal projection patterns in striatum

Similar to primates, rodent motor cortical projections onto striatum showed somatotopic organization (Nambu et al., 2011, Ebrahimi et al., 1992, Hintiryan et al., 2016). Corticostriatal input in both primates and rodents was shown to make specific patterns. Limbic cortex and amygdala input was constrained into immunohistochemically identifiable patchy regions called “patches” (Goldman-Rakic, 1982, Gerfen et al., 1987). MSNs into patches projected to dopamine cells (Goldman-Rakic, 1982, Gerfen et al., 1987). Sensory-motor cortex input was occupying the regions around the patches, called “matrix”, and MSNs in the matrix region projected to SNr (Goldman-Rakic, 1982, Gerfen et al., 1987). In primates sensory-motor cortical input to striatum, representing the same body part, diverges into partially connected “set of zones” called matrisomes which then project onto a small group of spatially constrained neurons on GPe (Graybiel et al., 1994, Flaherty et al., 1991). Matrisomes, subregions of matrix that receive similar sensory-motor input, might be multiple regions of

integration of information related to the specific body part (Graybiel et al., 1994, Flaherty et al., 1991). In rodents, divergence and convergence of cortical input onto striatum have been addressed (Mailly et al., 2013, Hintiryan et al., 2016, Heilbronner et al., 2016). Even though, projections from mouse cortex onto striatum has been described in detail and showed somatotopic organization, and different levels of convergence and divergence, it has not been shown matrisome-like patterns and if "divergence-reconvergence" of specific sensory-motor input exist rodents (Graybiel et al., 1994, Flaherty et al., 1991, Hintiryan et al., 2016, Heilbronner et al., 2016). Therefore, in rodents, less is known about how striatum processes cortical information to allow action selection.

In chapter 3, we labeled primary and secondary orofacial motor cortex and showed that their input was restricted to ventrolateral striatum. Primary and sensory motor cortex projected onto the same striatal region with primary orofacial motor cortex projecting more laterally and secondary orofacial motor cortex projecting more medially. Forelimb region of secondary motor cortex projected dorsal to secondary orofacial motor cortex input. All these projection patterns were similar to observations reported for primate putamen (Nambu, 2011).

Striatal activity during spontaneous sensory-motor events (that are not associated with particular outcomes)

In striatum, neurons were shown to respond to sensory stimuli of both single modality and of multimodal nature (Brown et al., 1996, Nagy et al., 2005, Nagy et al., 2006, Schultz et al., 2009). Visual, auditory and somatosensory receptive fields appear to be extremely large and

they did not show somatotopic organization in striatum (Brown et al., 1996, Nagy et al., 2005, Nagy et al., 2006, Schultz et al., 2009). The sites of sensory integration in striatum of rodents have not been studied as much as the motor outputs of the striatal populations (Reig, et al., 2014). However, it appears that somoatotopic organization model might not explain the integration of sensory information in striatum. Even though sensory feedback is required for proper execution of movement, somatotopic organization model seems to partially explain the motor output of striatum, but sensory integration in striatum might be happening via different mechanisms (Reig, et al., 2014).

Electrophysiological recordings from primate putamen showed increase in activity related to movement of tongue, arm and leg (DeLong, 1972). In mouse striatum, both striatonigral and striatopallidal pathway cells showed increase in activity preceding angular velocity of contralateral turns (Tecuapetla et al., 2014). Strong turn related activity in dorsolateral striatum was also observed during early stages of training in a T-maze task (Jog et al., 1999). Single unit recordings in dorsolateral striatum of mice showed correlations with movement of specific body parts such that more cells in dorsal part of dorsolateral striatum fired during forelimb, hind limb, trunk and whisker movements and more cells in ventrolateral striatum fired during orofacial movements such as, licking, tongue reaching and jaw movements (Carelli, et al., 1991, Mittler, et al., 1994). This somatotopy observed in mouse striatum was also observed in primate putamen (Nambu, 2011).

In adult mice, “natural actions” such as grooming, locomotion and consummatory-orofacial movements are some of the movements that require little experience for their accurate execution (Colonnese et al., 1996, Aldridge, et al., 1998, Jin et a., 2010). During postnatal development, or even during embryonic development, these action sequences are performed frequently and crystalized into “neutral actions” with specific “action syntaxes” that show little variability in their performances (Lashley, 1951, Colonnese et al., 1996, Aldridge, et al., 1998). In rats, even though some phases of the grooming syntactic chain are observed as early as E20-E21, the stereotyped “grooming action syntax” is only observed on the second-third postnatal week (Colonnese et al., 1996, Berridge et al., 1992). This grooming action syntax development coincided with the developmental window for striatal maturation, and striatal (DLS) lesions caused chronic deficits in the grooming action syntax (Fentress, 1992, Berridge et al., 1992). These observations suggest that striatum might be necessary to create “action syntax”, i.e. the serial order of action (Lashley, 1951, Berridge et al., 1992). The same group also showed that SNr cells responded with higher rates to the same grooming phases depending on if they were performed within the grooming synthetic chain or independent of the chain (Meyer-Luehmann, et al., 2002).

In rats, adult pattern of locomotion was also observed at the end of second postnatal week (Vinay et al., 2002). Even though locomotion is a much simpler action sequence compared to grooming, activity of basal ganglia structures preceded both actions sequences (Meyer-Luehmann, et al., 2002, Tecuapetla et al., 2014). SNr cells started

increasing their firing rate before grooming syntax chain initiation and they slowly decay during chain (Meyer-Luehmann, et al., 2002). Striatal cells of both pathways also increased their activity before initiation of contralateral turning and decayed fastly (Cui et al., 2013, Tecuapetla et al., 2014). Therefore, it is possible that these "neutral action-sequences" are encoded differently in basal ganglia compared to novel action sequences (Jin, et al., 2010).

However, it is also possible that movement related responses at different stages of instrumental conditioning are encoded differently in different parts of the striatum. It was previously suggested that, in humans, in early stages of instrumental conditioning anterior striatum showed correlations with movement and in late stages posterior striatum showed movement related activity (Jueptner, et al., 1997, Graybiel, 1998). Similar shift of activity during acquisition and consolidation of an instrumental action were observed between dorsomedial (associative) and dorsolateral (sensory-motor) striatum (Miyachi, et al., 1997, Miyachi, et al., 2002, Yin et al., 2009, Jin et al., 2010).

Single unit recordings from striatum showed that striatal cells increased firing during different spontaneous behaviors (motor events) with some units start increasing firing before the event, and some decay slower and some faster (Carelli, et al., 1991, Mittler, et al., 1994, Venkatraman, et al., 2010). In addition to limb movement related increase in firing rate in striatum, increase in mean firing rate during spontaneous active state (locomotion) compared to quiescent phase, in all basal ganglia structures (striatum, GPe, SNr and STN)

was observed in rats during spontaneous movements (Shi, et al., 2004)

The studies discussed above suggest that increases in striatal activity of both pathways before spontaneous and instrumental actions might be necessary for their initiation. Tecuapetla et al., 2016 also suggested that balanced activity of both pathways is necessary for their proper initiation and execution. However, the role of striatonigral and striatopallidal populations in initiation and execution of instrumental actions is still not clear.

Most of these studies were performed in DLS. However, one of the challenges in interpretation of DLS activity comes from its heterogeneous input from motor cortex, therefore heterogeneous motor functions. DLS activity has been implicated in the control of locomotion and different limb movements (Carelli, et al., 1991, Mittler, et al., 1994, Venkatraman, et al., 2010, Hintiryan et al., 2016).

The ventrolateral striatum has been suggested to be involved in orofacial motor control and receive input mostly from orofacial motor cortex (von Krosigk, et. al., 1992, Mittler, et al., 1994, Hintiryan et al., 2016). Therefore it suggests a less heterogeneous motor function compared to DLS, and a novel model for understanding the role of striatonigral and striatopallidal pathways in initiation and execution of instrumental actions, action selection.

Specific movements such as saccades, mastication, vocalization, swallowing, and locomotion are thought to be generated by specific neural networks in brainstem and spinal cord, called central rhythm

generators (CPG) (Hikosaka et al., 1983, Scott et al., 2003, Dusterhoft et al., 2000, Grillner et al., 2003, Amirali et al., 2001). It was previously suggested that basal ganglia might be involved in action selection via two (path)ways; modulating thalamocortcial networks therefore modulating its own functioning, and modulating brainstem motor networks therefore modulating motor output directly (Hikosaka et al., 2000).

Coordinated orofacial movements were suggested to be controlled via specific brainstem circuits (CPG's) such as PcRT, IRt, Gi (Travers, et al., 1997, von Krosigk, et. al., 1992, Stanek, et al., 2014). Therefore, studying the role of ventrolateral striatum in orofacial motor control could also help us understand the circuit mechanisms via which basal ganglia acts on specific CPG controlled actions to allow proper action selection and motor control.

REFERENCES

Albin, R. L., Young, A. B. & Penney, J. B. (1989) The functional anatomy of basal ganglia disorders. Trends Neurosci. **12**, 366–375

Aldridge, J.W., Berridge, K.C.(1998) Coding of serial order by neostriatal neurons: A "Neutral action" approach to movement sequence. J. Neurosci. 18(7):2777-2787

Alexander, G.E., Crutcher, M.D. (1990) Functional architecture of basal ganglia circuits: neural substrates of parallel processing. Trends Neurosci. 13: 266-271

Amirali, A., Tsai, G., Schrader, N., Weisz, D., Sanders, I. (2001) Mapping of brainstem neuronal circuitry active during swallowing. Ann. Otol. Rhinol. Laryngol. 110:502-513

Bergman, H., Graybiel, A.M., Kimura, M., Plenz, D., Seung, H.S., Surmier, D.J., Wickens, J.R. (2004) Microcircuits: The interface between neurons and global brain function, Report of the 93rd Dahlem Workshop, Berlin, April 25-30 2004: 165-190

Berridge, K.C., Whishaw, I.Q. (1992) Cortex, striatum and cerebellum: Control of a serial order in a grooming sequence. Exp Brain Res 90: 275-290

Bolam, J.P., Smith, Y. (1992) The striatum and the globus pallidus send convergent synaptic inputs onto single cells in the entopeduncular nucleus of the rat: a double anterograde labeling study combined with postembedding immunocytochemistry for GABA. J. Comp. Neurol. 321: 456-476

Brown, E.E., Hand, P.J., Divac, I. (1996) Representation of a single vibrissa in the rat neostriatum: peaks of energy metabolism reveal a distributed functional module. Neuroscience 75: 717-728

Carelli, R., M., West, M., O. (1991) Representation of the body by single neurons in the dorsolateral striatum of the awake, unrestrained rat. J. Comp. Neurology 309:231-249

Chevalier, G., Vacher, S., Deniau, J.M., Desban, M. (1985) Disinhibition as a basic process in the expression of striatal functions. I. The striato-nigral influence on tecto-spinal/tecto-diencephalic neurons. Brain Res. 334(2):215-26

Chevalier, G., Deniau, J., M. (1990) Disinhibition as a basic process in the expression of striatal functions. TINS, 13(7): 277-280

Colonnese, M., Stallman, E. L., Berridge, K. C. (1996) Ontogeny of action syntax in altricial and precocial rodents: Grooming sequences of rat and guinea pig pups. Behavior, 133:1165-1196

Cui, G., Jun, S. B., Jin, X., Pham, M.D., Vogel, S.S., Lovinger, D.M., Costa, R.M. (2013) Concurrent activation of striatal direct and indirect pathways during action initiation. Nature 494(7436): 238-42.

Day, M., Wang, Z., Ding, J., An, X., Ingham, C., A., … Arbuthnott, G., W., & Surmeier, D., J. (2006) Selective elimination of glutamatergic synapses on striatopallidal neurons in Parkinson's disease models. Nat. Neurosci. 9:251-259

Dautan, D., Huerta-Ocampo, I., Witten, I.B., Deisseroth, K., Bolam, J.P., Gerdjikov, T., Mena-Segovia, J. (2014) A major external source of cholinergic innervation of the striatum and nucleus accumbens originates in the brainstem. J.Neurosci. 34(13): 4509-18

DeLong, M.R. (1978) Activity of basal ganglia neurons during movement. Brain Research 40: 127-135

Deniau, J., M., Chevalier, G. (1985) Disinhibition as a basic process in the expression of striatal functions. . II. The striato-nigral influence on thalamocortical cells of the ventromedial thalamic nucleus. Brain Res. 334(2):227-33

Dusterhoft, F., Hausler, U., Jurgens, U. (2000) On the speech for the vocal pattern generator. A single unit recording study. Neuroreport 11:231-234

Ebrahimi, A., Pochet, R., Roger, M. (1992) Topographical organization of the projections from physiologically identified areas of the motor cortex to the striatum in the rat. Neuroscience Research 14: 39-60

Fentress, J.C. (1992) Emergence of pattern in the development of mammalian movement sequences. J. Neurobiol. 23(10): 1529-56

Flaherty, A.W., and Graybiel, A.M. (1991). Corticostriatal transformations in the primate somatosensory system. Projections from physiologically mapped body-part representations. J. Neurophysiol. 66, 1249–1263.

Gerfen , C.R. (1985) Neostriatal mosaic: I. Compartmental organization of projections from the striatum to the substantia nigra in the rat. J. Comp. Neurol. 236(4): 454-76

Gerfen , C.R., Herkenham, M., Thibault, J. (1987) Neostriatal mosaic: II. Patch- and matrix-directed mesostriatal dopaminergic and non-dopaminergic systems. J. Neurosci. 7(12): 3915-3934

Gerfen, C., R., Engber, T., M., Mahan, L., C., Susel, Z., Chase, T., N., Monsma, F., J., Sibley, D., R. (1990) D1 and D2 dopamine receptor regulated gene expression of striatonigral and striatopallidal neurons. Science 250 (4986):1429-1432

Gerfen, C. R. (1992) Neostriatal mosaic: multiple levels of compartmental organization. TINS 15(4): 133-139

Gerfen, C. R., Surmier, D. J., (2011), Modulation of striatal projection system by dopamine. Annu Rev Neurosci (34): 441-466

Gittis, A.,H. , Berke, J.D., Bevan, M.D., Chan, C.S., Mallet, N., Morrow, M.M., Schmidt, R. (2014) New roles of the external globus pallidus in basal ganglia circuit and behavior. J. Neurosci. 34 (46): 15178-15183

Goldman-Rakic, P.S. (1982) Cytoarchitectonic heterogeneity of the primate neostriatum: Subdivisions into island and matrix cellular components. J. Comp. Neurol. 205: 398-413

Graybiel, A.M., Aosaki, T., Flaherty, A. W., Kimura, M. (1994) Basal ganglia and adaptive motor control. Science, 265:1826-1831

Graybiel, A. M. (1998) The basal ganglia and chunking of action repertoires. Neurobiol. Learn. Mem. 70(1/2): 119-136

Grillner, S. (2003) The motor infrastructure: from ion channels to neural networks. Nat. Rev. Neurosci. 4: 573-586

Helibronner, S.R., Rodrigues-Romaguera, J., Quirk, G.J., Groenewegen, H.J., Heber, S.N. (2016) circuit based corticostriatal homologies between rat and primate. Biol. Psychiatry 80(7): 509-521

Hikosaka, O., Wurtz, R.H. (1983) Visual and occulomotor functions of monkey substantia nigra pars reticulate. Vol.II. Visual response related to fixation of gaze. J. Neurophysiol. 49: 1254-1267

Hikosaka, O., Takikawa, Y., Kawagoe, R. (2000) The role of basal ganglia in the control of purposive saccadic eye movements. Physiol. Rev. 80:953-978

Hintiryan, H., Foster, N.F., Bowman, I., Bay, M., Song, M.Y., Guo, L., Yamashita, S., Bienkowski, M. S., Zingg, B., Zhu, M., Yang, X.W., Shih, J.C., Toga, A.W., Dong, H.W. (2016) The mouse cortico-striatal projectome. Nat. Neurosci. 19(8): 1100-14

Jueptner, M., Stephan, K.M., Frith, C.D., Brooks, D.J., Frackowiak, R.S.J., Passingham, R.E. (1997a) Anatomy of motor learning. 1.Frontal cortex and attention to action. J. Neurophys. 77(3): 1313-24

Jin, X., Costa, R.M. (2010) Start/stop signal emerge in nigrostriatal circuit during sequence learning. Nature 466(7305): 457-462

Jin, X., Tecuapetla, F., Costa, R.M. (2014) Basal ganglia subcircuits distinctively encode the parsing and concatenation of action sequences. Nat. Neurosci. 17(3): 423-30

Jog, M.S., Kubota, Y., Connolly, C.I., Hillegaart, V., Graybiel, A.M. (1999) Building neural representations of habits. Science 286(5445): 1745-9

Kravitz, A.V., Freeze, B.S., Parker, P.R., Kay, K., Thwin, M.T., Deisseroth, K., Kreitzer, A.C. (2010) Regulation of parkinsonian motor behaviors by optogenetic control of basal ganglia circuitry. Nature 466(7306): 622-6

Kreitzer, A. (2009) Physiology and pharmacology of striatal neurons. Annu.Rev. Neurosci. 2009. 32:127-47

Lashley, K.S. (1951) The problem of serial order in behavior. In Jeffress, L.A. (ed.), Cerebral Mechanisms in Behavior. Wiley, New York, pp. 112-146

Mailly, P., Aliane, V., Groenewegen, H.J., Heber, S.N., Deniau, J.M. (2013) The rat prefrontostriatal system analyzed in 3D: Evidence for multiple interacting functional units. J. Neurosci. 33(13):5718-27

Mallet, N., Ballion, B., Le Moine, C., Gonon, F. (2006) Cortical input and GABA interneurons imbalance projection neurons in the striatum of Parkinsonian rats. Journal of Neurosicence 26(14): 3875-3884

Mallet, N., Micklem, B. R., Henny, P., Brown M.T., Williams, C., Bolam, J.P., Nakamura, K.J., Magill, P.J. (2012) Dichotomous organization of the external globus pallidus. Neuron 74(6): 1075-86

Mallet, N., Schmidt, R., Leventhal, D., Chen, F., Amer, N., Boraud, T., Berke, J.D. (2016) Arkypallidal cells send a stop signal to striatum. Neuron 89(2): 308-16

Meyer-Luehmann, M., Thonbson, J., Berridge, K.C., Aldridge, J.W. (2002) Substantia nigra pars reticulata neurons code initiation of a serial pattern: implications for natural action sequences and sequential disorders. Eur. Journ. Neurosci. 16: 1599-1608

Miyachi, S., Hikosaka, O., Miyashita, K., Karadi, Z., Rand, M.K. (1997) Differential roles of monkey striatum in learning of sequential hand movements. Exp. Brain Res. 115: 1-5

Miyachi, S., Hikosaka, O., Lu, X. (2002) Differential activation of monkey striatal neurons in the early and late stages of procedural learning. Exp. Brain Res. 146: 122-126

Mink, J.W. (1996) The basal ganglia: Focused selection and inhibition of competing motor programs. Prog. Neurobiol. 50: 381:425DeLong, M.R. (1990) Primate models of movement disorders of basal ganglia origin. Trends Neurosci. 13:281-285

Mittler, T., Cho, J., Peoples, L., L., West, M., O. (1994) Representation of the body in the lateral striatum of freely moving rats: single neurons related to licking. Exp Brain Res 98: 163-167

Nambu, A. (2011) Somatotopic organization of primate basal ganglia. Front Neuroanat. 5:26

Nagy, A., Paroczy, Z., Norita, M., Benedek, G. (2005). Multisensory responses and receptive field properties of neurons in the substantia nigra and in the caudate nucleus. Eur. J. Neurosci. *22*, 419–424.

Nagy, A., Eordegh, G., Paroczy, Z., Markus, Z., Benedek, G. (2006). Multisensory integration in the basal ganglia. Eur. J. Neurosci. 24, 917–924.

Reig, R., Silberberg, G. (2014) Multisensory integration in mouse striatum. Neuron 83: 1200-1212

Reiner, A., Albin, R.,L., Anderson, K.,D., D'Amato, C., D., Penney J., B., & Young, A., B. (1988) Differential loss of striatal projection neurons in Huntington disease. Proc Natl Acad Sci USA 85(15): 5733-5737

Saunders, A., Oldenburg, I.A., Berezovski, V.K., Johnson, C.A., Kingery, N.D., Elliot, H.L., Xie, T., Gerfen, C.R., Sabatini, B.L. (2015) A direct GABAergic input from the basal ganglia to frontal cortex. Nature 521, 85-89

Schultz, J.M., Redgrave, P., Mehring, C., Aertsen, A., Clements, K.M., Wickens, J.R., Reynolds, J.N. (2009) Short latency activation of striatal spiny neurons via subcortical visual pathways. J. Neurosci. 29: 633-6347

Scott, G., Westberg, K.G., Vrentzos, N., Kolta, A., Lund, J.P. (2003) Effects of lidocaine and NMDA injections into the medial pontobulbar reticular formation on mastication evoked by cortical stimulation in anesthetized rabbits. Eur. J. Neurosci. 17:2156-2162

Shen, W., Flajolet, M., Greengard, P., Surmeier, D.J., (2008) Dichotomous dopaminergic control of striatal synaptic plasticity. Science 321:848-851

Shi, L.H., Luo, F., Woodward, D.J., Chang, J.Y. (2004) Neural responses in multiple basal ganglia regions during spontaneous and treadmill locomotion task in rat. Exp. Brain. Res. 157: 303-314

Silberberg, G., Bolam, J. P. (2015) Local afferent synaptic pathways in the striatal microcircuitry. Curr. Op. Neur. 33: 182-187

Smith, Y., Bolam, J.P., (1989) Neurons of the substantia nigra reticulata receives a dense GABA containing input from the globus pallidus in the rat. Brain Research, 493:160-167

Smith, Y., Bevan, M.D., Shink, E., Bolam, J.P. (1998) Microcircuitry of the direct and indirect pathways of the basal ganglia. Neuroscience 86(2): 353-387

Stanek, E., Cheng, S., Takatoh, J., Han, B. X., Wang, F. (2014) Monosynaptic premotor circuit tracing reveals neural substates for oro-motor coordination. Elife 2014; 3:e02511

Surmeier, D.J., Ding, J., Day, M., Wang, Z., Shen, W. (2007) D1 and D2 dopamine receptor modulation of striatal glutamatergic signaling in striatal medium spiny neurons. TINS 30(5): 228-235

Tecuapetla, F., Koos, T., Tepper, J.M., Kabbani, N., Yeckel, M.F. (2009) Differential dopaminergic modulation of neostriatal synaptic connections of striatopallidal axon collaterals. J.Neurosci. 29: 8977-8990

Tecuapetla, F., Matias, S., Dugue, G. P., Mainen, Z.F., Costa, R.M. (2014) Balanced activity in basal ganglia projection pathways is critical for contraversive movements. Nat. Commun. Jul 8; 5:4315.

Tecuapetla, F., Jin, X., Lima, S.Q., Costa, R.M. (2016) Complementary contributions of striatal projection pathways to action initiation and execution. Cell 166(3): 703-15

Travers, J.B., Dinardo, L.A., Karimnamazi, H. (1997) Motor and premotor mechanisms of licking. Neurosci. Biobehav. Rev. 21(5): 631-47

Venkatraman, S., Jin, X., Costa, R.M., Carmena, J.M. (2010) Investigating neural correlates of freely behaving rodents using inertial sensors. J. Neurophys. 104(1): 569-575.

Vinay, L., Brocard, F., Clarac, F., Norreel, J.C., Pearlstein, E., Pflieger, J.F. (2002) Development of posture and locomotion: An interplay of endogenously generated activities and neurotropic actions by descending pathways. Brain Res Brain Res Rev 40 (1-3): 118-129

von Krosigk, M., Smith, Y., Bolam, J. P.& Smith, A. D. (1992) Synaptic organization of gabaergic inputs from the striatum and the globus pallidus onto neurons in the substantia nigra and retrorubral field which project to the medullary reticular formation. Neuroscience 50(3): 531-549

Yin, H.H., Knowlton, B.J. (2004) Contributions of striatal subregions to place and response learning. Learn. Mem. 11(4): 459-462

Yin, H.H., Mulcare, S.P., Hilaro, M.R., Clouse, E., Holloway, T., Davis, M.I., Hansson, A.C., Lovinger, D.M., Costa, D.M. (2009) Dynamic reorganization of striatal circuits during the acquisition and consolidation of a skill. Nat. Neurosci. 12(3): 333-41

CHAPTER 2| DIFFERENT STRIATAL DOMAINS PROJECT ONTO SPECIFIC AREAS OF THE DOWNSTREAM TARGETS

DIFFERENT STRIATAL DOMAINS PROJECT ONTO SPECIFIC AREAS OF THE DOWNSTREAM TARGETS

SUMMARY

Striatonigral and striatopallidal pathway cells comprise >90% of striatal cells. They express different dopamine receptors and project onto different target structures. Striatonigral pathway cells project onto SNr while striatopallidal pathway cells project onto GPe. It has been shown that different striatal populations project onto different parts of SNr and GPe. However, a systematic study showing the projection patterns of these populations throughout the structures, and comparing projections of different, simultaneously labeled populations was missing.

We used transgenic lines to label striatonigral and striatopallidal pathway cells specifically. We simultaneously labeled two domains of each pathway populations using two different fluorescent proteins, EYFP and tdTomato. We mapped projection patterns of 9 different striatonigral and striatopallidal populations onto SNr and GPe.

We showed that DMS, DLS, VLS populations project onto different regions of SNr and GPe, creating parallel pathways. The intra-striatal position of striatopallidal pathway cells was directly translated onto GPe by their projections, on both dorsoventral and mediolateral axis. However, striatonigral pathway projections made complex patterns in SNr. They inverted their intra-striatal cell body position on dorsoventral axis, and translated it directly on the mediolateral axis. Striatonigral pathway projections seemed to wrap around SNr making complex patterns that require 3D reconstruction for their interpretation.

INTRODUCTION

Striatonigral and striatopallidal MSNs are homogeneously intermingled in the mouse striatum, except perhaps for the most posterior part of the striatum, analogous to caudate tail in primates, which appears to be populated mostly by striatonigral cells and to contain fewer striatopallidal cells (Gangarossa et al., 2013).

The distributions of corticostriatal projections from different cortical regions permitted the division of the dorsal striatum into three domains that receive functionally distinct inputs; the dorsomedial (DMS), dorsolateral (DLS) and ventrolateral striatum (VLS) (Ebrahimi et al., 1992). This classification has also been used to define developmental patterns of striatal circuits (Bayer et al., 1982). The development of striatal domains follows two gradients; from posterior to anterior and from ventrolateral to dorsomedial. According to this pattern, the ventrolateral striatal cells were born earliest, dorsolateral striatal cells were born after and dorsomedial striatal cells were born the latest (Bayer et al., 1982).

In rodents, the VLS receives input from orofacial and head motor cortex, while the DLS receives input from forelimb, whisker and trunk motor cortex, and the most medial part of DLS receives input from hind limb and trunk motor cortex (Deniau et al., 1996, Ebrahimi et al., 1992, Hintiryan et al., 2016). Throughout the mouse striatum, only a small dorsomedial region does not receive motor input, but receives input from visual areas and more associative cortical areas (Hintiryan et al., 2016)

The combination of retrograde and anterograde labeling of different striatal populations showed that different striatal regions project onto

different parts of SNr (Gerfen et al., 1985, Deniau et al., 1992, Deniau et al., 1996). However, in these studies the regions were not divided into these three domains; DMS, DLS and VLS. In some studies, the cortical input was labeled together with their SNr output to relate the postsynaptic SNr region with the presynaptic cortical region (Deniau et al., 1996). However, to our knowledge, a detailed mesoscopic mapping of direct and indirect pathway projections onto SNr and GPe from genetically defined subpopulations of striatonigral and striatopallidal cells is missing, in the mouse.

Based on the input maps and developmental patterns we defined DMS, DLS and VLS as functionally different dorsal striatum domains (Deniau et al., 1996, Ebrahimi, et al., 1992, Hintiryan, et al., 2016). We produced AAV2.2-EF1a-DIO-EYFP-WPRE and AAV2.2-EF1a-tdTomato-WPRE viruses to simultaneously express different fluorescent proteins in different dorsal striatal domains. We used D1-Cre (FK150-Cre) and D2-Cre (Adora-Cre) mouse lines to target striatonigral or stiatopallidal subpopulations. 250-300 nl of each virus was injected and 3-4 weeks expression time was allowed.

We also considered the anterior-posterior axes and therefore we mapped the output of 9 striatal domains: anterior-dorsomedial (aDMS), mid-dorsomedial (mDMS) and posterior-dorsomedial (pDMS), anterior-dorsolateral (aDLS), mid-dorsolateral (mDLS) and posterior-dorsolateral (pDLS), and anterior-ventrolateral (aVLS), mid-ventrolateral (mVLS) and posterior-ventrolateral (pVLS) domains. We labeled two different domains simultaneously using two different fluorescent proteins, and compared their projection patterns onto target regions. The data below shows the projections of

striatonigral and striatopallidal subpopulations onto the specific regions of GPe and SNr, and will hopefully permit soon the 3D reconstruction of these pathways. Therefore, for the moment, the discussions on the projection patterns observed below are based on qualitative observations.

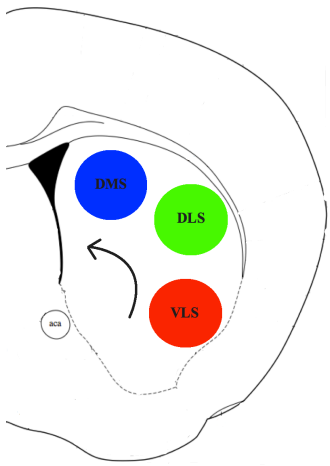

Figure 2.1 | Diagram showing three domains of dorsal striatum; dorsomedial striatum (DMS), dorsolateral striatum (DLS), ventrolateral striatum (VLS). (The arrow indicates their developmental order.)

RESULTS

We produced viruses, with the same promoters, and that only differ in the fluorescent proteins they express. Therefore, we cloned tdTomato fluorescent protein into a pAAV-EF1a-DIO-EYFP-WPRE construct replacing EYFP, and used AAV2.2-EF1a-DIO-EYFP-WPRE and pAAV-EF1a-DIO-tdTomato-WPRE for Cre dependent expression of EYFP and tdTomato in different striatal domains. We used D1-Cre (FK150-Cre) and D2-Cre (Adora2a-Cre) transgenic mouse lines. We injected 250-300nl virus in each domain and waited for 3-4 weeks expression time.

We optimized coordinates for each transgenic line separately. Nine different domains were labeled: aDMS, mDMS, pDMS, aDLS, mDLS, pDLS, aVLS, mVLS, and pVLS. Sequential images of whole brain slices were acquired at 10X magnification.

Projections of striatonigral and striatopallidal neurons from different domains targeted different downstream areas

Striatonigral projections of different striatal domains seemed to have different patterns of projection onto SNr. Relative mediolateral position of cell bodies in striatum seemed to be conserved by their projections onto the target structures, i.e., medial striatal domains targeted medial parts of SNr while lateral striatal domains projected onto the lateral parts of SNr. However, on the dorsoventral axis, striatal position was inverted by their projections, i.e., more dorsal striatal populations projected more ventrally and ventral striatal populations projected more dorsally onto SNr. Striatonigral projections kept their relative mediolateral position and never crossed each other to reach their target region in SNr. Therefore, they made parallel pathways projecting onto SNr.

Unlike striatonigral cells, striatopallidal populations projected onto GPe directly translating their striatal cell body position, on both mediolateral and dorsoventral axis. Striatopallidal populations also kept their mediolateral relative position on GPe and never crossed each other to reach their target region on GPe. Therefore, striatopallidal pathway projections also made parallel pathways projecting onto GPe.

Striatonigral projections on aSNr and pSNr showed differences

aDMS, aDLS, mDMS and mDLS striatonigral projections targeted larger, relatively dorsal regions of SNr, closer to SNc. However, on posterior-SNr (pSNr) they stayed on the most ventrolateral site, away from SNc. Interestingly, aVLS and mVLS projections targeted dorsolateral sites on anterior-SNr (aSNr) and kept targeting dorsolateral sites of pSNr, but they increased the targeted area on pSNr compared to aSNr. pDMS, pDLS, and pVLS striatonigral domains projected on small regions and did not seem to change the size of their target area throughout SNr. Therefore, it is likely that on aSNr all aDMS, aDLS, mDMS, mDLS, aVLS and mVLS might be occupying similar regions. However, on pSNr, aVLS and mVLS projections seemed to be occupying impressively larger areas compared to aDMS, aDLS, mDMS and mDLS projections.

Example images from injection sites, from anterior-SNr (aSNr), mid-SNr (mSNr), and posterior-SNr (pSNr) are presented in Figure 2.1, Figure 2.2, and Figure 2.3. For each image, we separated two fluorescent protein channels and used Otsu's method to convert images to binary (Otsu, 1979). We took each binary channel of the same image as vectors and calculated their correlation coefficient. We calculated the level of spatial overlap, independent of the intensity of the signal of two labeled populations using Pearson's correlation coefficient. We used Pearson's correlation coefficient as a measure of spatial overlap of projections.

Example images in Figure 2.1, Figure 2.2 and Figure 2.3 suggested that projections from different striatonigral domains might show different levels of overlap at different anterior posterior levels of SNr.

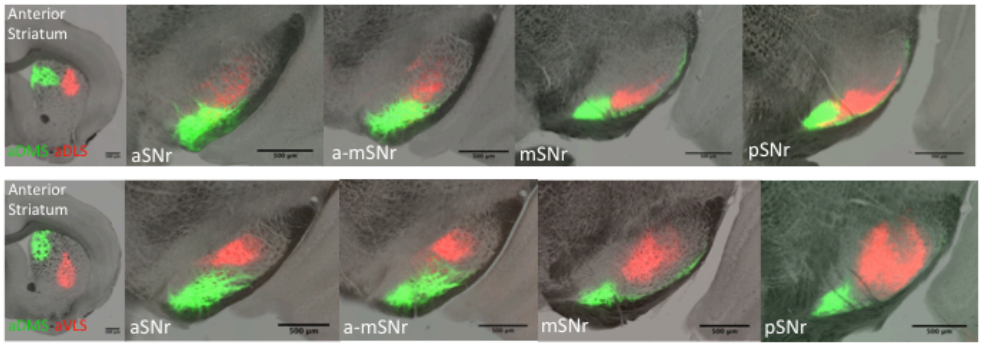

Figure 2.2 | Example images of striatonigral pathway aDMS-aDLS and aDMS-aVLS double labeled populations showed different projection patterns onto SNr. Non-overlapping aDMS-aDLS populations partially overlapped on aSNr and mSNr but not on pSNr (aDMS-aDLS: r_striatum=-0.01, r_aSNr= 0.1, r_mSNr= 0.2, r_pSNr= -0.006, Pearson's correlation coefficient, n=2). Non-overlapping aDMS-aVLS populations targeted non-overlapping SNr regions (aDMS-aVLS: r_striatum=-0.01, r_aSNr= -0.02, r_mSNr= -0.02, r_pSNr= -0.02, Pearson's correlation coefficient, n=2).

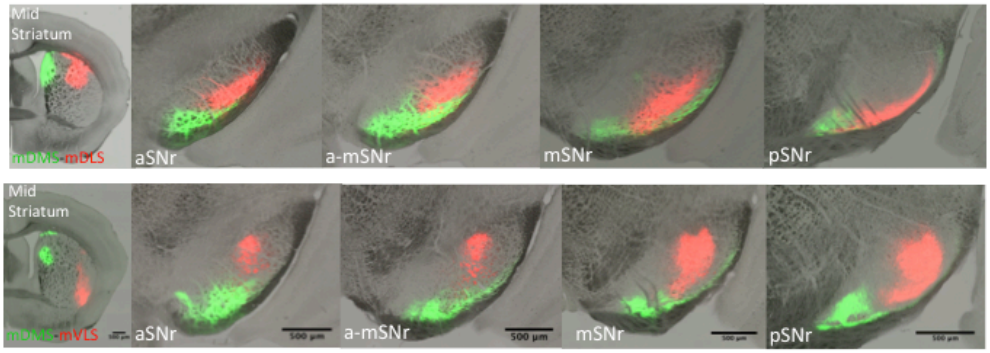

Figure 2.3 | Example images of direct pathway mDMS-mDLS and mDMS-mVLS populations showed different projection patterns on SNr. Targeted area of projections was different on the aSNr, mSNr and pSNr. Non-overlapping mDMS-mDLS and mDMS-mVLS populations targeted non-overlapping SNr regions (mDMS-mDLS: r_striatum=-0.01, r_aSNr= -0.009, r_mSNr= -0.009, r_pSNr= 0.03,

mDMS-mVLS: r_striatum=-0.005, r_aSNr= -0.02, r_mSNr= -0.02, r_pSNr= -0.04, Pearson's correlation coefficient, n=2).

aDMS striatonigral populations projected on the most ventrolateral SNr. mDMS projections targeted the same region however they also targeted the thin ventrolateral layer of SNr that was suggested to be occupied by mostly superior colliculus (SC) projecting cells (Grofova, et al., 1989). pDMS projected only to the thin ventrolateral layer of SNr.

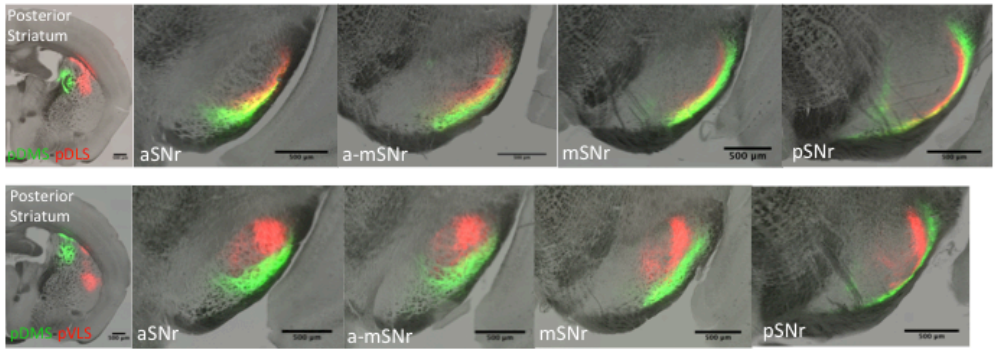

Figure 2.4 | Example images of direct pathway pDMS-pDLS and pDMS-pVLS populations showing different projection patterns on SNr. Targeted area of projections was different on the aSNr, mSNr and pSNr. Non-overlapping pDMS-pDLS populations partially overlapped on aSNr, mSNr, and pSNr (r_striatum=-0.01, r_aSNr= 0.4, r_mSNr= 0.4, r_pSNr= 0.4, 2D-Pearson's correlation coefficient, n=2) pDMS-pVLS populations targeted non-overlapping SNr regions (pDMS-pVLS: r_striatum=-0.01, r_aSNr= 0.03, r_mSNr= -0.03, r_pSNr= -0.01, Pearson's correlation coefficient, n=2).

DLS striatonigral projections generally targeted the SNr regions between the targets of DMS and VLS projections. mDLS projections targeted similar but more ventral regions on SNr compared to aDLS projections. pDLS projections targeted the most ventral (thin layer) regions around the projections of aDLS and mDLS.

VLS projections generally occupied similar regions to DLS projections on aSNr, but extended their projection area on pSNr, on the dorsolateral site of pSNr. aVLS and mVLS projected on similar regions with mVLS targeting more ventral compared to aVLS projections. pVLS projections targeted similar but more dorsolateral regions on SNr compared to aVLS and mVLS projections.
pDMS and pDLS seemed to project only on the thin ventrolateral layer along the anterior posterior axis of SNr, which was reported to be occupied by cells projecting to SC (Grofova, et al., 1989). Therefore, it is possible that pDMS and pDLS striatonigral populations are mostly targeting SC circuits.
It was previously suggested that striatonigral projection patterns resemble the corticostriatal projection patterns (Gerfen, 1985). Our results supported this observation. Similar to corticostriatal projections targeting the whole anterior-posterior axis of striatum, each labeled striatonigral population targeted the whole anterior-posterior axis of SNr.

Striatopallidal projections of different populations showed similar patterns on aGPe and mGPe

We also observed that on the mediolateral axis, DMS and DLS projections of striatopallidal cells directly translate their striatal cell body position onto GPe, creating vertical bands, similar to striatopallidal projection patterns described before (Wilson, et al., 1982, Hazrati, et al., 1992, Sadek et al., 2007).
Example images in Figure 2.4 and Figure 2.5 suggested that non-overlapping striatopallidal populations targeted non-overlapping GPe

regions. DMS, DLS and VLS populations projected on different regions on GPe. Therefore, as suggested above, it is possible that striatopallidal projections are more segregated compared to striatonigral projections.

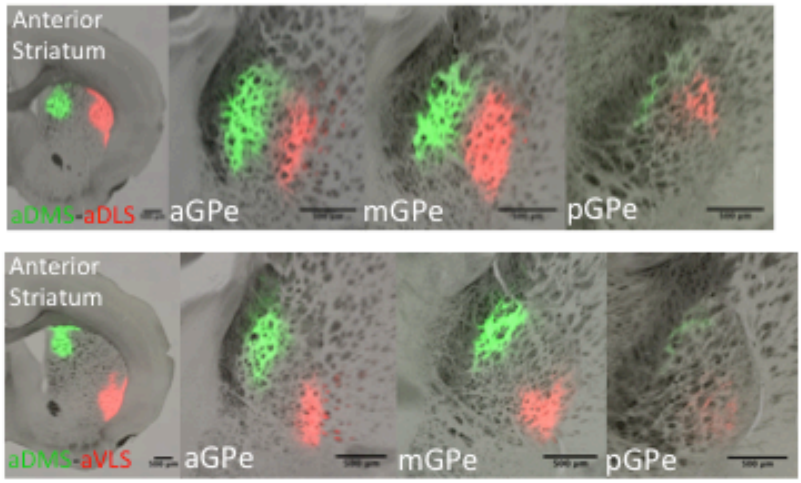

Figure 2.5 | Example images of striatopallidal pathway aDMS-aDLS and aDMS-aVLS populations showed different projection patterns on GPe. Non-overlapping aDMS-aDLS and aDMS-aVLS populations targeted non-overlapping GPe regions (aDMS-aDLS: r_striatum=-0.01, r_GPe_1= -0.02, r_GPe_2= -0.02, r_GPe_3= -0.01, aDMS-aVLS: r_striatum=-0.01, r_GPe_1= -0.02, r_GPe_2= -0.03, r_GPe_3= -0.01, Pearson's correlation coefficient, n=3).

Both aDMS and mDMS projected onto GPe occupying the most medial region, creating the most medial band onto GPe. aDLS and mDLS occupied the most lateral region of GPe creating the most lateral band. However aVLS and mVLS projections occupied the most ventrolateral region of GPe, sometimes creating a V-shape, but not a vertical band.

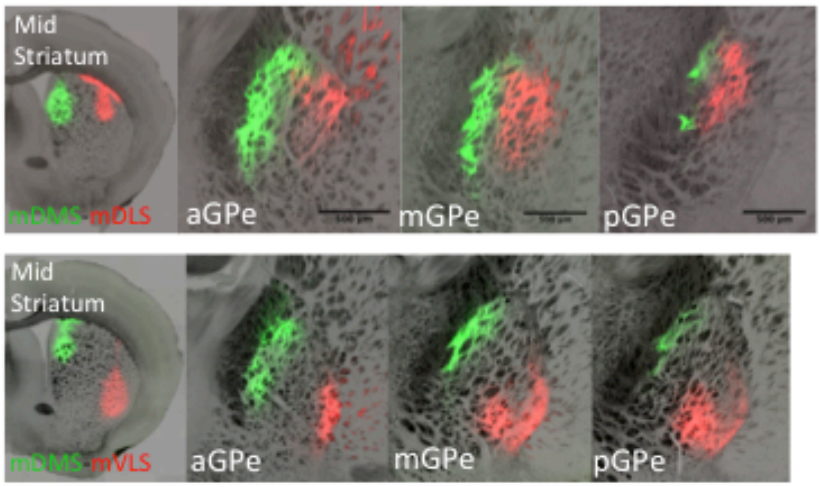

Figure 2.6 | Example images of indirect pathway mDMS-mDLS and mDMS-mVLS populations showed different projection patterns on GPe. Non-overlapping mDMS-mDLS and mDMS-mVLS populations targeted non-overlapping GPe regions (mDMS-mDLS: r_striatum=-0.01, r_GPe_1= -0.03, r_GPe_2= -0.01, r_GPe_3= -0.01, mDMS-mVLS: r_striatum=-0.01, r_GPe_1= -0.03, r_GPe_2= -0.04, r_GPe_3= -0.01, Pearson's correlation coefficient, n=3)

Interestingly all aDMS, mDMS, aDLS, mDLS, aVLS, and mVLS targeted strongly onto aGPe and mGPe but sent weak projections onto pGPe. Even though it was suggested that the most posterior striatum showed low expression of D2 receptors, and fewer striatopallidal neurons, it will be important to map the projections of the most posterior striatopallidal populations (Gangarossa et al., 2013).

DISCUSSION

Anatomical mapping of circuits is important not only to understand the structural organization of the brain, but also for it functional understanding. Anatomical data can sometimes lead to functional predictions. One way to map striatonigral and striatopallidal

projections onto their target regions would be to create a projectome, and report projection patterns of each population in detail and leave the functional interpretations to the readers. However, it is very hard to test specific hypothesis on connectome or projectome data reported thus far, since it has been hard to reach the data and analyze it for specific questions. Therefore, another approach is to start with functional questions and functional domains, analyze anatomical data for specific functional domains, and report the answers to specific questions.

Accordingly, we started with defining three striatal functional domains, DMS, DLS, and VLS, based on previous anatomical and functional data, and compared their projection patterns onto their target regions. We used AAVs that express EYFP and tdTomato and simultaneously labeled two subpopulations of either striatonigral or striatopallidal populations using D1-Cre (FK150-Cre) and D2-Cre (Adora2a-Cre) mouse lines. We labeled 9 different subpopulations described before by keeping DMS populations as reference and labeling either DLS or VLS on the same anterior-posterior axis. We acquired whole brain anatomical data. This technique allowed us to compare projection patterns within and between brains. The data collected can hopefully help identifying projection patterns that might be plausible candidates to explain functional data (see example in chapter 3).

Using this approach, we showed that both striatonigral and striatopallidal population projections created parallel pathways. Both pathway projections followed similar organization on the

mediolateral axis, by conserving their relative mediolateral striatal position onto the target structures, but they also followed different organizational rules.

In one hand, striatonigral projections inverted their cell body position on the dorsal-ventral axes, suggested larger degrees of overlap, and crated complex shapes in SNr. On the other hand, striatopallidal projections translated their striatal position directly onto GP creating vertical bands and V-shaped bands.

In primates, it was suggested that GPi receives most of the limb and trunk input while SNr receives mostly orofacial and occulomotor input (Nambu, 2011). In the mouse SNr, VLS populations in general, target larger regions that DMS and DLS populations. Therefore, it is still possible that, in the mouse, a larger population of SNr is involved in orofacial motor and occulomotor control, compared to other motor functions.

It was previously suggested that basal ganglia is involved in action selection via two (path)ways, modulating thalamocortcial networks, and modulating brainstem motor networks (Hikosaka et al., 2000). It was also suggested that anterior two thirds of SNr projects to thalamus and SC, and the posterior one third of SNr projects to thalamus and brainstem (Grofova, et al., 1982, Deniau, et al., 1996). All the striatonigral populations that were labeled projected to the whole anterior-posterior axis of SNr. DMS and DLS striatonigral populations of anterior, mid and posterior striatum projected on larger areas on aSNr and to smaller areas on pSNr. However, unlike DMS and DLS populations, VLS striatonigral populations projected on larger areas on pSNr compared to aSNr.

Therefore, aSNr, via its stronger thalamic projections, might be providing information feeding back to the thalamo-cortico basal-ganglia loops. pSNr, via its stronger projections to brainstem, might be directly modulating the premotor regions, motor output. It is likely that DMS, DLS and VLS target thalamo-cortico-basal-ganglia loops similarly, but VLS sends stronger motor output compared to DMS and DLS.

Our labeling techniques do not discriminate between patch and matrix compartments of striatum, but it was previously suggested that anterior striatum receives more input from limbic cortex regions and have more patches compared to the other striatal regions (Gerfen et al., 1987, Graybiel, 1998). It was suggested that anterior striatum was involved execution of instrumental actions in early stages of learning while posterior striatal was involved in execution of instrumental actions in late stages of learning (Jueptnter et al., 1997a, Yin et al., 2004, Yin et al., 2009). If we take this at facevalue, together with the fact that pSNr is the motor output region of SNr, then it would be expected that the posterior striatum would be projecting weaker to aSNr and stronger to pSNr (Grofova, et al., 1982). Our first observations suggested that pDMS, pDLS and pVLS populations might indeed be projecting into smaller regions on aSNr, than aDMS, aDLS and aVLS populations. However, the same comparison on pSNr requires more analysis. Therefore, it is likely that posterior striatum and pSNr might be involved in execution in late stages of learning, while anterior populations might be involved in early stages of instrumental learning (Jueptnter et al., 1997a, Hikosaka, et al., 2000, Yin et al., 2004, Yin et al., 2009).

It was also suggested that striatonigral projections create layers around SNr, form “onion-like” structures, and the dendritic fields of SNr projection cells were distributed within these layers of converging inputs (Faul et al., 1978, Grofova et al.,1982, Deniau et al., 1996). To understand the organization of such a complex structure coronal, or sagittal images of SNr would not be sufficient. Therefore, 3D reconstruction of projections would be necessary to understand the organization of different striatopallidal population projections onto SNr. We are currently pursuing these efforts.

Similar to primates’ putamen projections, in the mouse, we showed that somatotopic organization on the striatum was directly projected onto GPe via striatopallidal projections (Nambu, 2011).

DMS projected strongly onto aGPe and mGPe. DMS projections seemed to occupy larger region than DLS or VLS projections onto aGPe, and its projections seemed weaker on the pGPe.

It was previously suggested that two types of cells showed different intrinsic projection patterns in GPe (Stanek et al., 2007). The first group was located within the 100um thick, outer layer of GPe that was on the striatal border and was occupied by cells that arborized within the same layer and send collaterals to the inner layer of GPe (Stanek et al., 2007). Second group was arborized only within the larger inner layer of GPe (Stanek et al., 2007). We did not observe differences in the striatopallidal projection patterns between the inner and the outer layer of GPe. It is likely that these two structures did not differ in their striatal input but only differ in their within-GPe arborizations.

It was previously suggested that PV+ cells were located more laterally on GPe and cells expressing Lhx6 were located more medially (Mastro, et al., 2014). These cells were also shown to project onto different targets; PV+ cells projected stronger onto Pf, SNr and STN, while Lhx6 expressing cells projected stronger onto DLS, SNc and Rt (Mastro, et al., 2014). We observed that medial part of GPe received only DMS input and lateral region received DLS and VLS input. DMS input might be transmitted to target structures by Lhx6 population such as DLS, SNc and Rt, whereas, DLS and VLS input might be transmitted to Pf, SNr and STN via PV+ cells, distributing information from different domains of striatopallidal pathway to different circuits.

Even though specific regions of SNr and GPe received specific input from striatum, dendritic fields of SNr and GPe cells span large areas, with striatal input targeting distal dendrites of both GPe and SNr cells (Grofova et al., 1982, Smith et al, 1998, Stanek et al., 2007, Bolam et al., 2000). Therefore, even though these observations do not clarify the advantages of having parallel projecting striatonigral and striatopallidal pathways, circuit mapping shows that striatal cells that receive specific motor input project to regions of SNr which in turn projects to downstream motor regions involved in same specific movements (Deniau et al., 1996, Grofova et al., 1989). Therefore, large dendritic fields of SNr and GPe cells might allow them to integrate different contextual input to gate motor information to the pre-motor output centers, while also allowing specific actions to be performed in different contexts, in a cue guided manner or self initiated.

It would be interesting to compare the dendritic regions of GPe and SNr targeted by functionally similar striatal domains compared to functionally different striatal domains. These differences might help us better understand the information processing on basal ganglia output cells.

In summary, corticostriatal projections, striatonigral and striatopallidal projections showed complex projection patterns, and the complexity increased by large dendritic fields of SNr and GPe cells. All these circuit complexity might allow movement patterns to be learned and executed in different contexts, in response to different stimuli.

In order to study the complex anatomical patterns together with their motor functions on initiation and execution of specific movements, on the rest of the thesis we focused on the anterior-ventrolateral striatum and in addition to its striatonigral and striatopallidal projections, we investigated the role of this region in naïve and instrumental orofacial actions.

MATERIAL AND METHODS

Animals

All procedures were reviewed and performed in accordance with the Champalimaud Center of the Unknown Ethics Committee guidelines and approved by the Portuguese Veterinary General Board (Direccao Geral de Veterinaria, approval 0421/000/000/2014). GENSAT BAC transgenic lines D1-Cre (FK150) and D2- Cre (Adora2a) are used to specifically target striatonigral or striatopallidal cells. Animals between 3-6 months of age, that were housed in normal light cycle

were used in these experiments. Experiments were performed during the light cycle.

Cloning

pAAV-EF1a-DIO-EYFP-WPRE (Addgene plasmid #27056) construct was used as backbone. tdTomato was amplified from pAAV-CAG-flex-tdTomato (provided by Champalimaud Virus Platform) adding Nhe1(GCTAGC) at the 3' and Asc1 (GGCGCGCC) restriction sites at the 5' ends with PCR and inserted into the backbone. The full length of end product pAAV-EF1a-DIO-tdTomato-WPRE was sequenced no significant mutations were observed. AAV2.2-EF1a-DIO-tdTomato-WPRE virus was produced University of North Carolina at Chapel Hill vector core and the virus is available at University of North Carolina at Chapel Hill vector core for distribution. AAV2.2-EF1a-DIO-EYFP-WPRE virus was also purchased from University of North Carolina at Chapel Hill vector core.

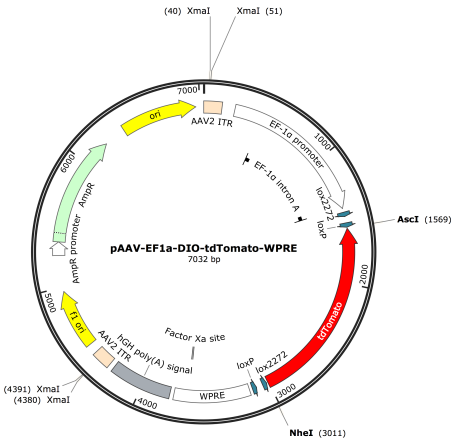

Figure 2.7 | Map of pAAV-EF1a-DIO-tdTomato-WPRE construct produced by inserting tdTomato into pAAV-EF1a-DIO-EYFP-WPRE using Asc1 and Nhe1 restriction sites. (Virus will be distributed by University of North Carolina at Chapel Hill vector core)

Surgery

Double injections of 250-300nl AAV2.2-EF1a-DIO-EYFP-WPRE (University of North Carolina, titer $1.85x10^{12}$) and AAV2.2-EF1a-DIO-tdTomato-WPRE (University of North Carolina, titer $2.7x10^{12}$) were injected in aDMS, mDMS, pDMS, aDLS, mDLS, pDLS, aVLS, mVLS and pVLS using DMS injections as reference and changing the second injections site between DLS and VLS. Fluorescent proteins were randomly switched between injection sites. Coordinates of the injection sites were optimized as for aDMS (D1-Cre mice; AP: +1.15mm, ML:1.2mm, DV:2.4mm, D2-Cre mice; AP:+1.15mm, ML:1.42mm, DV:2.2mm), mDMS (D1-Cre; AP:+0.55mm, ML:1.42mm, DV:2.35mm, D2-Cre-mice; AP:+0.55mm, ML:1.43mm, DV:2.33mm) and pDMS (D1-Cre mice; AP:-0.42mm, ML: 2.43 mm, DV:2.3mm), aDLS (D1-Cre mice; AP:+1.15mm, ML: 2.28 mm, DV:2.32mm, D2-Cre mice; AP:+1.15mm, ML: 2.66 mm, DV:2.35mm), mDLS (D1-Cre mice; AP:+0.55mm, ML: 2.7 mm, DV:2.35mm, D2-Cre mice; AP:+0.6mm, ML: 2.75 mm, DV:2.35mm,) and pDLS (D1-Cre mice; AP:-0.42mm, ML: 3.15 mm, DV: 2.35mm), and aVLS (D1-Cre mice; AP:+1.15mm, ML:1.9 mm, DV:3.15 mm, D2-Cre mice; AP:+1.15mm, ML:2.25mm, DV:3.2 mm), mVLS (D1-Cre mice; AP:+0.55mm, ML:2.6mm, DV:3.1 mm, D2-Cre mice; AP:+0.6mm, ML:2.65mm, DV:3.25mm) and pVLS (D1-Cre mice; AP:-0.42mm, ML: 3.16 mm, DV: 3.38 mm) domains. GENSAT BAC transgenic lines FK150-Cre were used for D1 labeling population and Adora2a-Cre line was used for labeling D2 population. FK150-Cre is the only line where we can reliably label dorsal and ventral striatal D1 populations together (Gerfen et al., 2013).

D1 and D2 Cre lines used showed differences in their brain size. Therefore coordinates were optimized for both lines. D2 expression is very weak in posterior striatum (Gangarossa, et al., 2013). Therefore posterior D2 population labeling was not included.

Histology

3-4 weeks post-injection mice are perfused with 4% PFA and incubated in 4% PFA for 24h. 50um slices of the whole brain are sliced acquired using vibratome. The order of the slices is kept during slicing for reconstruction of the whole brain.

Imaging

Slices with maximum intensity of expression were identified separately for cell bodies in striatum and axons on SN, GPi and GPe. Exposure times below saturation level for each condition aware recorded for each channel. Recorded exposure times are fixed and used for each structure. Images are acquired using wide field fluorescence scanning microscope (Zeiss Axioimager M2) at 10X. Multichannel images were acquired using EYFP, mRFP filters and bright field (DIC) channels for every image. Alexa Fluor-647nm was used as a secondary antibody for cell type staining and imaged using Cy5 filter. DAPI, Nissl filters ware used depending on the labeling.

Image Analysis

Each brain was injected with two fluorescent protein and relative positioning of either DMS with either VLS or DLS. DMS was kept as a reference on all the injections. Non-overlapping populations were targeted in striatum. Therefore projections of DLS and VLS relative to DMS projections were analyzed. Each image was separated to its channels. Each fluorescent protein imaging channel was converted to

binary image using Otsu's method for tresholding (Otsu, 1979, Hunnicutt, et al., 2014). Correlation coefficient of these binary-converted images was calculated as a measure of special overlap between channels (labeled populations), independent of the pixel intensity.

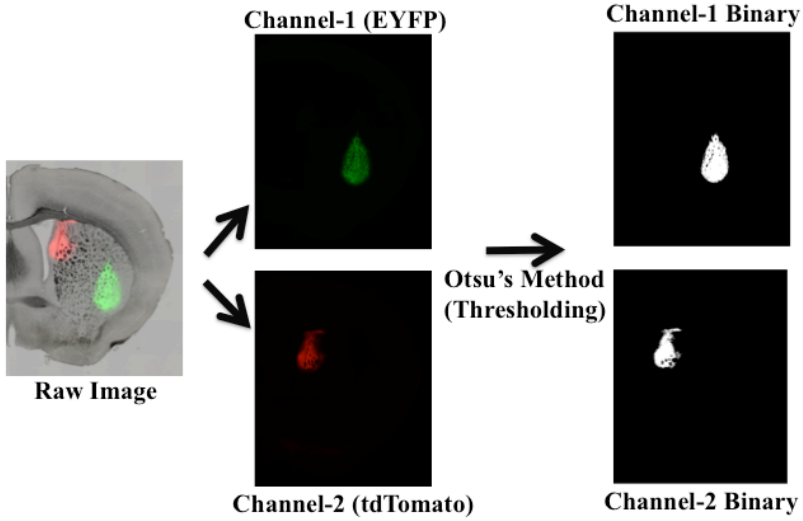

Figure 2.68| Workflow for 2D Pearson's correlation coefficient calculations for simultaneously labeled two populations in striatum, and their axons on the target regions. Each channel for each image was converted to binary image using Otsu method. Spacial correlations of binary images were calculated to measure if populations and their projections overlapped.

ACKNOWLEDGEMENTS

We would like to thank F.Tecuapetla for his comments and valuable discussions that inspired this work. A.Vaz and M.Correira for mouse colony management. This research was supported by INDP Graduate Programme, FCT fellowship, HHMI to R.M.C, ERA-NET NEURON, 7th Framework Programme.

AUTHOR CONTRIBUTIONS

S.Multu and R.M.Costa designed the experiments, S.Mutlu performed the experiments.

REFERENCES

Bayer, S.A. (1983) Neurogenesis in the rat neostriatum. Int. J. Devl. Neuroscience 2(2): 163-175

Bolam, J.P., Hanley, J.J., Booth, P.A.C., Bevan, M.D. (2000) Synaptic organization of basal ganglia. J.Anat. 196: 527-542

Colonnese, M.T., Stalman, E.L., Berridge, K.C. (1966) Ontogeny of action syntax in altrical and precocial rodents: Grooming sequences of rat and guinea pig pups. Behavior 133(15/16): 1165-1195

Deniau, J.M., Chevalier, G. (1992) The lamellar organization of the rat substantia nigra pars reliculata: Distribution of projection neurons. Neuroscience, 46(2): 361-377

Deniau, J.M., Menetrey, A., Charpier, S. (1996) The lamellar organization of the rat substantia nigra pars reliculata: Segregated patterns of striatal afferents and relationship to topography of corticostriatal projections. Neuroscience, 73(3): 761-781

Ebrahimi, A., Pochet, R., Roger, M. (1992) Topographical organization of the projections from physiologically identified areas of the motor cortex to the striatum in the rat. Neuroscience Research 14: 39-60

Faull, R.L., Mehler, W.R. (1978) The cells of origin of nigrotectal, nigrothalamic and nigrostriatal projections in the rat. Neuroscience 3(11): 989-1002

Gangarossa, G., Espallergues, J., Mailly, P., De Bundel, D., d'Exaerde, A., Herve, D., Girault, J., A., Valjent, E., Krieger, P. (2013) Spatial distribution of D1R- and D2R- expressing medium sized spiny neurons differs along the rostro-caudal axis of the mouse dorsal striatum. Front. Neural Circuits 7(124): 1-16

Gerfen, C. R. (1985) Neostriatal mosaic 1:Compartmental organization of projections from the striatum to substantia nigra in the rat. J. Comp. Neurol. 236(4): 454-476

Gerfen , C.R., Herkenham, M., Thibault, J. (1987) Neostriatal mosaic: II. Patch- and matrix-directed mesostriatal dopaminergic and non-dopaminergic systems. J. Neurosci. 7(12): 3915-3934

Gerfen, C. R., Engber, T. M., Mahan, L. C., Susel, Z., Chase, T., N., Monsma, F. J., Sibley, D. R. (1990) D1 and D2 dopamine receptor regulated gene expression of striatonigral and striatopallidal neurons. Science 250 (4986): 1429-1432

Gerfen, C. R. (1992) Neostriatal mosaic: multiple levels of compartmental organization. TINS 15(4): 133-139

Gerfen, C. R., Surmier, D. J., (2011), Modulation of striatal projection system by dopamine. Annu Rev Neurosci (34): 441-466

Gerfen, C., R., Paletzki, R., Heintz, N., (2013) GENSAT- BAC Cre-recombinase driver lines to study the functional organization of cerebral cortical and basal ganglia circuits. Neuron 80(6):1368-1383

Graybiel, A. M. (1998) The basal ganglia and chunking of action repertoires. Neurobiol. Learn. Mem. 70(1/2): 119-136

Grofova, I., Deniau, J. M., Kitai, S.T. (1982) Morphology of the substantia nigra pars reticulata projection neurons intracellularly labeled with HRP. J. Comp. Neurology 208:352-368

Hazrati, L.N., Parent, A. (1992) The striatopallidal projection displays a high degree of anatomical specificity in the primate. Brain Res. 592(1-2): 213-227

Hikosaka, O., Takikawa, Y., Kawagoe, R. (2000) The role of basal ganglia in the control of purposive saccadic eye movements. Physiol. Rev. 80:953-978

Hintiryan, H., Foster, N.F., Bowman, I., Bay, M., Song, M.Y., Guo, L., Yamashita, S., Bienkowski, M. S., Zingg, B., Zhu, M., Yang, X.W., Shih, J.C., Toga, A.W., Dong, H.W. (2016) The mouse cortico-striatal projectome. Nat. Neurosci. 19(8): 1100-14

Hunnicutt, B., J., Long, B., R., Kusefoglu, D., Gertz, K., J., Zhong, H., & Mao, T. (2014) A comprehensive thalamocortical projection map at the mesoscopic level. Nat. Neurosci. 17(9): 1276-1285

Jueptner, M., Stephan, K.M., Frith, C.D., Brooks, D.J., Frackowiak, R.S.J., Passingham, R.E. (1997a) Anatomy of motor learning. 1.Frontal cortex and attention to action. J. Neurophys. 77(3): 1313-24

Nambu, A. (2011) Somatotopic organization of the primate basal ganglia. Front. Neuroanat. Apr 20;5:26.

Mastro, K., Bouchard, R.S., Holt, H.A., Gittis, A.H. (2014) Transgenic mouse lines subdivide external segment of the globus pallidus (GPe) neurons and reveal distinct GPe output pathways. J Neurosci. 34(6): 2087-99.

Otsu, N. (1979) Threshold selection method from gray level histograms. IEEE SMC-9(1): 62-66

Shen, W., Flajolet, M., Greengard, P., Surmeier, D.J., (2008) Dichotomous dopaminergic control of striatal synaptic plasticity. Science 321:848-851

Smith, Y., Bevan, M.D., Shink, E., Bolam, J.P. (1998) Microcircuitry of the direct and indirect pathways of the basal ganglia. Neuroscience 86(2): 353-387

Stanek, E., Cheng, S., Takatoh, J., Han, B. X., Wang, F. (2014) Monosynaptic premotor circuit tracing reveals neural substates for oro-motor coordination. Elife 2014; 3: e02511

Wilson, C.J., Phelan, K.D. (1982) Dual topographic representation of neostriatum in the globus pallidus of rat. Brain Res. 243(2): 354-9

Yin, H.H., Knowlton, B.J. (2004) Contributions of striatal subregions to place and response learning. Learn. Mem. 11(4): 459-462

Yin, H.H., Mulcare, S.P., Hilaro, M.R., Clouse, E., Holloway, T., Davis, M.I., Hansson, A.C., Lovinger, D.M., Costa, D.M. (2009) Dynamic reorganization of striatal circuits during the acquisition and consolidation of a skill. Nat. Neurosci. 12(3): 333-41

CHAPTER 3 | ANATOMICAL AND FUNCTIONAL MAPPING OF VENTROLATERAL STRIATUM POPULATIONS CONTROLLING LICKING

ANATOMICAL AND FUNCTIONAL MAPPING OF VENTROLATERAL STRIATUM POPULATIONS CONTROLLING LICKING

SUMMARY

It was suggested that the ventrolateral striatum (VLS) might be involved in orofacial movements. However, the contribution of anatomical circuits and functional properties of VLS populations to orofacial movements in naive and trained mice have yet to be established. We showed that VLS receives input from primary and secondary orofacial motor cortex and that VLS striatonigral pathway project onto dorsolateral "core" region of SNr. Cells in this "core" region of SNr were shown to project to medullary reticular formation, a brain stem nuclei involved in orofacial movements. We also showed that VLS striatopallidal pathway projects onto ventrolateral region of GPe. However, the target regions of these cells are yet to be established.

Optogenetic stimulation of striatonigral pathway VLS cells induced licking in naive freely moving mice, while stimulation of striatopallidal pathway VLS cells did not show an immediate motor effect.

We developed a head fixed olfactory guided operant task to investigate the role of striatonigral and striatopallidal VLS populations in instrumental orofacial movements, specifically in licking. We trained mice to respond to different odors by licking for water, suppressing licking to avoid punishment, withholding licking to receive a delayed water reward and for no outcome. VLS

striatonigral pathway stimulations induced licking differently depending on the context. Lick rates during stimulations were the highest in go trials, lowest in no-go trials, and intermediate in wait and neutral trials. Striatopallidal pathway stimulations paused licking during stimulation period. Interestingly, population calcium imaging of VLS striatonigral and striatopallidal population activity suggested that both populations were active preceding initiation of licking in go trials. Striatonigral population decayed during execution of licking, without showing modulations by changes in the lick rates. However, striatopallidal population showed sustained activity during execution of licking. Our results support the idea that balanced activity of both pathways might be necessary for initiation and execution of instrumental actions.

INTRODUCTION

Anatomical mapping of different striatal population projections onto GPe and SNr suggested that spatially segregated striatal populations project mostly onto spatially segregated regions of GPe and SNr. Interestingly, striatonigral projections of VLS showed different projection patterns compared to DMS and DLS striatonigral populations. They occupied relatively larger areas on the “core”, dorsolateral region of SNr.

In addition, orofacial motor cortex has been shown to project onto ventrolateral striatum in primates and in mice (Nambu, 2011, Hintiryan, et al., 2016). Single unit recordings in lateral striatum showed correlations with movement of specific body parts, i.e. more cells in the dorsal part of dorsolateral striatum (DLS) fired during

forelimb, hind limb, trunk and whisker movements and more cells in ventrolateral striatum fired during orofacial movements such as, licking, tongue reaching, and jaw movements (Carelli et al., 1991, Mittler et al., 1994). Lesion studies, inducing different sizes of lesions, confirmed the somatotopic organization on anterior-DLS (aDLS), and showed that while anterior-DMS (aDMS) lesions did not have a chronic effect on spontaneous movement initiation and execution, aDLS lesions chronically impaired forelimb reaching, and aVLS lesions chronically impaired tongue reaching and showed weaker impairment on forelimb reaching (Pisa et. al., 1988, Pisa, 1988).

Microinjection of dopamine and acetylcholine agonists into VLS induced repetitive orofacial movements (Mittler et al., 1994). Dopamine depletion in VLS induced vacuous chewing (spontaneous chewing like jaw movements), reversible difficulty in chewing and facial tremors (Jicha et. al., 1991). Therefore, electrophysiological recording and lesion studies suggested that VLS is involved in orofacial movements. However, the role of striatonigral and striatopallidal aVLS populations in orofacial motor control, in initiation and execution of instrumental licking was not known.

In Chapter 2, we have shown that VLS was projecting onto ventrolateral GPe via its striatopallidal projections and onto dorsolateral SNr via its striatonigral projections. Electron microscopy studies showed that ventrolateral GPe and striatonigral VLS projections converged on the same cells in SNr (von Krosigk et. al., 1992). GPe axon terminals targeted soma and proximal dendrites of SNr cells, while striatal axon terminals targeted distal dendrites of the

same SNr cells (von Krosigk et. al., 1992). Simultaneous anterograde and retrograde tracing and electron microscopy studies showed that parvicellular reticular formation (PcRT), a medullary reticular formation structure, was one of the brainstem nuclei that monosynapticly innervated facial motor neurons that might be involved in mastication (von Krosigk, et. al., 1992, Mogoseanu et. al., 1993, Mogoseanu et. al., 1994). Interestingly, PcRT received direct input from the output of basal ganglia, SNr (von Krosigk, et. al., 1992). Therefore, it is possible that VLS striatonigral and striatopallidal populations modulate orofacial movements by controlling the activity of single SNr cells that project onto orofacial brainstem regions in medullary reticular formation. Therefore, understanding the role of striatonigral and striatopallidal VLS populations in control of orofacial movements might help us understand the role of striatonigral and striatopallidal pathways in action selection.

We used transgenic mouse lines to target cortical (Emx1-Cre), striatonigral (FK150-Cre), and striatopallidal (Adora2a-Cre) populations. We used the same anterograde tracing technique described in chapter 2 (AAV2.2-EF1a-DIO-EYFP-WPRE, AAV2.2-EF1a-tdTomato-WPRE) for simultaneously labeling different motor cortical regions and to map their projections onto striatum. We expressed channel rhodopsin in striatonigral or in striatopallidal populations using AAV2.1-EF1a-DIO-Chr2 (H134R)-WPRE and used optogenetic approaches to stimulate different populations. We investigated the importance of aVLS in control of licking, in freely

moving mice and in mice trained to modulate licking as an instrumental response.

RESULTS

Projections from primary and secondary orofacial motor cortex converged on the ventrolateral striatum

Both primary and secondary motor cortical regions have been suggested to be involved in the preparation, initiation and execution of specific movements (Sul et al., 2011, Li et al., 2015). In particular, the orofacial motor cortex has been implicated in the control of licking (Komiyama et al., 2010, Zingg et al., 2014, Li et al., 2015). Therefore, we mapped the projections of primary and secondary orofacial motor cortex to determine the span of orofacial motor cortical input onto striatum. It has been suggested that in primate striatum the primary and secondary motor cortex projections follow a somatotopic organization, with secondary motor cortex projections targeting more medially (Nambu, 2011). However, to our knowledge, a detailed comparison of primary and secondary motor cortex projections onto the mouse striatum has not been performed.

Primary and secondary orofacial motor cortices of mice were defined based on their corticocortical input (Zingg et al., 2014). To map their projections onto the striatum, we simultaneously labeled primary and secondary orofacial motor cortices using AAV2.2-EF1a-DIO-EYFP-WPRE, AAV2.2-EF1a-DIO-tdTomato-WPRE which expressed EYFP and tdTomato fluorescent proteins, respectively. We observed that projections from both regions onto the striatum were rather

restricted to the ventrolateral region of striatum (Figure 3.1). Projections from both regions reached the VLS along the entire anterior-posterior axis of striatum (Figure 3.1). On the anterior and mid VLS, secondary motor cortex projections targeted more medially than primary motor cortex projections, similar to the projection patterns observed in primates (Nambu, 2011). However, primary and secondary orofacial motor cortex projections mostly overlapped in the posterior striatum.

Forelimb regions of the secondary motor cortex targeted dorsolateral striatum, dorsal to the regions targeted by orofacial regions of the secondary motor cortex.

Secondary motor cortex areas receive more associative input than primary motor areas (Zingg et al., 2014). Therefore, we expected that if orofacial and forelimb motor cortical inputs converge onto striatum, secondary motor cortical projections might have higher chance of convergence than primary motor cortical projections. We labeled forelimb secondary motor cortex and orofacial secondary motor cortex and mapped their projections onto striatum. In general, forelimb secondary motor cortex projections target dorsolateral striatum, a region dorsal to that targeted by orofacial secondary motor cortex (Figure 3.2).

These cortical regions were also defined based on their corticocortical projections (Zingg et al., 2014). There was some overlap in the anterior ventrolateral striatum, but projections from forelimb areas were still more dorsal than projections of orofacial areas. In the mid

and posterior striatum, projections were more segregated, with forelimb secondary motor cortex projections targeting DLS and orofacial secondary motor cortical projections targeting VLS (Figure 3.3).

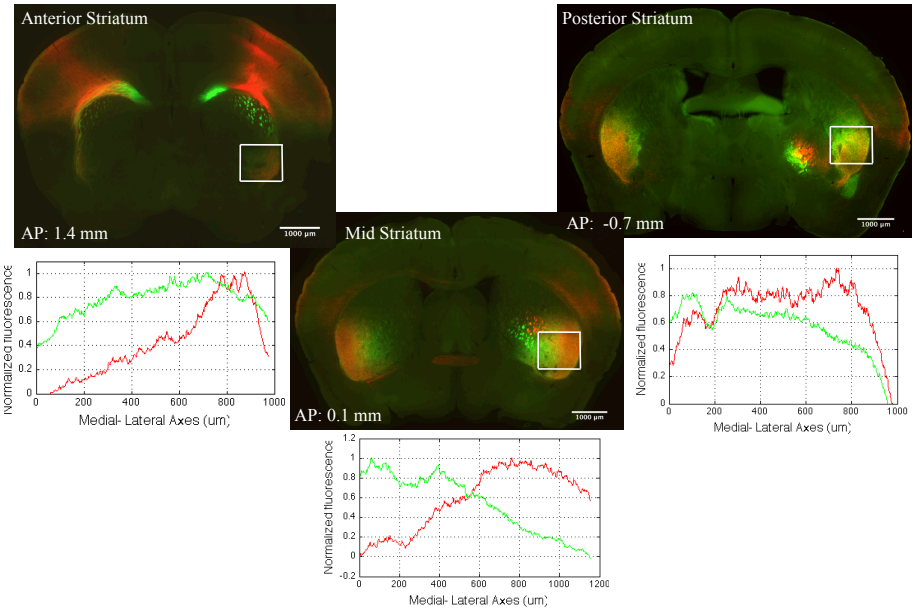

Figure 3.1| Primary- and secondary orofacial motor cortices projected on ventrolateral striatum (n=3). Primary orofacial motor cortex was labeled with viruses expressing tdTomato (AAV2.2-EF1a-DIO-tdTomato-WPRE) and secondary orofacial motor cortex was targeted with viruses expressing EYFP (AAV2.2-EF1a-DIO-EYFP-WPRE). Projections of these two populations targeted the VLS along the anterior-posterior axis of striatum.

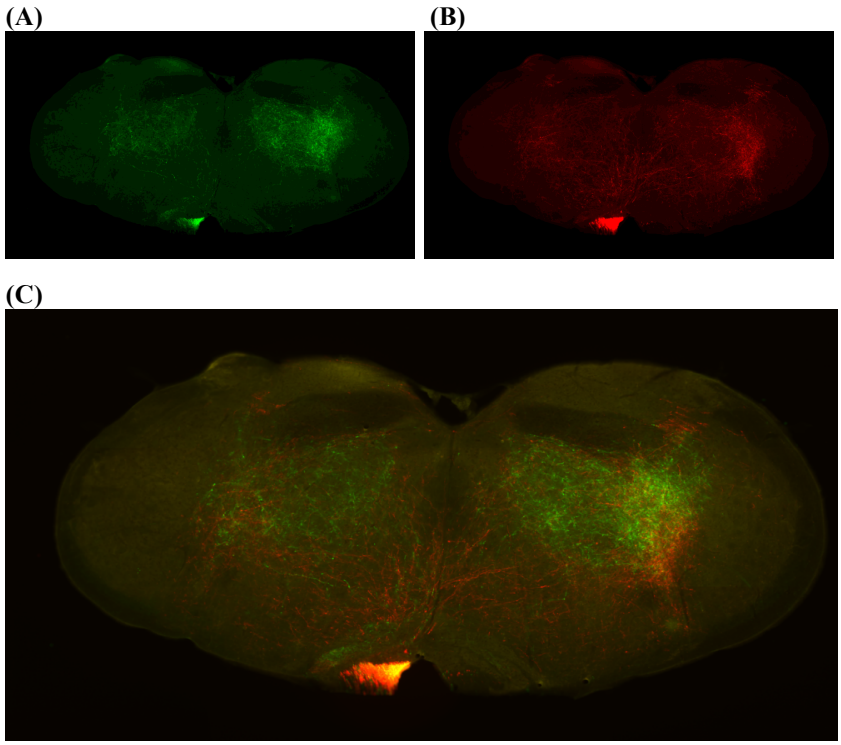

Figure 3.2| Simultaneously labeled, secondary orofacial and secondary forelimb motor cortex projections on brainstem reticular formation (n=2). Unilaterally labeled secondary orofacial motor cortex labeled with EYFP (A), and secordary forelimb motor cortex labeled with tdTomato (B) project on partially segregated regions of brainstem reticular formation. Spatial overlap of secondary orofacial and secordary forelimb motor cortex on brainstem reticular formation (C).

We observed that corticostriatal projection patterns on striatum of primates and mice showed similarities in two ways. First, orofacial motor cortex projections targeted more ventral compared to forelimb projections. Second, while both primary and secondary orofacial motor cortex projections targeted VLS, secondary orofacial motor cortex projections targeted more medial regions of VLS than primary orofacial motor cortex projections.

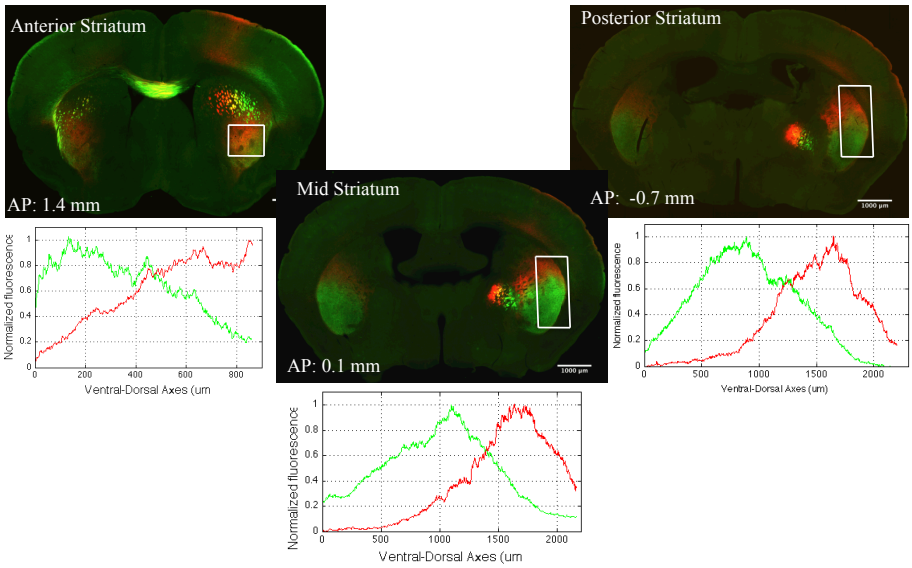

Figure 3.3| Secondary forelimb motor cortex projected dorsal to secondary orofacial motor cortex projections on striatum (n=2). Secondary orofacial motor cortex was labeled with viruses expressing EYFP (AAV2.2-EF1a-DIO-EYFP-WPRE) and secondary motor forelimb cortex was labeled with viruses expressing tdTomato (AAV2.2-EF1a-DIO-tdTomato-WPRE). Projections of these two populations diverged more in the mid and posterior striatum, and converged more in the anterior ventrolateral striatum.

In line with previous observations, these data suggest that ventrolateral striatum is the striatal region involved in orofacial motor control (Smith, et al., 1991, Ebrahimi et al., 1992, Hintiryan et al., 2016)

Optogenetic stimulation of striatonigral pathway aVLS induced orofacial movements while stimulation of striatopallidal pathway aVLS did not have an immediate motor effect.

We next examined if the striatal projection neurons in VLS were indeed involved in orofacial movements. To achieve this, we

expressed ChR2 in striatonigral and striatopallidal neurons in the VLS. The behavioral effects of optogenetic stimulations of different striatal populations were assessed using high-speed video recordings (60fps and 400fps) of freely moving mice in a small open field with a transparent floor. To perform automated high resolution, automated locomotion tracking the LocoMouse system was used (Figure 3.4, Figure 3.5, Machado, et al., 2015).

A small open field with transparent floor (25x18cm) was designed to permit visualization of the limbs and the mouth of the mice, (Figure 3). Mice were habituated to the open field for 2 days, with one session of 10 minutes per day. Stimulations of 5 seconds duration were performed at random times with a minimum interval of 2 minutes between stimulations for 30 min to 45 min long sessions, for 2-3 days after habituation. An infrared LED was used to indicate stimulation times as the videos were acquired.

Optogenetic stimulation of striatonigral and striatopallidal pathway aVLS populations were performed at 2, 5 and 10 Hz with 10ms pulses for 5 seconds durations. The effect of these stimulations on orofacial movements was assessed. The effect of these stimulations on orofacial movements specifically was investigated.

Striatonigral pathway aVLS stimulations induced head bobbing-like movements at 2Hz stimulations. 5Hz stimulations induced jaw movements. During 10Hz stimulations, mice stopped its ongoing movements, lowered its head and started licking. Striatopallidal pathway aVLS stimulations did not induce an immediate motor effect and did not induce consistent changes in the ongoing movement.

To examine the effect of these stimulations on orofacial movements and locomotion, we performed the same stimulations using the LocoMouse system (Machado et al., 2016, Figure 3.5). The LocoMouse system is composed of a narrow corridor and two boxes on both sides of the corridor. Side and bottom view of the mice during locomotion along the narrow corridor were projected on the same plane using a mirror with 45° angle (Machado, et al., 2016). Water deprived mice received water reward in both side boxes after each cross. Therefore, they learned to cross the corridor to receive water reward. Stimulations were performed in the middle of the corridor.

We are currently analyzing the primary effects of the stimulations on orofacial movements and limb movements, in collaboration with Neural Circuits and Behavior Laboratory at Champalimaud Center for the Unknown.

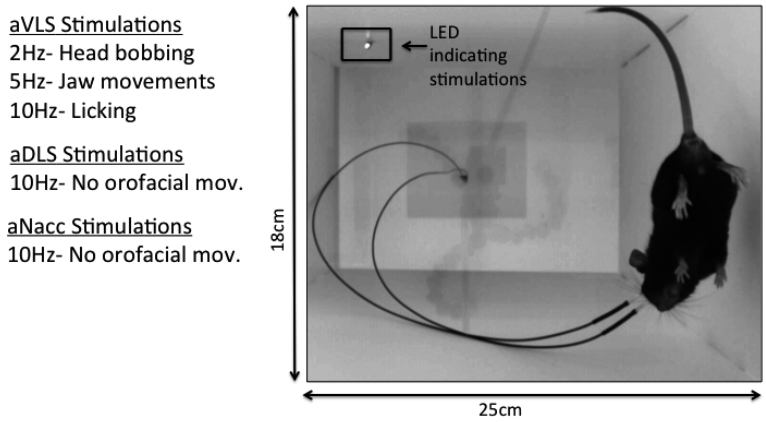

Figure 3.4 | Small open field with transparent floor was designed to observe the role of striatal different striatal populations on specific movements. A small open field (25cmX18cm) with transparent floor was used to observe the effect of striatal stimulations on specific movements in freely moving mice. An infrared LED was placed on the wall of the open-field to signal the stimulation times.

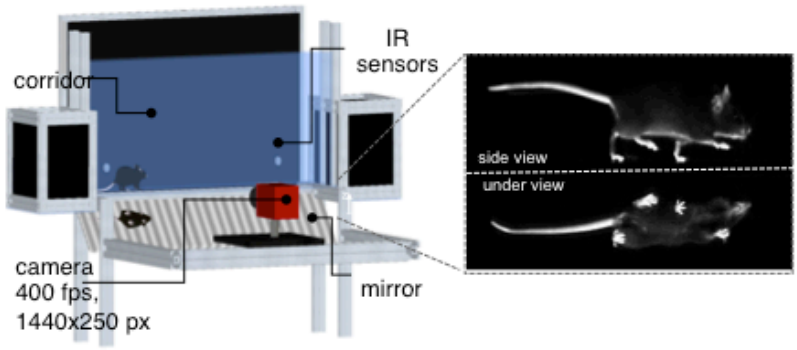

Figure 3.5| The LocoMouse setup was used to investigate the role of aVLS in orofacial movements and locomotion of freely moving mice. Two side boxes were connected by a glass corridor. Side and under image of the corridor was projected onto a single plane and recorded at 400fps. Limbs, nose and the tail could be tracked during locomotion for detailed analysis of circuit perturbations on specific locomotion parameters and orofacial movements.

The effect of 10Hz-5s stimulations on locomotion speed was assessed using a custom made tracking method described in Machado et al., 2016. Striatonigral pathway aVLS stimulations stopped locomotion; mice did not continue walking until the end of stimulation. Striatopallidal aVLS stimualtions did not change the locomotion speed (Figure 3.6).

It was previously shown that optogenetic stimulation of DMS striatonigral pathway induced locomotion and stimulations of DMS striatonigral pathway suppressed locomotion, without changing locomotion parameters such as stride-length and stance-width (Kravitz et al., 2010).

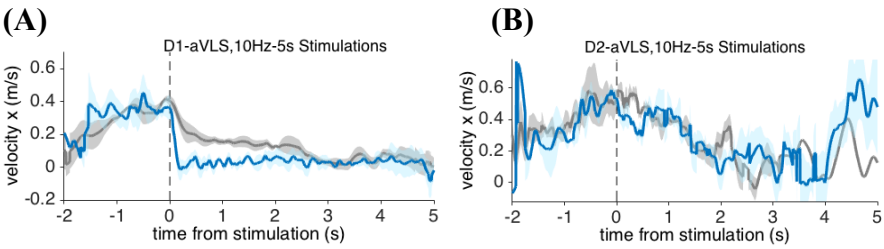

Figure 3.6 | Striatonigral aVLS stimulations reduces locomotion speed (n=4), while striatopallidal aVLS stimulations did not affect locomotion speed (n=4). (**A)** Striatonigral aVLS stimulations stopped locomotion at the onset of the stimulation for stimulated trials (blue). Non-stimulated trials (grey) also showed decrease in speed at the onset of the stimulation. We observed that mice learned the place for stimulation and spent more time exploring at the stimulation point in non-stimulated trials. (**B)** Striatopallidal aVLS stimulations did not show differences between stimulated (blue) non-stimulated trials (grey).

It will be interesting to see if manipulations of aDLS and aVLS, which are parts or sensory-motor striatum that receive specific motor input, would have an effect on specific locomotion parameters or in speed without changing the locomotion parameters.

Examining the role of aVLS in licking using an olfactory-guided operant task

After showing that aVLS stimulation induced orofacial movements and licking in freely moving naive mice, we asked if these circuits were important for modulating licking, under different conditions. In collaboration with Systems Neuroscience Laboratory at the Champalimaud Center for the Unknown, we modified a head fixed olfactory guided classical conditioning paradigm and developed a head fixed olfactory guided instrumental conditioning paradigm to condition mice to differentially modulate licking behavior in response

to 4 different odors that were associated with 4 different conditions. Go-odor indicated the availability of water after licking, no-go-odor indicated that air puff would be delivered if mice fails to suppress licking, wait odor indicated that a delayed water reward would be delivered if mice could withhold licking and wait for the go-tone, and neutral odor indicated no outcome (Matias et al., 2016, Cohen et al., 2012). Therefore, mice learned to lick to receive a water drop in response to the go-odor (Cuminaldehyde), to suppress licking to avoid an air puff in response to the no-go odor (Octanol) and to withhold licking to receive a delayed water reward in response to the wait odor (Carvone). In the fourth condition, the neutral odor, did not have an outcome. Therefore, mice learned not to lick in neutral trials (Limonene) (Figure 3.7).

All trials started with 1.5-3 second pretrial period (uniform probability distribution with 1.5-3 second borders), during which white noise was introduced. Odor was delivered for 1 second after the pretrial period followed by a 2 trace second (delay) period. It was previously shown that mice could make olfactory discrimination in <200ms (one sniff time), with >75% accuracy, even for odors that did not stimulate trigeminal nucleus (Resulaj et al., 2015). It was also suggested that reaction time was a function of decision time and a non-decision-sensory-motor delay (Resulaj et al., 2009). In many olfactory discrimination tasks a 1 second delay or trace period was used to allow mice >0.5s decision time (Uchida et al., 2003, Komiyama et al., 2010, Cohen et al., 2012). However, we used a 2 second trace period to permit longer decision times and to train the mice for longer lick bouts in go trials. A 1-7 second decision period

followed the trace period. Decision was the only period during which licking had outcomes depending on the trial type. The duration of the decision period changed between 1-7 seconds, as a Gaussian probability distribution with a mean of 4 seconds. The inter trial intervals were between 3-5 seconds (uniform probability distribution with 3-5 second borders). The durations of all the periods in the task were kept variable to impede mice from learning the timing of the events, and keep them engaged in the task (Figure 3.7).

Go trials started with a pretrial period followed by the go-odor and the trace period. Mice generally started licking during the trace period and the first lick in the decision period earned the mouse a 3 µl water drop with a simultaneous 100ms 6 KHz go tone. In no-go trials mice learned to stop licking in response to the no-go odor. If mice would lick during the decision period, the first lick triggered an air puff to the face for 100ms and a simultaneous 100 ms 10KHz no-go-tone. Wait trials were the most difficult trial type for water-deprived mice to learn. If they licked during the decision period, the inter-trial interval started and there was no outcome for the mice. However, if they waited for a variable duration between 3-5 seconds until they heard the go-tone, they received a 3 µl water drop. Therefore, this trial type required active waiting for the go-tone, i.e. active withholding of licking to receive reward (unlike actively avoiding punishment in no-go trials). Mice started with 5-10% correct wait trials with 1-2.5s waiting time. The waiting time was increased or decreased over 20-40 sessions for mice to learn to withhold licking until they heard a go tone for 50% of the wait trials. 20% of the water-deprived mice could not learn to wait for longer than 1s for

more than 15-30% of wait trials. Therefore, 80% of the mice learned the task with the desired percentage of correct trials.

This task allowed us to compare the effect of striatonigral and striatoplallidal aVLS stimulations on mice trained to lick to receive a water reward, to suppress licking to avoid punishment, to withhold licking to receive a delayed reward and in no-outcome conditions.

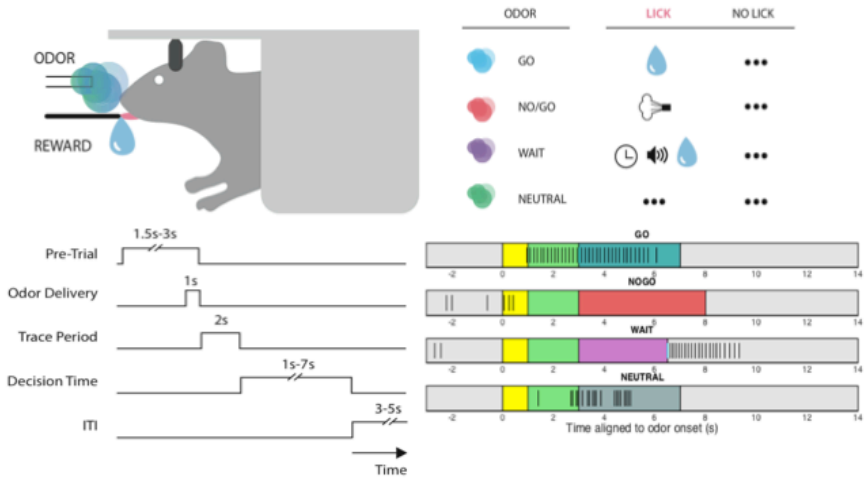

Figure 3.7 | Mice were trained in a head fixed-olfactory-guided operant task to modulate licking differently as an instrumental action in response to 4 different cues. Head fixed mice were trained to associate 4 different odors with 4 different outcomes and modulate licking according to these outcomes. Trials started with a variable duration pre-trial period followed by a 1 second odor delivery. The trace period was fixed for 2 seconds after odor delivery. The decision period was the only period during which licking had four different outcomes depending on the trial type. The order of the trial types were randomly changed with one limitation that the same trial type could not be introduced three times in a row.

Animals learned to perform olfactory guided-operant licking task

After the head-fixed habituation and pre-training period (mice learned to lick from a water port), mice learned the action-outcome associations for all 4 trial types in 25-45 sessions. Average reaction

time for go trials was 2.06± 0.92s for D1-Cre mice (FK150-Cre, n=4) and 1.44 ± 1.02s for D2-Cre mice (Adora2a-Cre, n=5) after the go odor onset. Therefore, mice started licking in trace period, in response to go odors.

D1-Cre and D2-Cre mice learned go trials with similar, 95.7±3.3 % (mean ± std %) and 96.5 ± 4.2 % (mean ± std %) correct trial performances respectively, and no-go trials with 95.9±2.1% (mean ± std %) and 96.42± 3.3% (mean ± std %) correct trial performance respectively (Wilcoxon rank sum test, $p>0.05$). Percentage of correct wait trial performances were lower within D1- Cre (FK150-Cre) mice, but were similar between D1- Cre (FK150-Cre) and D2-Cre (Adora2a-Cre) mice with 52.8±2.9% (mean ± std %) and 66.0±13.1% (mean ± std %) respectively (Wilcoxon rank sum test, $p>0.05$) (Figure 3.9).

After mice reached a stable performance for all trial types, optogenetic stimulations were performed for 5 sessions, over 5 days. Each session contained 200-250 trials per mice. Stimulations were performed at different times within a trial. Trace period stimulations were performed to determine the effect of stimulations 1s after odor onset and the licks induced in this period had no outcome. Decision stimulations were performed 3.5s after the odor onset and the licks induced in this period had outcome depending on the trial type.

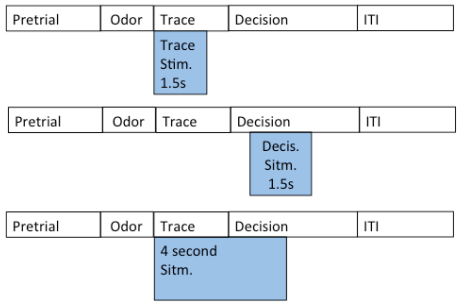

Figure 3.8 | Activity of striatal populations were manipulated using 10 different stimulation conditions. Optogenetic manipulations were performed at 2Hz, 5Hz and 10Hz, with 1.5 seconds durations starting at either 1 second after odor onset, I trace period, or 3.5 seconds after odor onset, in decision period. 2, 5 and 10Hz stimulations with 4 seconds duration were performed 1 second after odor onset.

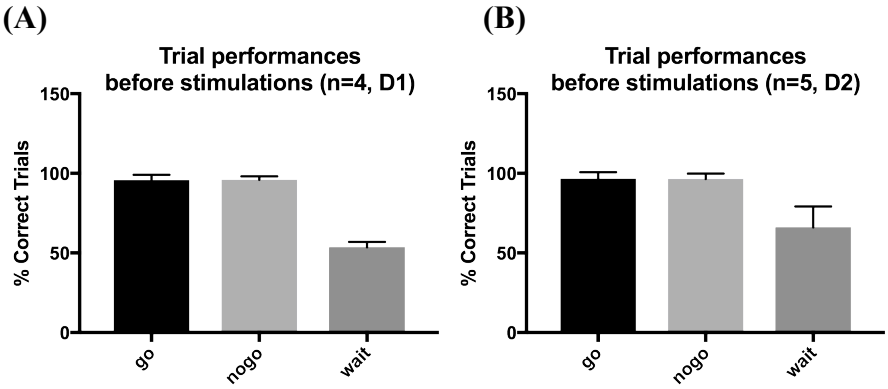

Figure 3.9 | Mice learned to modulate licking as an instrumental action in response to different odors. (A) D1-Cre (FK150-Cre) and **(B)** D2-Cre (Adora2a-Cre) mice reached to stable, close to 100% correct go trial and no-go trial performance. D1-Cre and D2-Cre mice reached similar percentages of correct in go, no-go and wait trials (Wilcoxon rank sum test, $p>0.05$). All mice were trained until they reach ≥50% correct wait trials. Optogenetic manipulations were performed 3 days after mice reached the desired stable performance.

4 seconds stimulations started 1s after the odor onset and continued 2s within the trace and 2 s within the decision period. Therefore, they were initiated early but still had the outcome of the trial.
Baseline firing rate of striatal neurons in awake mice was close to 5Hz (Costa et al., 2004, Tecuapetla et al., 2014). Therefore striatal populations were stimulated with lower than baseline frequency-2Hz, close to baseline frequency-5Hz and higher than baseline frequency-10Hz. Stimulations at frequencies of 2Hz, 5Hz and 10Hz – with 10ms pulses of blue light (473nm) and 2.5mW at the tip of the fiber – were used for all the stimulations. Therefore, 10 different stimulation conditions were randomly assigned to each trial; 2Hz-trace, 5Hz-trace, 10Hz-trace, 2Hz-decision, 5Hz-decision, 10Hz-decision, 2Hz-4s, 5Hz-4s, 10Hz-4s.

Stimulations of striatonigral aVLS population induced licking in every trial type

Striatonigral aVLS population stimulations induced licking in all trial types for 10Hz stimulations.
Liking induced by stimulations affected the trial performances and changed the average lick rates during stimulation compared to non-stimulated trials.
Lick rate histograms showed the change in lick rate across a trial. Lick rate histograms suggested that in go trials lick rates increased earlier for 5Hz and 10Hz stimulations compared to 2Hz and non-stimulated conditions (Figure 3.10 and Figure 3.11). In go trials lick rates during stimulation period did not change for 2Hz-4s, 5Hz-4s and 10Hz-4s stimulations compared to non-stimulated trials (2-way

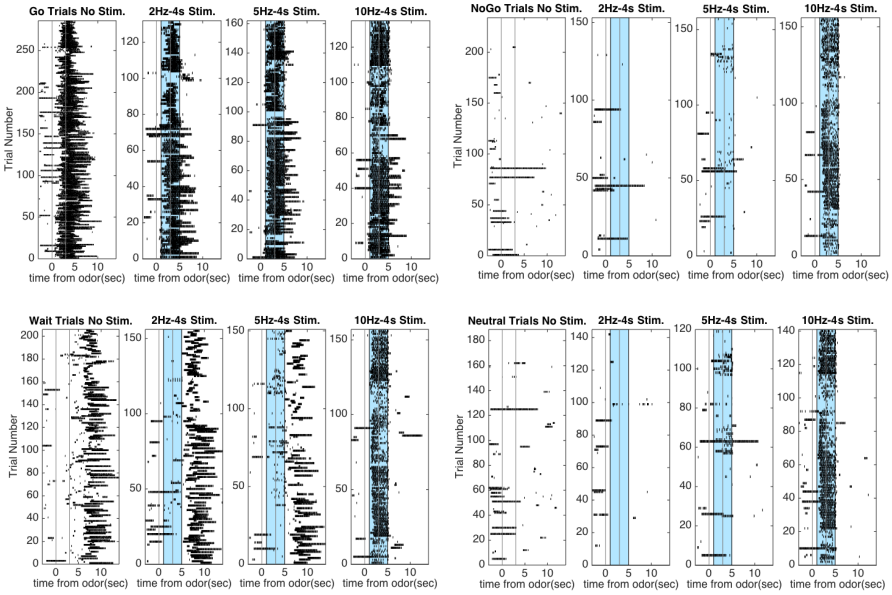

Figure 3.10| 4-seconds striatonigral pathway aVLS stimulations modulated licking for all trial types. Examples of single lick events across all trials and trial types, with no-stimulation and 2Hz-4s, 5Hz-4s, 10Hz-4s stimulated conditions were shown. 10Hz-4s stimulations increased lick rate in all trial types.

ANOVA, $p>0.05$). Average lick rates during 10Hz-4s stimulations increased for no-go, wait and neutral trials compared to non-stimulated trials (2-way ANOVA, $p=0.0001$, Dunnet's multiple comparison test, Figure 3.10 and Figure 3.11). 4 seconds stimulations did not change the percentage of correct go trials for any stimulation frequency compared to the non-stimulated trials (2-way ANOVA, $p>0.05$). 10Hz stimulations induced licks during the 4 seconds that stimulation was on. Therefore, 4 seconds stimulations induced licks during trace period and the first 2 seconds of the decision period in all trial types. 4 seconds stimulations decreased percentage of correct no-go trials for stimulations at 10Hz and 5Hz (2-way ANOVA, $p<0.05$, Dunnet's multiple comparison test), but not for 2Hz stimulation.

10Hz-4s stimulation decreased the percentage of correct wait trials, but 5Hz-4s, and 2Hz-4s stimulations did not (2-way ANOVA, $p<0.05$, Dunnet's multiple comparison test, Figure 3.11).

During 4 seconds stimulations, lick rate increased for 10Hz stimulations. During these stimulations mice were forced to lick 2 seconds in the trace period and 2 seconds in the decision period for all trial types. Mice were forced to lick to receive water in go trials, to lick to receive air puff in no-go trials, and to lick to forfeit delayed reward delivery in wait trials. 4 seconds stimulations also forced the mice to lick for no outcome during stimulation.

Lick rate histograms of trace period stimulated conditions show that, similar to 4seconds stimulated conditions, lick rate increased earlier for 5Hz and 10Hz stimulated trials compared to 2Hz stimulated and non-stimulated trials. Only 10Hz stimulations increased lick rate for all trial types (Figure 3.12).

Trace stimulations increased the lick rate in go trials during trace stimulation, compared to non-stimulated trials for 5Hz and 10Hz stimulations (2-way ANOVA, $p<0.05$, Dunnet's multiple comparison test), but not for 2Hz stimulations (Figure 3.12). Trace stimulations during no-go, wait and neutral trials increased lick rate only for 10Hz stimulations compared to non-stimulated trials (2-way ANOVA, $p<0.05$, Dunnet's multiple comparison test, Figure 3.12). Trace stimulations did not change the percentage of correct trials regardless of the stimulation frequency for any trial types (2-way ANOVA, $p>0.05$). After the 10Hz stimulations lick rates went back to baseline. Mice were able to recover from the effect of stimulation within the 0.5 second before the decision period started (Figure 3.12).

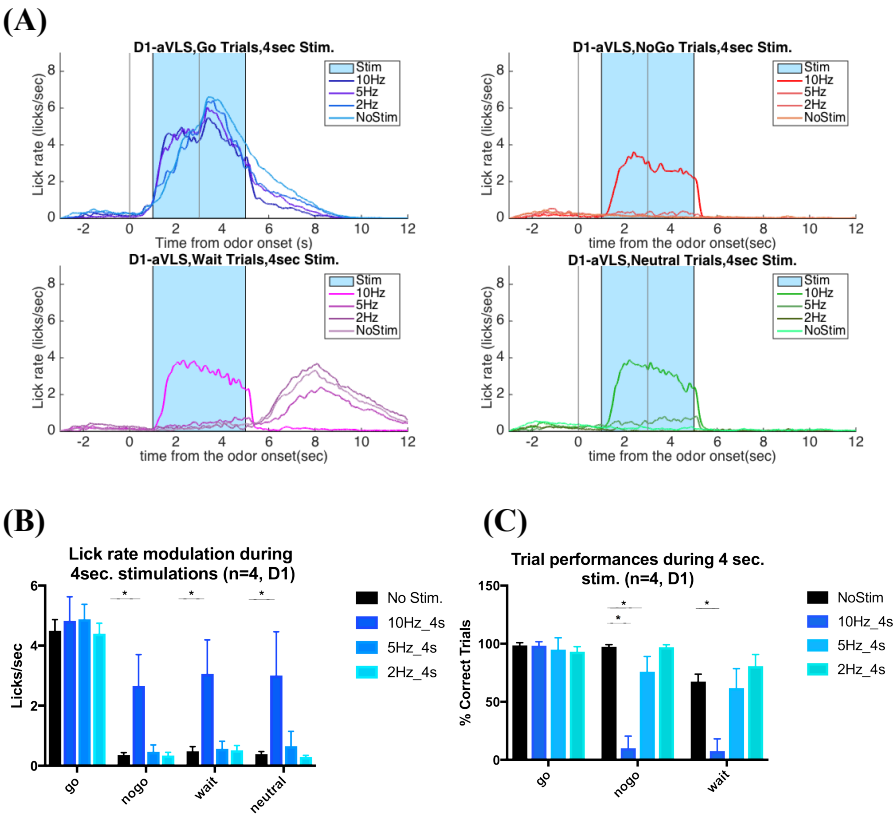

Figure 3.11 | Direct pathway aVLS stimulations for 4 seconds, induced licks and changed the percentage of correct trials for different trial types (n=4). **(A)** Lick rate histograms showed the lick rate changed during 4 seconds stimulations for all trial types. **(B)** Lick rate during stimulation period increased only for 10Hz-4s stimulations in no-go (Dunnet's multiple comparison test, p=0.0001), wait (Dunnet's multiple comparison test, p=0.0001) and neutral (Dunnet's multiple comparison test, p=0.0001) trials compared to non-stimulated trials. **(C)** 4 second stimulations changed the percentage of correct no-go, wait and neutral trials. Percentage of correct go trials did not change for trace period stimulated trials. Percentage of correct no-go trials decreased for 10Hz-4s stimulated trials (Dunnet's multiple comparison test, p=0.0001) and for 5Hz-4s (Dunnet's multiple comparison test, p=0.004) stimulated trials. Percentage of correct wait trials only decreased for 10Hz-4s stimulated trials (Dunnet's multiple comparison test, p=0.0001).

Lick rate histograms suggested that lick rates did not change in go trials for any stimulation frequency during decision period stimulations. Lick rate histograms also suggested that lick rates increased for no-go, wait and neutral trials during decision period stimulations. Similar to other stimulation types only 10Hz stimulations increased lick rate during decision period stimulations, for all trial types (Figure 3.13).

In line with lick rate histograms, decision stimulations did not change lick rate for go trials for any stimulation frequency (2-way ANOVA, $p>0.05$). Similar to trace stimulations, decision stimulations increased lick rate during stimulation for no-go, wait and neutral trials, only for 10Hz stimulations compared to non-stimulated trials (2-way ANOVA, $p<0.05$, Dunnet's multiple comparison test, Figure 3.12), and not for 2Hz- or 5Hz-decision period stimulations.

Decision stimulations did not change the percentage of correct go trials (2-way ANOVA, $p>0.05$). No-go (2-way ANOVA, $p<0.05$, Dunnet's multiple comparison test) and wait (2-way ANOVA, $p<0.05$, Dunnet's multiple comparison test) trial performances decreased for 10Hz-decision period stimulations, but not for 5Hz- or 2Hz-decision period stimulations (Figure 3.13).

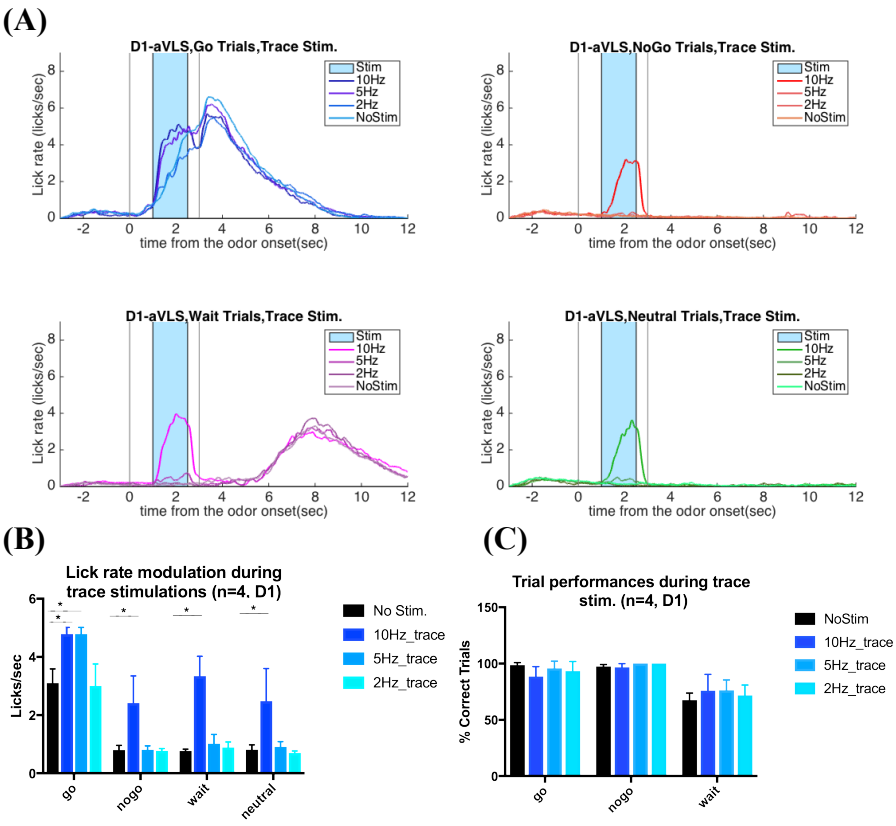

Figure 3.12 | Direct pathway aVLS stimulations for 1.5 seconds stimulations during trace period, induced licks, but did not change the percentage of correct trials for different trial types (n=4). **(A)** Lick rate histograms showed the lick rate changes during 1.5s trace stimulations for all trial types**. (B)** Lick rate was modulated during 10Hz-trace period stimulations. Lick rate increased during 10Hzand 5Hz trace stimulations in go trials (Dunnet's multiple comparison test, p=0.0001). In no-go trials (Dunnet's multiple comparison test, p=0.0002), wait trials (Dunnet's multiple comparison test, p=0.0001), and neutral trials (Dunnet's multiple comparison test, p=0.0001) only 10Hz-trace stimulations increased lick rates during stimulations, compared to non-stimulated trials. **(C)** Trace stimulations did not change the percentage of correct go, no-go and wait trials compared to non-stimulated trials for any stimulation frequency.

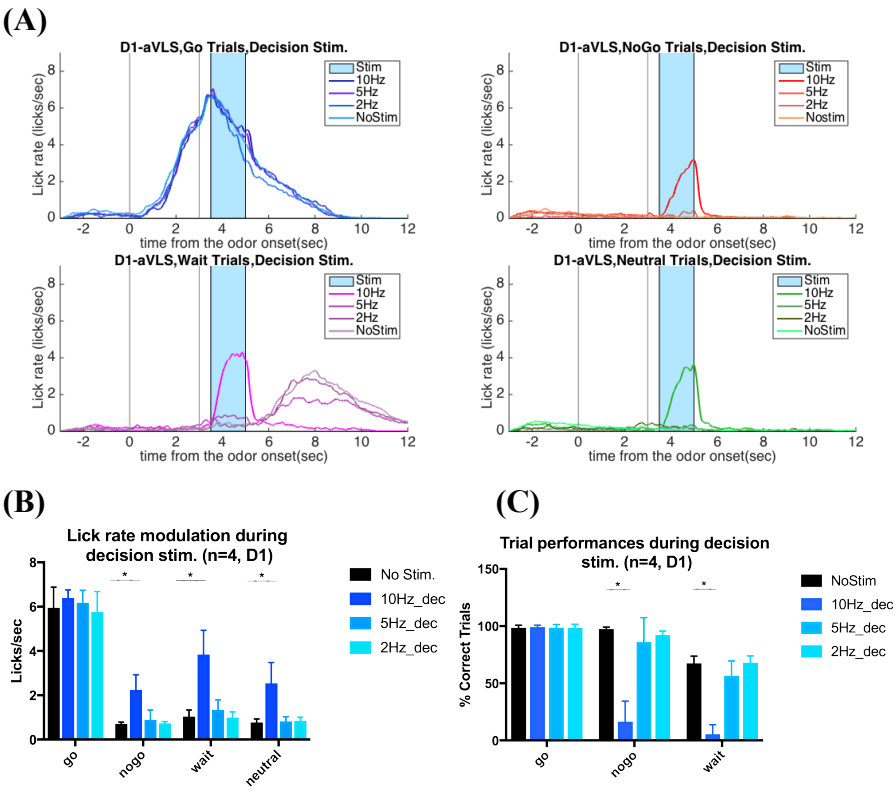

Figure 3.13 | Direct pathway aVLS stimulations for 1.5 seconds stimulations during decision period, induced licks, and changed the percentage of correct trials for different trial types (n=4). **(A)** Lick rate histograms showed the lick rate change during 1.5s decision period stimulations for no-go, wait and neutral trials**.** **(B)** Lick rate did not change during decision period stimulations for go trials. In no-go trials (Dunnet's multiple comparison test, p=0.0001), wait trials (Dunnet's multiple comparison test, p=0.0001), and neutral trials (Dunnet's multiple comparison test, p=0.0001) trials only 10Hz-decision period stimulations increased lick rates, compared to non-stimulated trials. **(C)** Decision stimulations did not change the percentage of correct go trials, but decreased the percentage of correct no-go and wait trials compared to non-stimulated trials for 10Hz-decision period stimulations (Dunnet's multiple comparison test, $p<0.05$).

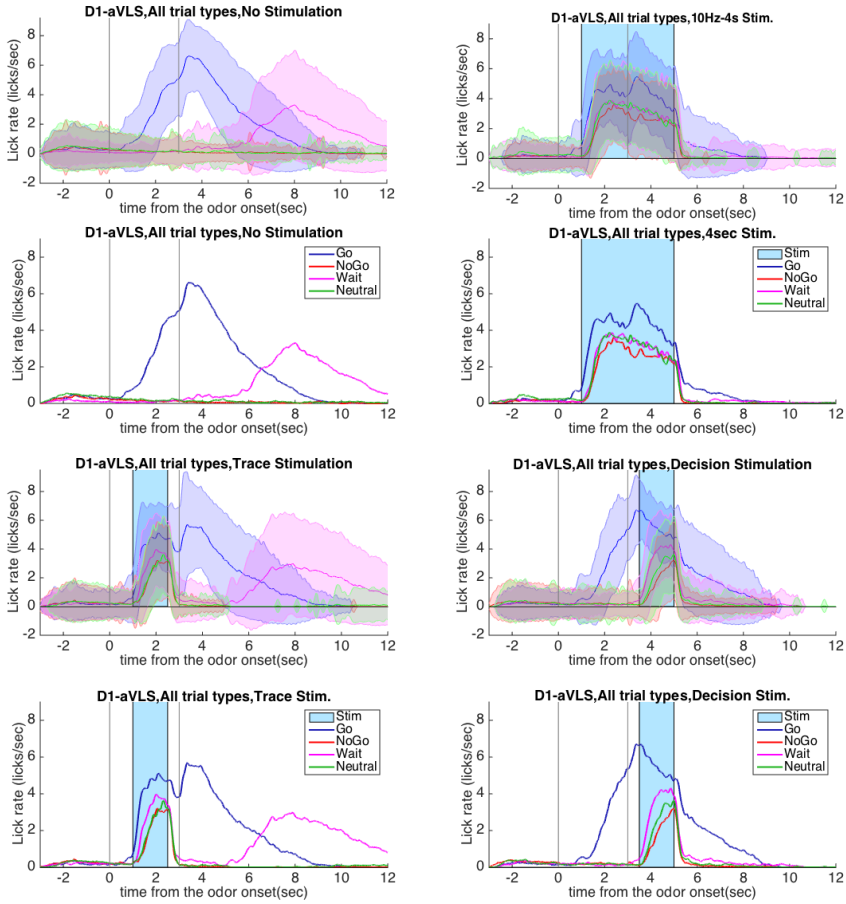

Figure 3.14 | Lick rate histograms suggested trial type dependent effect of 10Hz stimulations, for all stimulation types. Lick rate histograms suggested that during 4s stimulations, trace period stimulations and decision period stimulations lick rates increased differently in go, no-go, wait and neutral trials. During stimulations lick rates seem highest for go trials, lowest for no-go trials and intermediate for wait and neutral trials.

In addition to the observations above, lick rate histograms suggested that in non-stimulated trials lick rate was modulated when water was delivered. Non-stimulated trials showed lower anticipatory lick rate during trace periods and after the water delivery with first lick in the

decision period, mice showed a slight increase in lick rate. Therefore, during go trials mice modulated their lick rate in response to water delivery. Trace and 4 seconds stimulations during go-trials seemed to reduce the animals' ability to modulate lick rate in response to water (Figure 3.11 and Figure 3.12).

Stimulations of striatonigral aVLS population induced licking differently in go and no-go trials

We asked if the striatonigral aVLS population stimulations induced licking differently for different trial types. Therefore, we compared if direct striatonigral aVLS manipulations that induced licking were modulated differently by the context, in each trial type.

Lick rate histograms for 10Hz stimulations during trace period, 4s stimulation period and decision stimulation period suggested that lick rates during stimulation was highest for go trials and lowest for no-go trials, and intermediate for wait trials (Figure 3.14).

We compared the average lick rates for different stimulation times for stimulated and non-stimulated trials for different trial types, across animals (Figure 3.15, n=4). We found that for 10Hz-4s stimulations lick rates during stimulation in go trials, were higher than average lick rates for no-go trials (Friedman test, Dunnet's multiple comparisons test, $p=0.01$). 10Hz-4s stimulations increased average lick rates for no-go, wait and neutral trials. Average lick rates during 10Hz-4s stimulations were not different between no-go, wait and neutral trials, or between go, wait and neutral trials (Friedman test, $p>0.05$).

During 10Hz-trace stimulations again lick rates were higher for go trials compared to no-go trials (Friedman test, Dunnet's multiple

comparisons test, p=0.01, Figure 3.15). Lick rates during 10Hz-trace stimulations were not different between no-go, wait and neutral trials, or between go, wait and neutral trials (Friedman test, p>0.05). During 10Hz-decision stimulations, similar to other 10Hz stimulations, lick rates were higher for go trials compared to no-go trials (Friedman test, Dunnet's multiple comparisons test, p=0.006). Average lick rates during 10Hz-decision stimulations were not different between no-go, wait and neutral trials, or between go, wait and neutral trials (Friedman test, p>0.05, Figure 3.15).
Therefore, during 10Hz-4s, 10Hz-trace and 10Hz-decision stimulations average lick rates in go trials were different than lick rates in no-go trials. Mice were able to suppress the effect of direct pathway aVLS stimulations to avoid punishment, but not to receive delayed reward or in the absence of any outcome (Figure 3.15). Therefore, the effects of striatonigral aVLS stimulations were modulated differently by the context, in different trials.

Stimulations of striatonigral aVLS population facilitated initiation of licking in go trials

To evaluate if direct pathway aVLS stimulations facilitated the initiation of licking in go trials, as suggested by the lick rate histograms, we separated the trials during which mice did not initiate licking before the stimulation onset (77% of non-stimulated trials, 84% of 10Hz-4s stimulated trials, 85% of 5Hz-4s stimulated trials, 84% of 2Hz-4s stimulated trials, 77% of 10Hz-1.5s trace period stimulated trials, 81% of 5Hz-1.5s trace period stimulated trials, 81%

of 2Hz-1.5s trace period stimulated trials). We calculated the average delay to start licking for each condition, across animals.

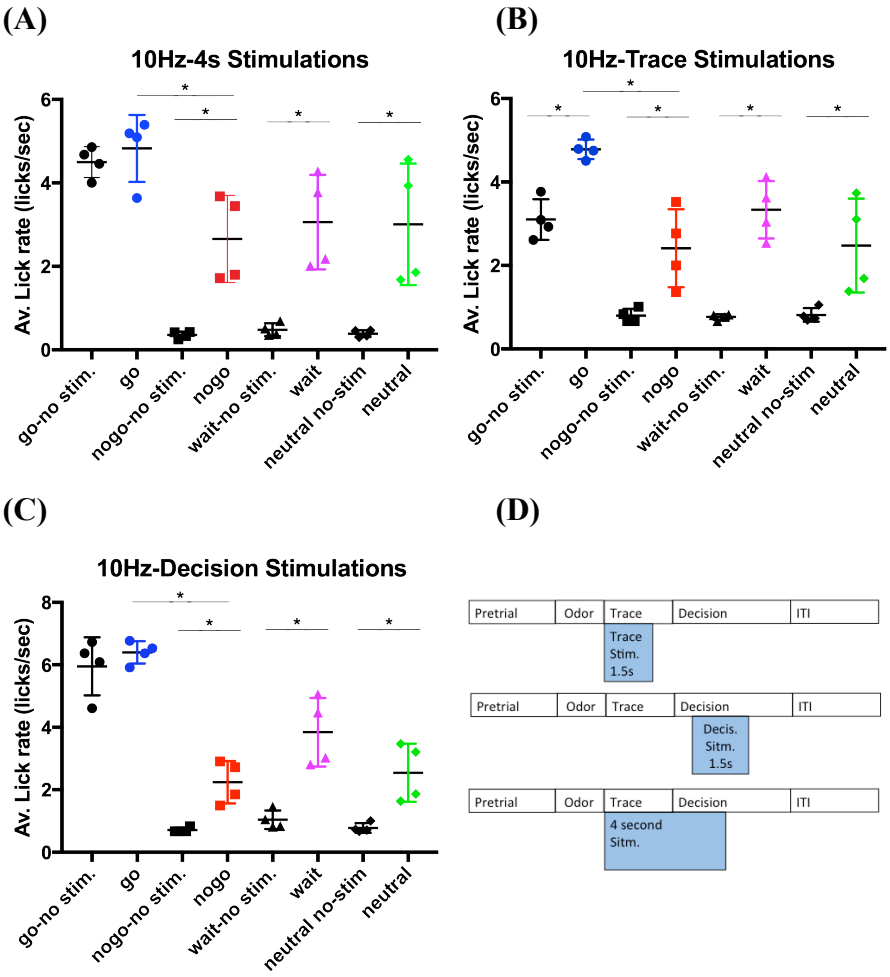

Figure 3.15| Average number of licks during striatonigral-aVLS stimulations, across animals (n=4). (A) Average lick rate during 10Hz-4s stimulations were only different between go and no-go trials (Friedman test, Dunnet's multiple comparison test, p=0.01). **(B)** Average lick rate during 10Hz trace stimulations were only different between go and no-go trials (Friedman test, Dunnet's multiple comparison test, p=0.006). **(C)** Average lick rate during 10Hz decision stimulations were only different between go and no-go trials (Friedman test, Dunnet's multiple comparison test, p=0.0061). **(D)** Schematic of the stimulation conditions within a trial.

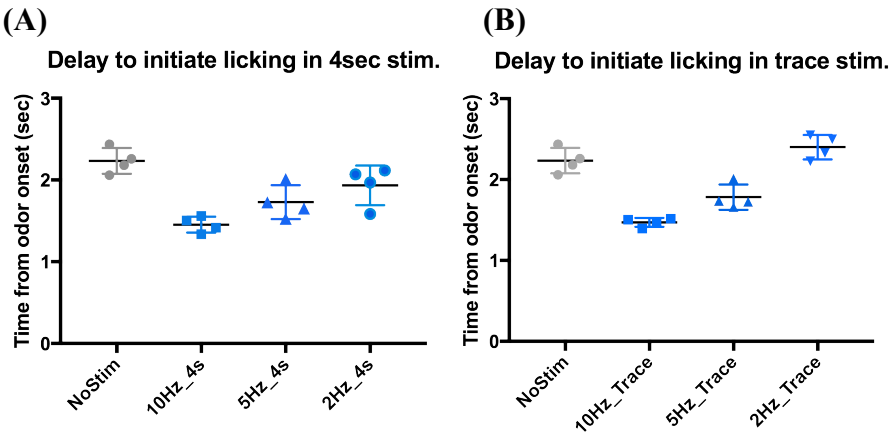

Figure 3.16 | The effects of striatonigral-aVLS stimulations on initiation of licking in go trials, across animals (n=4) (A) 10Hz-4s stimulations, but not 5Hz-4s and 2Hz-4s stimulations, facilitated initiation of go-lick bouts by reducing the delay to initiate (Friedman test, p=0.0009, Dunnet's multiple comparison test, p=0.003). (**B)** 10Hz-trace stimulations, but not 5Hz-trace and 2Hz-trace stimulations, facilitated initiation of go-lick bouts by reducing the delay to initiate (Friedman test, p=0.0009, Dunnet's multiple comparison test, p=0.04).

Only 10Hz stimulations facilitated initiation of licking (go-lick-bouts) compared to the non-stimulated trials, for both 4s stimulations (Friedman test, p=0.003) and trace stimulations (Friedman test, p=0.04, Figure 3.16).

Figure 3.17 shows the distribution of lick frequencies, during 10Hz 4s stimulation, in different trial types. In 97% (151/157) of go trials more than one lick was induced, with lick rate 5.97 ± 1.66 lick/sec (mean ± standard deviation). In 93% (162/174) of wait and 96% (165/175) of neutral trials more than one lick was induced, with lick rates 4.96± 1.82 and 4.95 ± 1.74 lick/sec respectively In go trials that are not stimulated mice, within the same time window, mice licked in

96% (343/356) of the trials with average rate of 6.69 ± 1.34 licks/sec. However, in nogo trials stimulations induced more than one lick only in 88% (148/167) of the trials with lick rate 4.64 ± 1.89 licks/sec. These results suggest that stimulations in go trials facilitate initiation (Figure 3.16) but reduce the average licking rate (Figure 3.17). Therefore, optogenetic activation of VLS direct pathway facilitated initiation but interfered with natural licking in go trials. Stimulations also induced licking at around 5 licks/sec while natural licking was around 7 licks/sec. It is possible that direct pathway stimulation itself is sufficient to induce licking but it is not sufficient to activate natural consumatory licking pattern, independent of conditions. We observe trial type modulation of indiced licking frequency. It is possible that stronger activations of VLS direct pathway might activate downstream licking CPG's stronger and induce licking at 7 licks/sec independent of condition. (We are using higher frequency stimulations to test this possibility.)

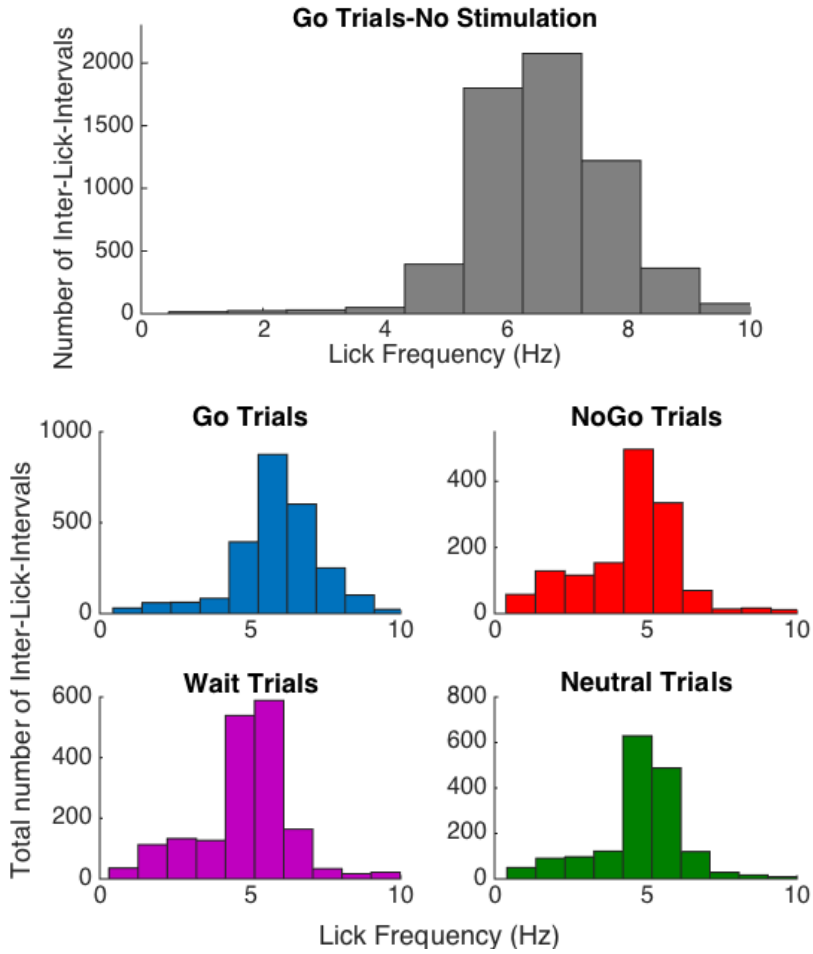

Figure 3.17| Distributions of lick frequencies, during 10Hz-4s stimulations in different trial types (n=4). In go trials average lick frequency during 10Hz-4s stimulations is 5.97 ± 1.66 licks/sec, in nogo trials 4.64 ± 1.89 licks/sec in wait trials it is 4.96 ± 1.82 licks/sec, and in neutral trials 4.95 ± 1.74 licks/sec. While in go trials that are not stimulated mice lick at average rate 6.69 ± 1.34 licks/sec within the same time window.

Stimulations of striatopallidal aVLS population stopped licking in go trials

Striatopallidal aVLS population stimulations stopped or delayed licking in all trial types. Lick rate histograms suggested that lick rates were reduced for Striatopallidal aVLS stimulations for 4 second, during go trials gradually, depending on the stimulation frequency (Figure 3.19). We also observed that at the stimulation-off time few licks were induced in no-go, wait and neutral trials (Figure 3.18).
In line with the observations from the lick rate histograms, we found that in go trials, 4s stimulations decreased lick rate for 2, 5 and 10Hz stimulations (2-way ANOVA, Dunnet's multiple comparisons test, $p=0.0001$). Lick rates during stimulations did not change for no-go, wait and neutral trials for any frequency of stimulation (2-way ANOVA, $p>0.05$). In no-go, wait and neutral trials it was not possible to see reduction in lick rates since the baseline conditions involved close to zero lick rates (Figure 3.18-19).

10Hz-4s stimulations reduced the percentage of correct go trials compared to non-stimulated trials (2-way ANOVA, $p<0.05$). Mice stopped licking during stimulations. However after stimulation they were able to lick within the variable decision period (1-7sec) and consume water. Therefore, the percentage of correct go trials did not decrease sharply. The percentage of correct no-go trials only decreased for 5Hz stimulations (2-way ANOVA, Dunnet's multiple comparisons test, $p=0.01$).

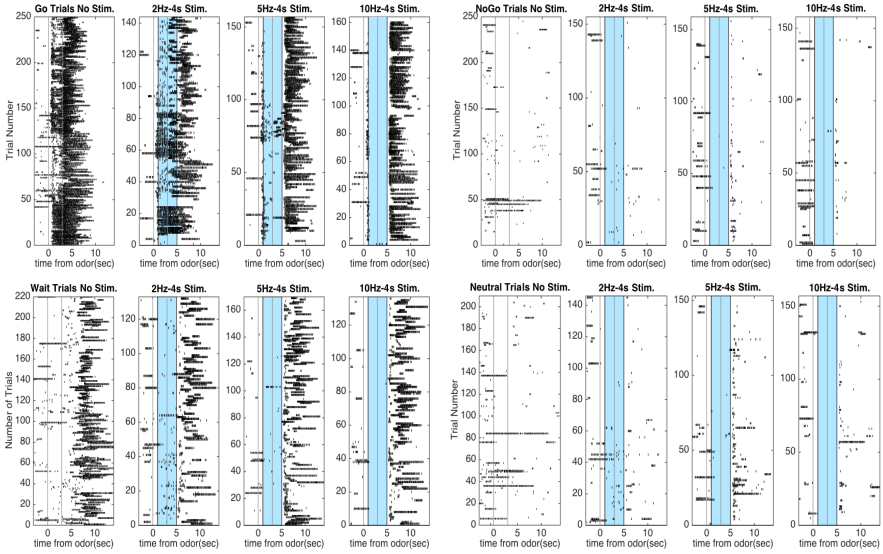

Figure 3.18| 4-seconds striatopallidal pathway aVLS stimulations paused licking for all trial types. Examples of single lick events across all trials and trial types, with no-stimulation and 2Hz-4s, 5Hz-4s, 10Hz-4s stimulated conditions were shown. 10Hz-4s stimulations paused licking in all trial types.

The percentage of correct no-go trials might be reduced due to the stimulation-off effect. This effect of indirect pathway cells was reported in other studies where optogenetic activation of indirect pathway was performed (Kravitz et al., 2012). The offset effects of indirect pathway optogenetic stimulations observed in our experiments were smaller than reported effects (Kravitz et al., 2012). Stimulation-off effect was also observed in wait and neutral trials. Therefore reduction in the percentage of correct wait trials was also observed for these trial types. Interestingly, percentage of correct wait trials decreased for 2Hz and 5Hz, but not for 10Hz stimulations (2-way ANOVA, Dunnet's multiple comparisons test, 2Hz-p=0.001, 5Hz-p=0.0003, Figure 3.19).

Lick rate histograms for trace period stimulated trials suggested similar effects to 4s stimulated trials, such that lick rates seemed to be reduced only in go trials gradually depending on the stimulation frequency (Figure 3.19). When we compare lick rates during trace period stimulations we saw that lick rate decreased for 2, 5and 10Hz stimulations (2-way ANOVA, Dunnet's multiple comparisons test, 2Hz and 5Hz- p=0.0001, 10Hz-p=0.0004, Figure 3.20). Lick rates during trace stimulations did not change for no-go, wait, and neutral trials for any stimulation frequency (2-way ANOVA, $p>0.05$, Figure 3.20).

Stimulations during the 1.5s trace period did not change the percentage of correct go and no-go trials for none of the stimulation frequencies (2-way ANOVA, $p>0.05$). The offset effect of stimulation was observed for trace stimulations. However, it did not affect the percentage of correct trials. Therefore, trace stimulations did not change the percentage of correct no-go trials. However, the above statement might not be true for wait trials since the percentage of correct wait trials was reduced compared to non-stimulated wait trials, for stimulations at all frequencies (2-way ANOVA, Dunnet's multiple comparisons test, 2Hz-p= 0.0002, 5Hz-p=0.0007, 10Hz-p=0.0001, Figure 3.20).

Lick rate histograms suggested a gradual decrease in lick rates during decision period stimulations in go trials and no change in lick rate in other trial types for any stimulation frequency (Figure 3.21). When we compared average lick rates, we saw that go lick rates decreased for 5Hz and 10Hz stimulations but not for 2Hz stimulations (2-way ANOVA, Dunnet's multiple comparisons test, p=0.001). No change

in lick rates during decision period stimulations in no-go, wait and neutral trials was observed (2-way ANOVA, $p>0.005$, Figure 3.21). Stimulations during decision period did not affect the percentage of correct go trials for any stimulation frequency (2-way ANOVA, $p>0.05$). In most of the go trials, water was already consumed for 0.5sec before the stimulation onset. Therefore, even though decision stimulations stopped licking in go trials, the percentage of correct go trials was not affected by these stimulations. In no-go and wait trials, 5 and 10Hz stimulations, but not 2Hz stimulations reduced the percentage of correct trials compared to non-stimulated trials (2-way ANOVA, Dunnet's multiple comparisons test, nogo-5Hz $p=0.005$, nogo-10Hz, $p=0.01$, wait-5Hz $p=0.0001$, wait-10Hz $p=0.0009$, Figure 3.20).

Lick rate histograms showed the average effect of striatopallidal pathway aVLS 10Hz stimulations on all trials, for all trial types (Figure 3.20, 3.21). When we compared the effect of 10Hz stimulations on different trial types we saw that indirect pathway aVLS stimulations stopped licking during stimulations independent of trial type and independent of the stimulation time in the trials. Gradual decrease in lick rate was observed in go trials depending on stimulation frequency. Increase in lick rates at the offset of stimulations was observed in no-go, wait and neutral trials (Figure 3.21, 3.22). Lick rate histograms also suggested that stimulation-off effect might show differences between trial types (Figure 3.21, 3.22).

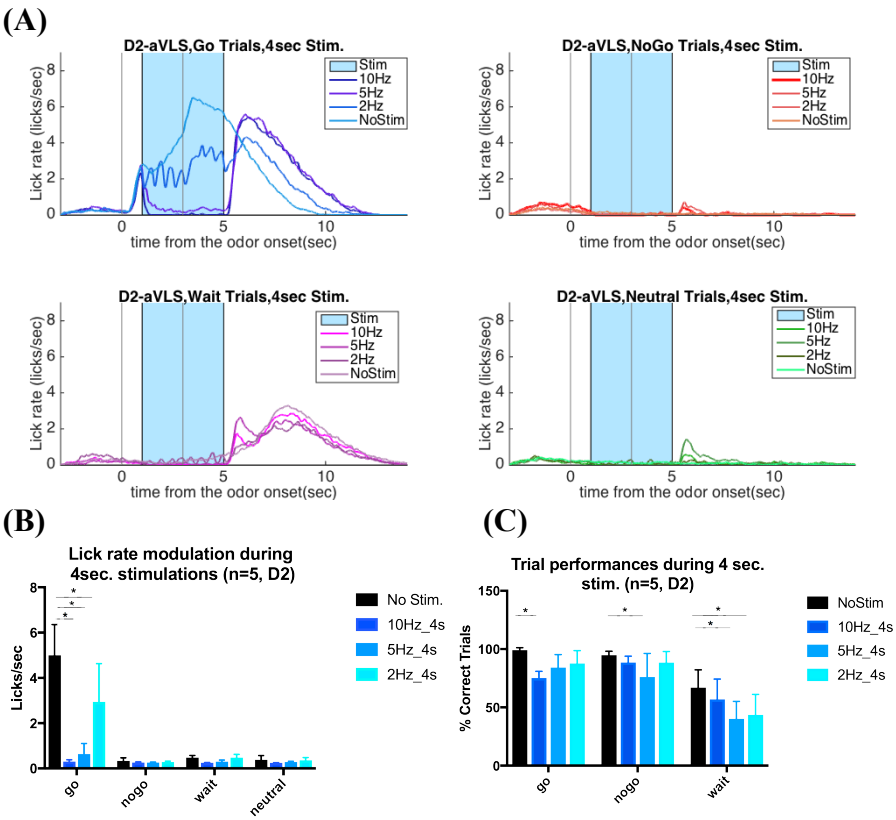

Figure 3.19| Indirect pathway aVLS stimulations for 4s, stopped licking and changed the percentage of correct trials for different trial types (n=5). **(A)** Lick rate histograms showed the lick rate change during 4 seconds stimulations for all trial types**. (B)** Lick rates decreased gradually during 10Hz-4s, 5Hz-4s and 2Hz-4s stimulations in go trials (Dunnet's multiple comparison test, p=0.0001). Lick rates during stimulation did not change in no-go, wait and neutral trials compared to non-stimulated trials. **(C)** Percentage of correct go trials decreased for 10Hz-4s stimulations (Dunnet's multiple comparison test, p=0.0012). Percentage of correct no-go trials decreased only for 5Hz-4s stimulations (Dunnet's multiple comparison test, p=0.01), and percentage of correct wait trials decreased for 5Hz-4s (Dunnet's multiple comparison test, p=0.0003), and 2Hz-4s stimulations (Dunnet's multiple comparison test, p=0.0014).

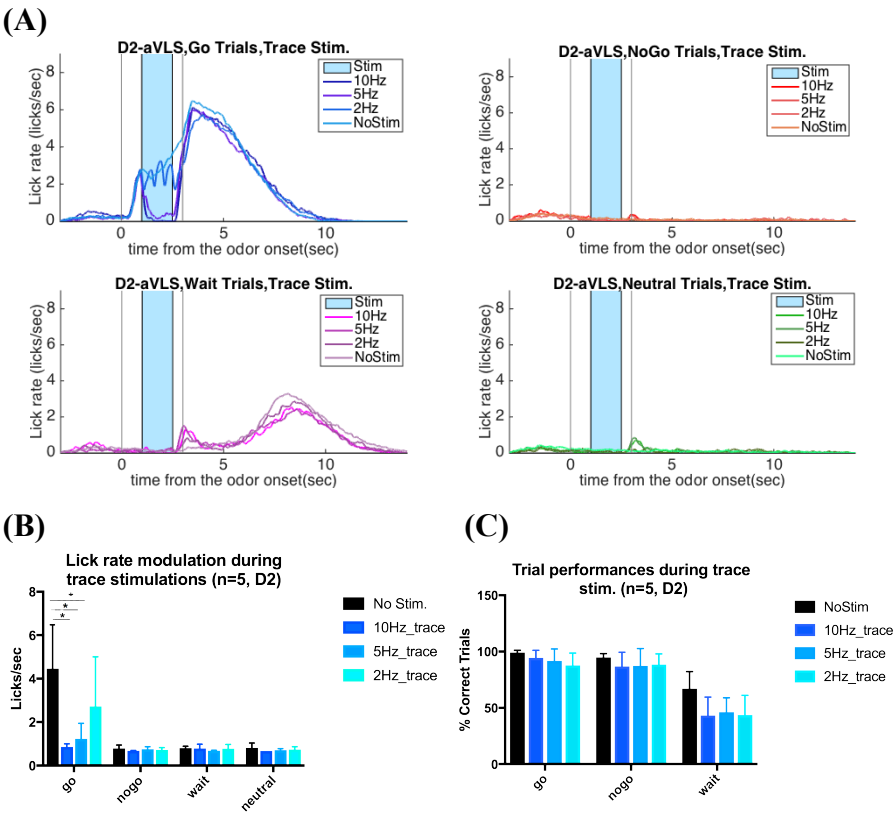

Figure 3.20 | Indirect pathway aVLS stimulations for 1.5 s during trace period, reduced lick rate, but did not change the percentage of correct trials for different trial types (n=5). (**A)** Lick rate histograms showed the lick rate change during 1.5s trace period stimulations for all trial types**. (B)** Lick rates decreased during 10Hz-trace (Dunnet's multiple comparison test, p=0.0001), 5Hz-trace (Dunnet's multiple comparison test, p=0.0001) and 2Hz-trace (Dunnet's multiple comparison test, p=0.0004) period stimulations. Lick rates during stimulation did not change in no-go, wait and neutral trials for any stimulation frequency. **(C)** Trace stimulations did not change the percentage of correct go, no-go and wait trials compared to non-stimulated trials.

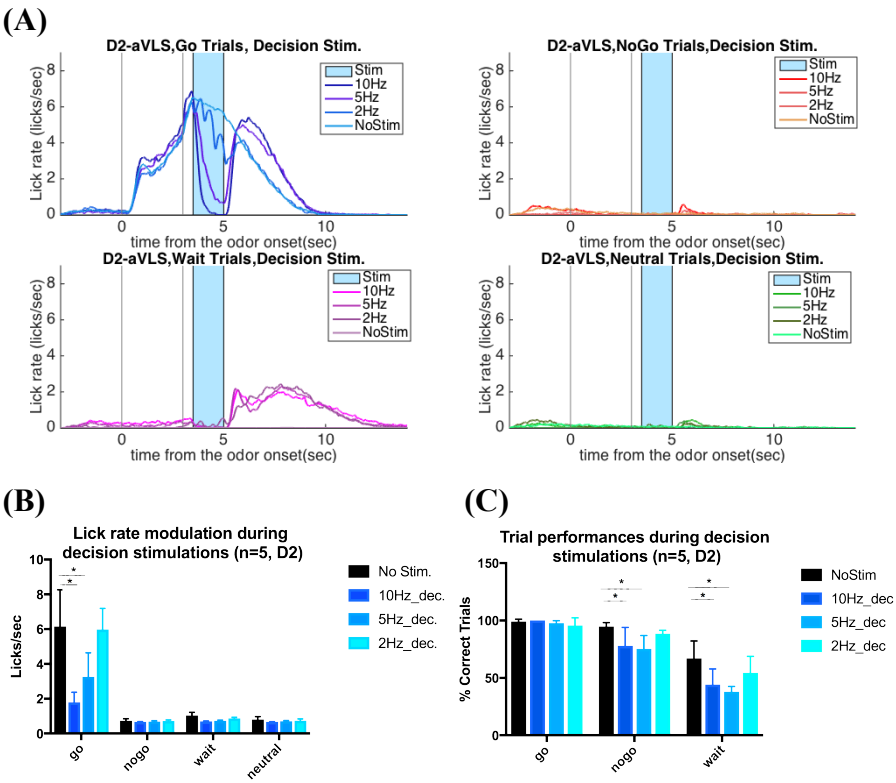

Figure 3.21 | Indirect pathway aVLS stimulations for 1.5 s during decision period, reduced lick rate, and changed the percentage of correct trials for different trial types (n=4). (**A**) Lick rate histograms showed the lick rate change during 1.5 s decision period stimulations for go trials. (**B**) In go trials, lick rates during stimulation decreased gradually for 5Hz (Dunnet's multiple comparison test, p=0.0001), and 10Hz (Dunnet's multiple comparison test, p=0.0001) stimulations. Lick rates during stimulation did not change in no-go, wait and neutral trials for any stimulation frequency. **(C)** Decision stimulations did not change the percentage of correct go trials, but decreased no-go and wait trial performances compared to non-stimulated trials for 5Hz (no-go; trials-Dunnet's multiple comparison test, p=0.005 and wait trials; Dunnet's multiple comparison test, p=0.001) and 10Hz (no-go trials; Dunnet's multiple comparison test, p=0.009 and wait trials-Dunnet's multiple comparison test, p=0.01) decision period stimulations.

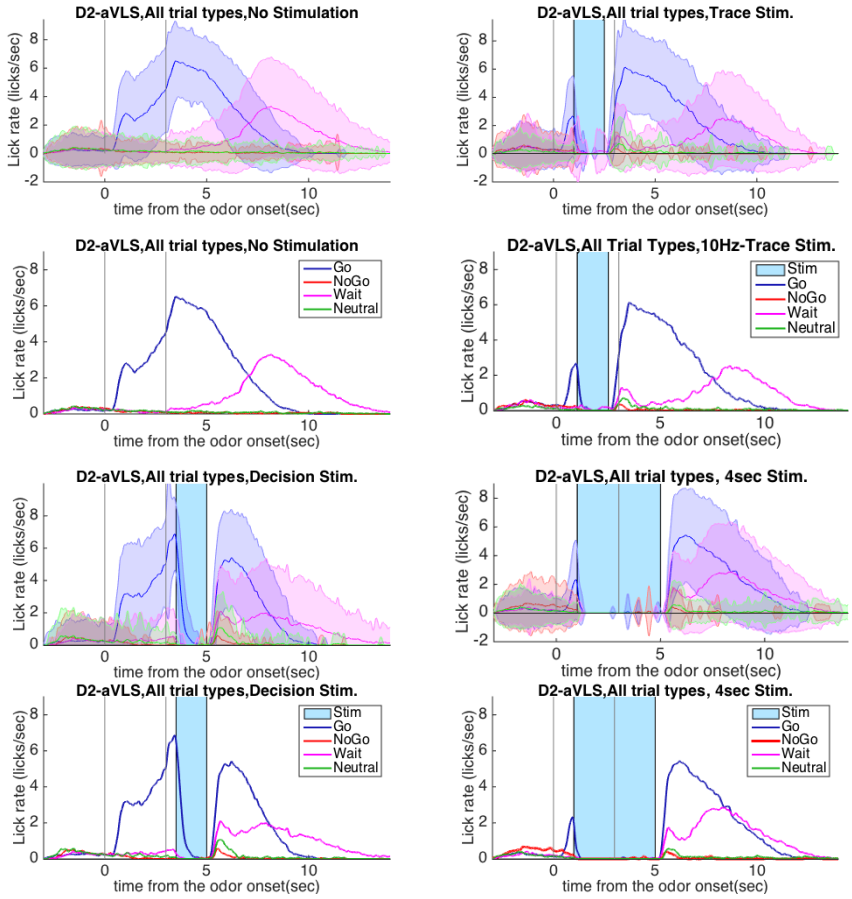

Figure 3.22 | Lick rate histograms suggested that 10Hz stimulations of indirect pathway aVLS populations decreased or paused licking during stimulation in all trial types. Lick rate histograms suggested that during 10Hz-4s stimulations, 10Hz-trace period stimulations and 10Hz-decision period stimulations decreased or paused licking in go, no-go, wait and neutral trials.

We asked if the indirect pathway aVLS stimulations during go trials had different effects on the recovery times depending on if licking was initiated before the stimulation onset or not. We separated the go trials in which licking was initiated between the odor onset and the stimulus onset. These trials were called stopped go trials.

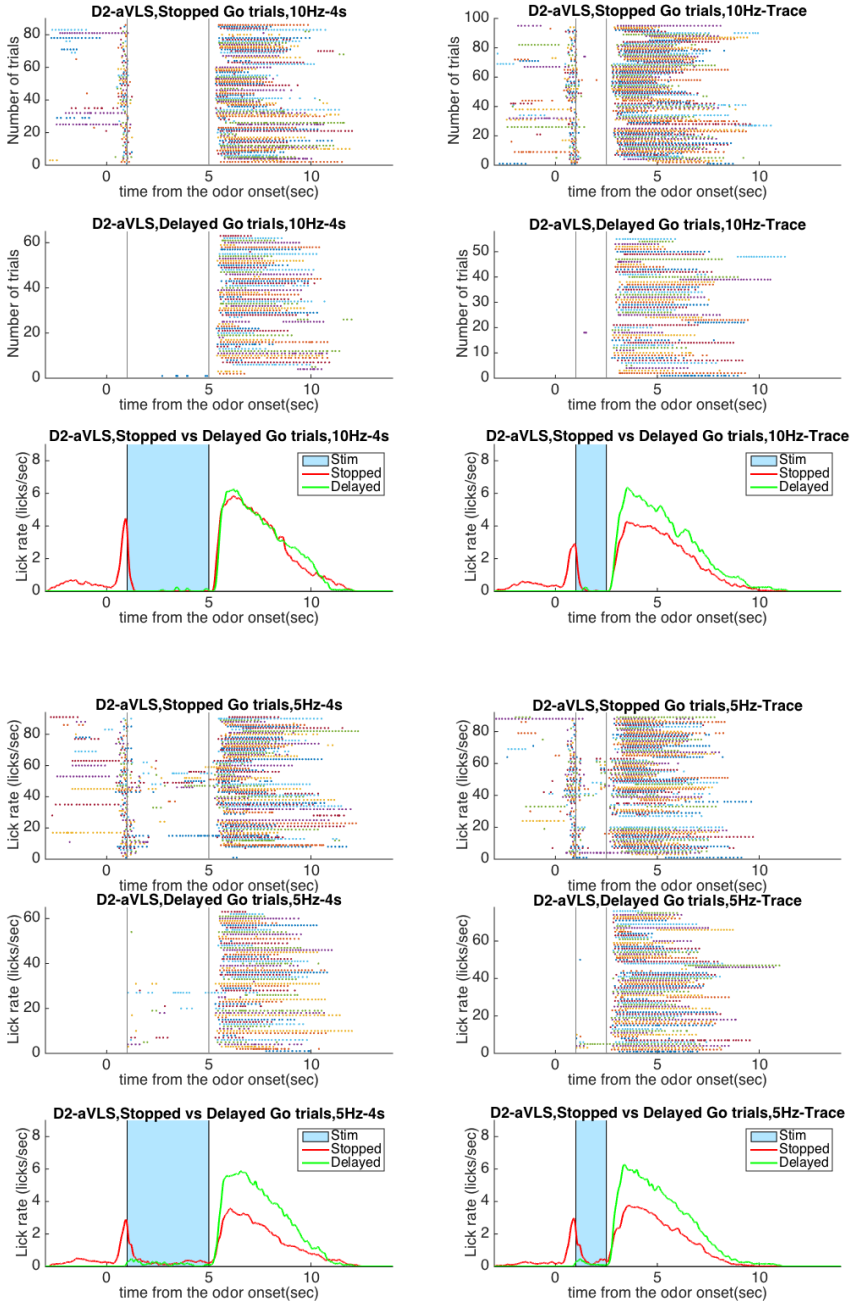

Figure 3.23 | Stopped and delayed go trials recovered similarly after 5Hz and 10Hz indirect pathway aVLS stimulations.

Go trials, during which licks were not detected between the odor onset and stimulation-onset were separated, and called delayed go trials. Stopped and delayed go trials did not show differences in their recovery time for 10Hz and 5Hz stimulations (Figure 3.22). Only 4 seconds stimulations and trace stimulations are analyzed, since almost all the trials were initiated before the decision period.

aVLS stimulations of EYFP expressing control animals did not induce or stopped licking

To compare if the effect of optogenetic of stimulations in striatonigral and striatopallidal aVLS populations was due to the activation of these specific population via channel rhodopsin induced depolarization, we infected the same populations with EYFP and performed the same optogenetic stimulations. We pooled together the data from three D1-Cre and two D2-Cre mice since they learned the task similarly (detailed comparison on page 75). None of the stimulation frequencies for 4s, trace and decision period stimulations changed the percentage of correct trials any trial type (2-way ANOVA, $p>0.05$, Figure 3.24, Figure 3.25, and Figure 3.27). Optogenetic stimulations on these mice did not induce or reduce lick rates compared to the non-stimulated trials in any trial type (2-way ANOVA, $p>0.05$, Figure 3.24, Figure 3.25, Figure 3.26, and Figure 3.27).

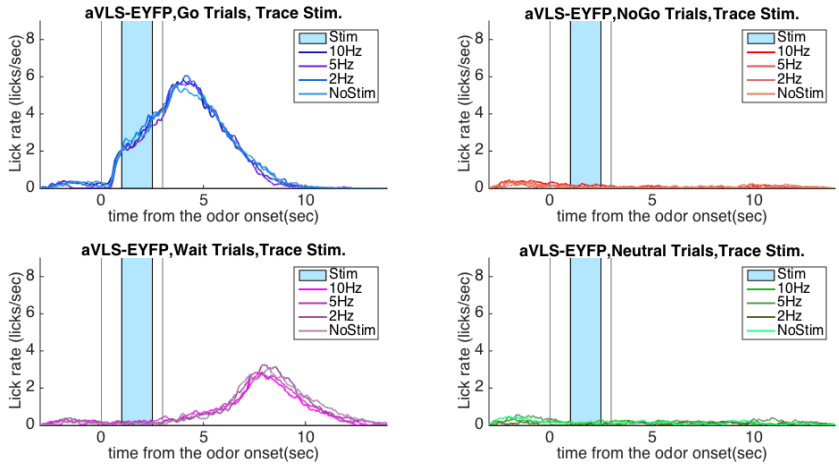

Figure 3.24| aVLS stimulations for 1.5s trace period did not change lick rate in EYFP expressing mice (n=5).

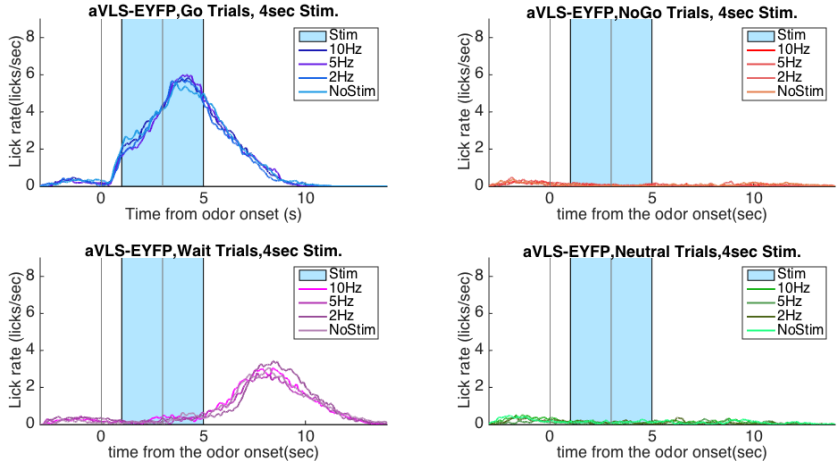

Figure 3.25 | aVLS stimulations for 4s during did not change lick rate in EYFP expressing mice (n=5).

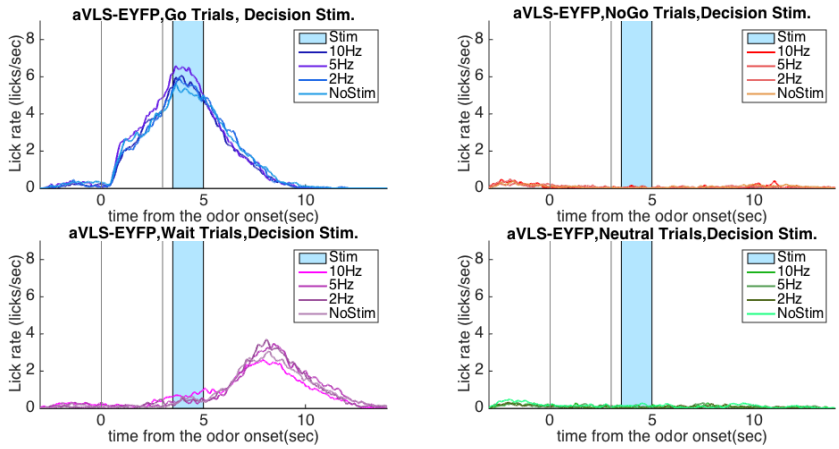

Figure 3.26| aVLS stimulations for 1.5s during decision period did not change lick rate in EYFP expressing mice (n=5).

Stimulations of striatonigral-aNAcc population did not induce or stop licking in any trial type

We compared if the neighboring direct pathway stimulation would have similar effects to direct pathway aVLS stimulations. Stimulations did not induce or stop licking. Only 10Hz stimulations during go trials might have slightly decreased the lick rate during 4s and decision stimulations. Trial performances did not show difference between stimulated trials and non-stimulated trials for any trial type (Figure 3.27, Figure 3.28, Figure 3.29, Figure 3.30, and Figure 3.31).

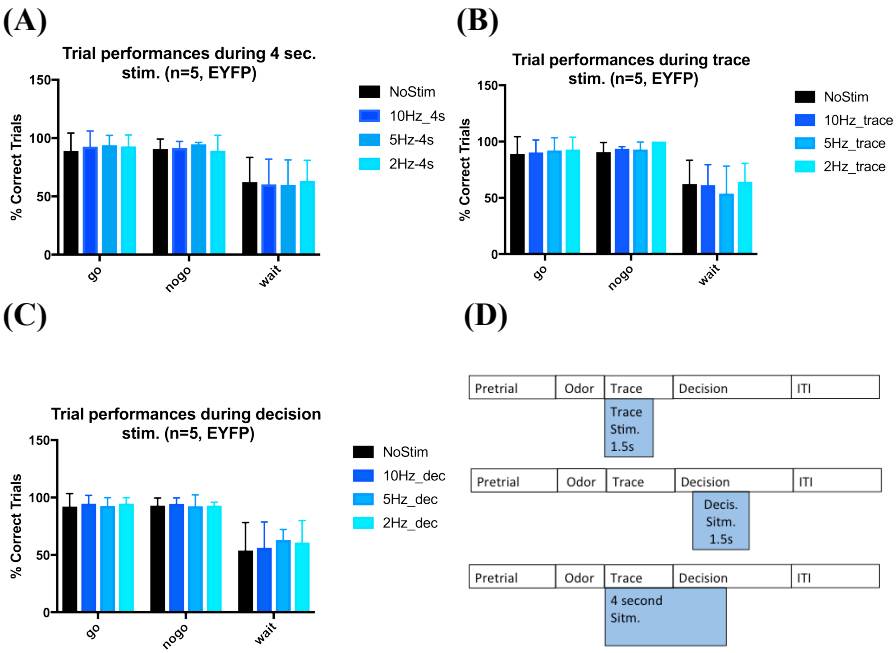

Figure 3.27 | Optogenetic stimulations of EYFP expressing aVLS populations did not change percentages of correct trials for any trial type (n=5). (A) 4 seconds stimulations did not change the percentage of correct trials for 2Hz, 5Hz and 10Hz stimulations for any trial type. **(B)** Trace period stimulations did not change the percentage of correct trials for 2Hz, 5Hz and 10Hz stimulations for any trial type. **(C)** Decision period stimulations did not change the percentage of correct trials for 2Hz, 5Hz and 10Hz stimulations for any trial type. **(D)** Schematic of the stimulation conditions within a trial.

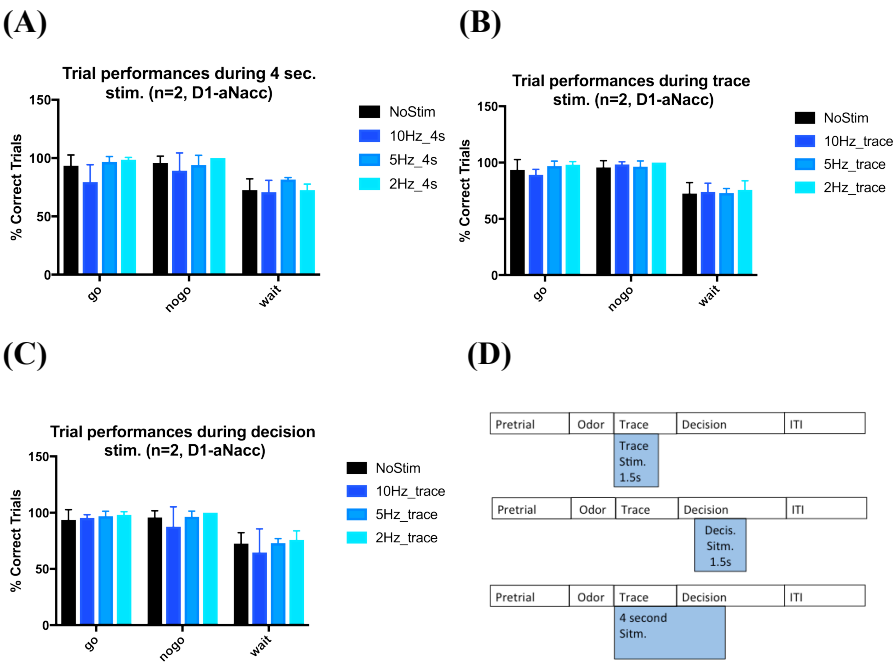

Figure 3.28 | Effect of striatonigral aNacc stimulations on the percentage of correct trials for different trial types (n=2). (A) 4s stimulations did not change the percentage of correct trials for 2Hz, 5Hz and 10Hz stimulations for any trial type. **(B)** Trace period stimulations did not change the percentage of correct trials for 2Hz, 5Hz and 10Hz stimulations for any trial type. **(C)** Decision period stimulations did not change the percentage of correct trials for 2Hz, 5Hz and 10Hz stimulations for any trial type. **(D)** Schematic of the stimulation conditions within a trial.

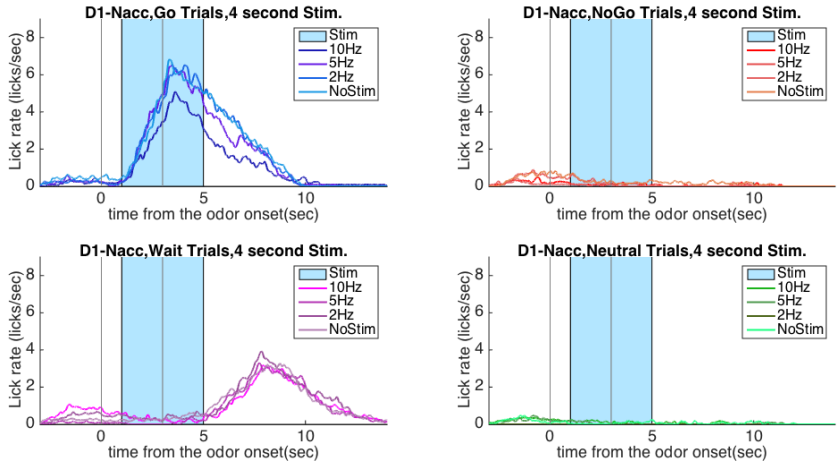

Figure 3.29 | Striatonigral-aNacc stimulations for 4s did not change lick rate in any trial type (n=2).

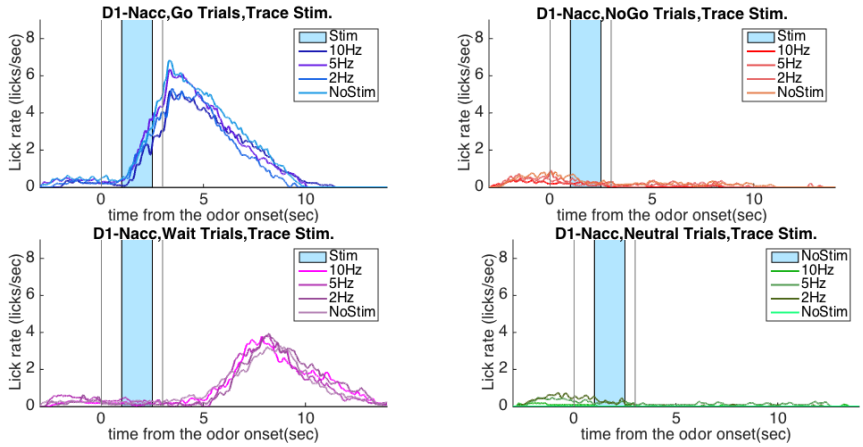

Figure 3.30 | Striatonigral-aNacc stimulations for 1.5s during trace period did not change lick rate in any trial type (n=2).

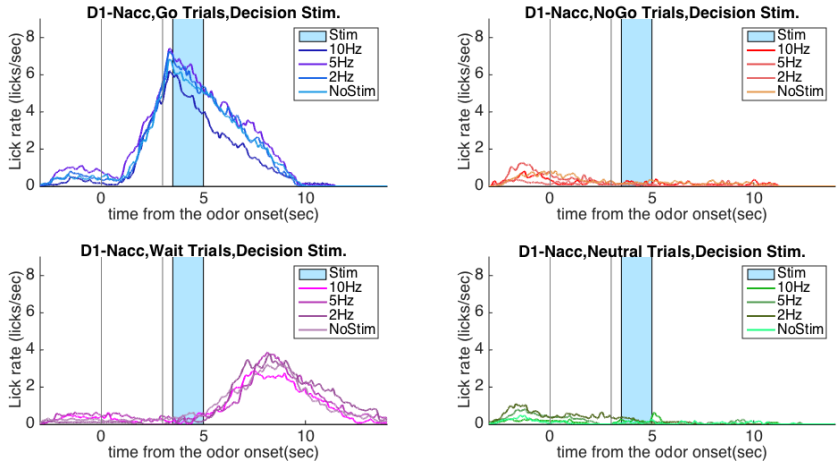

Figure 3.31 | Striatonigral-aNacc stimulations for 1.5s during decision period did not change lick rate in any trial type (n=2).

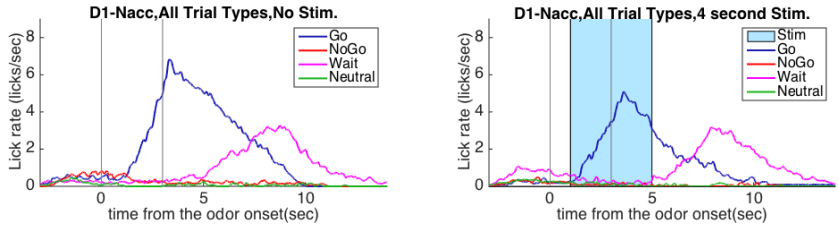

Figure 3.32| Striatonigral-aNacc stimulations for 4s did not change lick rate in any trial type compared to the non-stimulated trials (n=2).

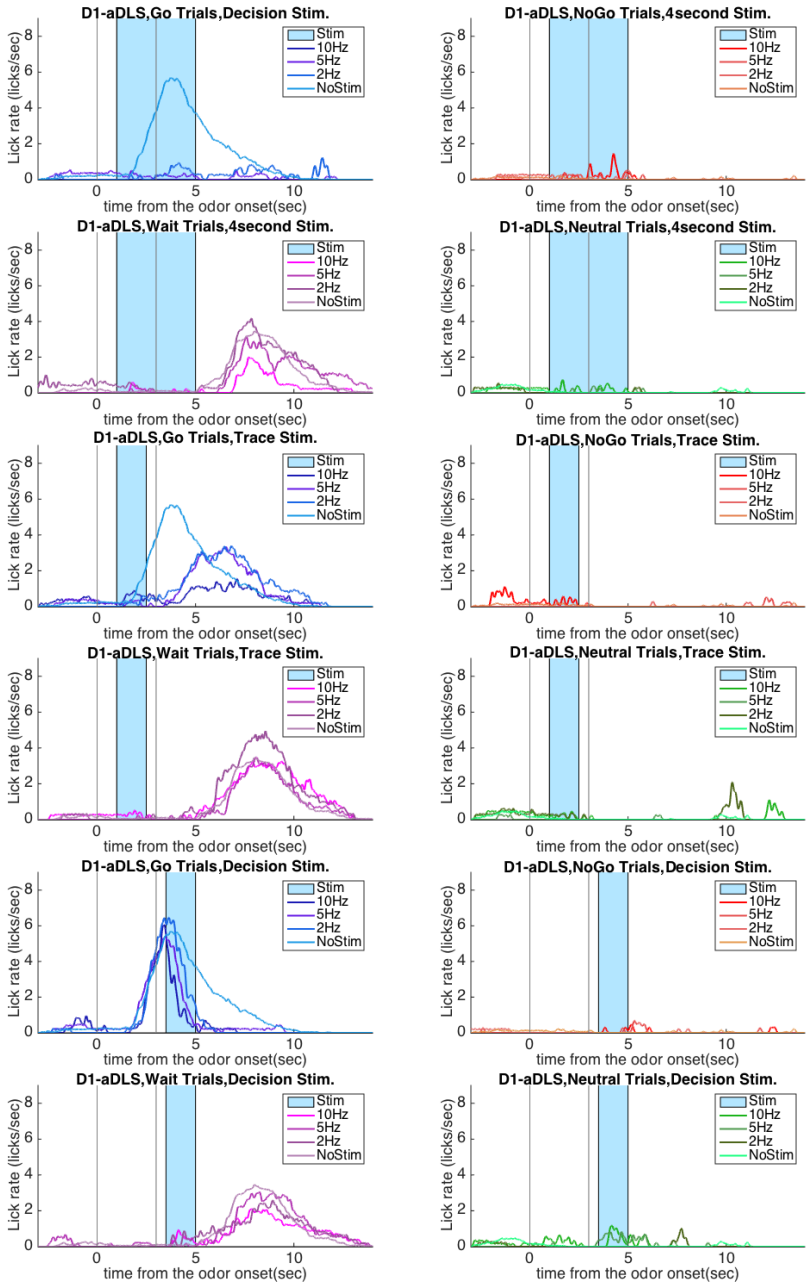

Supplementary Figure 1 | Striatonigral-aDLS stimulations decreased or canceled licking in go trials (n=1). Our preliminary results that stimulations of striatonigral aDLS population canceled licking and mice did not continue or start licking after stimulation offset in go trials. Stimulations also seemed to induce body movements. Stimulations did not induce licking

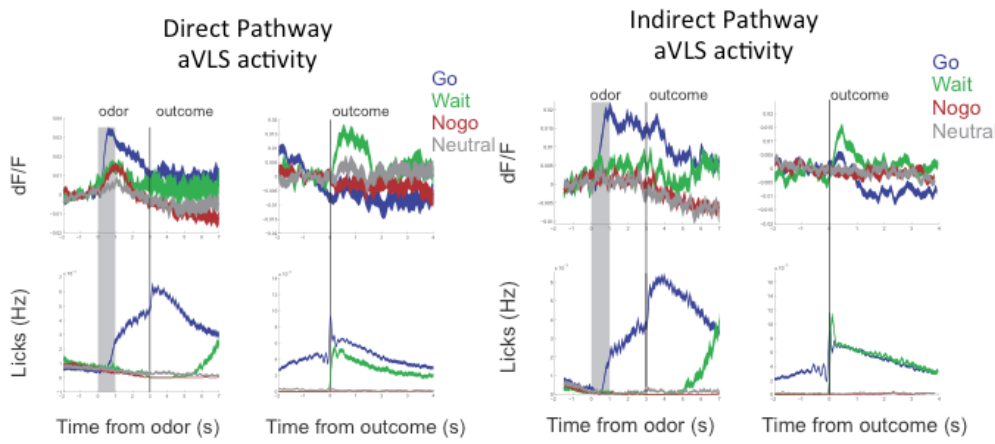

Supplementary Figure 2 | Population activity of striatonigral aVLS (n=1) and striatopallidal aVLS (n=1) populations suggested that both pathways were coactive during initiation but striatopallidal pathway was also active during execution of instrumental licking. We performed bulk population calcium imaging of striatonigral and striatopallidal aVLS populations during head fixed olfactory guided operant task, using GCaMP6f expressed in either pathway populations. Population imaging techniques used in these experiments were explained elsewhere (Matias et al., 2016). We observed that striatopallidal aVLS was active preceding the initiation of licking in go trials and decayed without being modulated by changes in lick rate during execution. We observed odor responses for all trial types only in striatonigral population activity. Reward modulations of striatonigral activity were only observed in wait trials. Striatopallidal pathway aVLS was also active preceding initiation of licking in go trials. However, striatopallidal pathway aVLS activity was sustained during execution of licking, until the water reward was obtained. Modulations in the striatopallidal pathway aVLS activity preceded modulations in lick rate, in go trials. We also observed water reward modulations in striatopallidal pathway aVLS activity in go and wait trials.

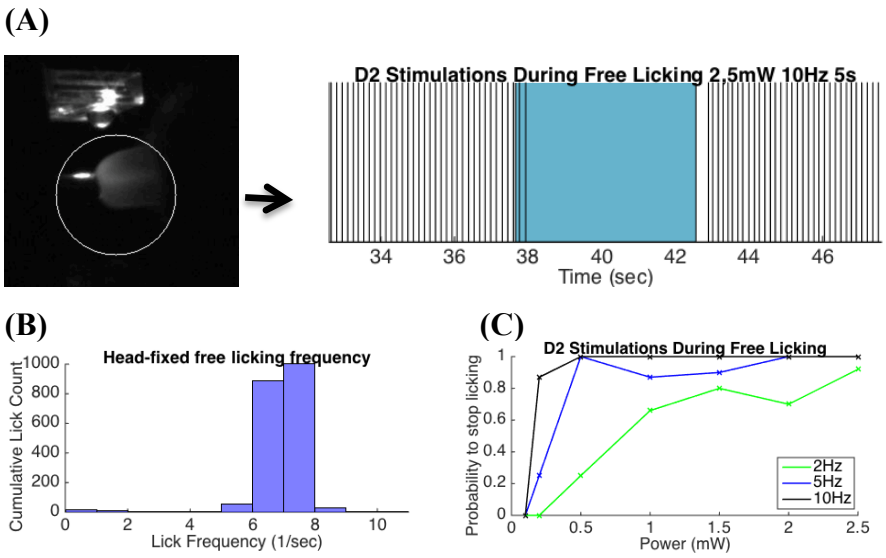

Supplementary Figure 3| Striatopallidal pathway stimulations stopped head fixed free licking for laser power <2.5mW. **(A)** Free licking of mice was recorded using 60fps videos. Video analysis was performed on manually chosen ROI, by subtracting the first frame from all the frames. **(B)** Head-fixed mice showed stable licking frequencies similar to natural licking frequency of mice (Travers et al., 2007). **(C)** Striatopallidal pathway stimulations stopped free licking for 0.5mW laser power.

DISCUSSION

We have shown that orofacial primary and secondary motor cortical regions project onto ventrolateral striatum. The most rostral part of striatum received motor input from forelimb motor cortical regions but not mid and posterior striatum. However, orofacial motor cortical regions projected only on VLS regions of anterior, mid and posterior striatum. Anatomical mapping of cortciostriatal projections suggest VLS might be the striatal region involved in orofacial motor control.

We observed different jaw movements with 5Hz and licking with 10Hz striatonigral pathway aVLS stimulations. Different sites of medullary reticular formation (Gi, PcRT and IRt) are thought to be involved orofacial movements (Travers et al., 1997). Retrograde labeling using rabies viruses, from different orofacial muscles showed that same premotor neurons innervate different muscles and might be controlling precise complex orofacial movements (Stanek et al., 2014). Specific premotor neuron pools might be controlling not specific muscles but complex, coordinated movements by targeting multiple muscles (Stanek et al., 2014). Therefore, downstream basal ganglia pathways controlling orofacial movements was shown to involve medullary reticular formation structures but the details of their roles in orofacial motor control is not clear (Travers et al., 1997, Scott et al., 2003, Stanek et al., 2014). However, it was suggested that VLS striatonigral and striatopallidal populations (via GPe) converge on single SNr cells that project to medullary reticular formation structures (von Krosigk, et al., 1992).

Optogenetic activation of striatonigral pathway aVLS cells induced orofacial movements and licking in freely moving mice. However, striatopallidal pathway aVLS stimulations paused licking during the stimulation freely drinking head fixed mice (Supplementary Figure 3).

We investigated the secondary effects of aVLS 10Hz stimulations in locomotion. We showed that striatonigral pathway aVLS 10Hz stimulations in addition to inducing liking, stopped locomotion. Stopping locomotion might be due to inhibitory intra-striatal connections within striatonigral pathway cells, via the mechanism

known as “lateral inhibition” (Mink et al., 1996, Tecuapetla et al., 2009). Or it might be due to competing motor programs activated by synchronous optogenetic activation of direct pathway cells (Mink et al., 1996). The same 10Hz stimulations when performed on striatopallidal pathway paused ongoing movement briefly (<0.5s). However, they did not stop locomotion of freely moving mice, and they did not stop ongoing movement in general. Therefore, optogenetic stimulations in freely moving mice, suggested that striatonigral pathway aVLS population, together with striatopallidal pathway aVLS population, are involved mainly in orofacial motor control.

We have also shown that the orofacial motor roles of aVLS striatonigral pathway cells were conserved but modulated in mice trained to change its licking as an instrumental response for different outcomes. Therefore, in addition to inducing licking in naive freely moving mice, optogenetic activation of striatonigral pathway aVLS cells induced licking differently depending on the context, in trained mice.

We trained mice to modulate its licking in response to different cues such that they learned to lick to receive a water reward in response to the go-odor, suppress licking in response to the no-go-odor, and withhold licking until they hear the go-tone in response to the wait-odor. Mice also learned not to lick for no-outcome in response to the neutral odor. We manipulated striatonigral and striatopallidal pathway aVLS populations using optogenetic stimulations. These circuit manipulations were sufficient to change the learned responses of mice in all trial types.

Direct pathway aVLS stimulations induced higher lick rates in go trials compared to no-go trials, regardless of the period of the trial the stimulations were performed. Lick rates induced by stimulations were similar for wait and neutral trials compared to go and no-go trials. This difference in the motor output of striatonigral pathway aVLS population stimulations, in different trial types, suggested that mice were able to modulate the motor output activated by striatonigral pathway stimulations depending on the context, learned outcome of the trial. They were able to suppress licking induced by stimulations in no-go trials, to avoid punishment, but not in wait trials to avoid loss of a delayed reward, or in no-outcome neutral trials. aVLS striatonigral pathway 10Hz stimulations also facilitated initiation of licking.

Optogenetic activation of striatopallidal pathway aVLS stopped licking in mice trained to modulate its licking as an instrumental response for different outcomes. Striatopallidal pathway aVLS stimulations paused licking in go trials. Delay to start licking after stimulation offset did not show differences between stopped and delayed go trials. Therefore the effect of indirect pathway aVLS stimulation did not seem to change the decision of mice to initiate licking, but only paused the execution of licking during stimulation period and recovered the learned response after stimulation.

2, 5 and 10Hz stimulations showed a gradual suppression on lick rates in go trials, independent of the period of the trial the stimulations were performed. We could not address if the effects of indirect pathway aVLS stimulations modulated licking differently depending on the context, since our task did not involve licking at different

motivational states but only for go trials. Therefore, we could not claim that the motor output of striatopallidal pathway aVLS population would be modulated by the context.

Interestingly, striatopallidal pathway stimulation offset induced licking in different trial types. This effect could be one of the mechanisms that might explain why we did not see differences in recovery times after stimulations, between stopped and delayed trials. Stimulus off effect might be explained by two-step, pause and cancel model of action suppression (Mallet et al, 2016). Two types of GPe cells were shown to be involved in stopping actions differently (Mallet et al., 2012, Mallet et al., 2016). Fast GPe-STN-SNr pathway and slow GPe-Striatum pathway were suggested to act on stopping actions in different time scales (Mallet et al., 2016). It is possible that stimulation of aVLS striatopallidal pathway simultaneously activated at least these two pathways that and release of this simultaneous activation at the offset of stimulation might be causing inactivation of both fast and slow suppression pathway. Therefore, the fast suppression pathway (GPe-STN-SNr) might be briefly silencing SNr cells and induce licks at the offset of the stimulation, until the slow suppression pathway (GPe-Striatum) recovered. This effect might also be explained by a momentary network imbalance, or due to intra-striatal connections between direct and indirect pathway (Tecuapetla et al., 2009). However, it was also shown that SNr received direct projections from GPe, which could account for a third inhibitory pathway for action suppression (Smith et al., 1991, von Krosigk et al., 1992).

Striatonigral pathway aNAcc stimulations showed immediate motor effect in naïve freely moving mice with minimal orofacial effects (mostly forelimb), but did not change the responses in head fixed olfactory guided operant task. This control experiments were performed because aNacc and aVLS were only 500-600 μm away from each other. Previous lesion and pharmacological studies that targeted large regions around VLS and suggested that both VLS and Nacc might be involved in orofacial motor control (Pisa et. al., 1988, Mittler et al., 1994, Jicha et. al., 1991).

We also, showed that aDLS stimulations did not induce licking in naive freely moving mice and in trained mice to modulate licking in different context. Our preliminary work showed that aDLS stimulations did not induce licking in trained mice but stopped or canceled licking.

We are currently working on calcium imaging of population activity of aVLS striatonigral and striatopallidal pathway during olfactory guided operant task performance. Our preliminary results suggested that striatonigral pathway is active during initiation, preceding licking in go trials. However, striatonigral population activity decayed monotonically, without being modulated by changes in lick rate (Supplementary Figure 2). Therefore high levels of sustained activity of striatonigral population might not be necessary for the execution of instrumental licking. Striatonigral population also showed odor responses for all trial types and water reward responses in wait trials. In go trials, striatopallidal pathway was also active preceding initiation of licking. Unlike striatonigral population, striatopallidal population showed sustained activity during licking and decayed

preceding the decay in lick rate. Striatopallidal population did not show odor responses in any trial type but showed responses to water reward in both go and wait trials (Supplementary Figure 2). Therefore, active suppression of instrumental actions might not require increase in indirect pathway population activity.

Our preliminary results supports the previous observations that both pathways are active during initiation of instrumental actions, in both self initiated and cue guided conditions (Jog et al., 1999, Jin et al., 2010, Cui et al., 2013, Tecuapetla et al., 2014, Jin et al., 2014, Tecuapetla et al., 2016). They also suggest that salient cues might be encoded only in striatonigral population, but not in striatopallidal population, supporting previous report by Sippy et al., 2015.

It was also shown that subpopulations of both pathways showed start-stop related, sustained, or inhibited activity during instrumental action (Jog et al., 1999, Jin et al., 2010, Jin et al., 2014). Sustained activity was observed in larger percentage of striatonigral population and inhibited activity was observed in a larger percentage of striatopallidal population (Jin et al., 2014). However, we did not observe lick rate modulations in striatopallidal aVLS activity. Interestingly we observed modulations preceding both initiation and execution in indirect pathway activity. Considering the limitations of population calcium imaging techniques, we could not make direct comparisons with electrophysiological recording. However, we conclude that activity in both pathways might be necessary for action selection and initiation, and that striatopallidal pathway might be guiding the execution showing a permissive role as suggested by Tecuapetla et al., 2016.

Optogenetic inactivation of striatonigral and striatopallidal DLS suggested that balanced activity of both pathways were necessary for proper execution of instrumental actions (Tecuapetla et al., 2016). It remains to be tested if activity of both pathways in aVLS would be necessary for initiation and execution of instrumental actions Next, we are planning to optogenetically silence striatonigral and striatopallidal aVLS populations and assess their necessity in the head fixed olfactory guided operant task performance. It would be interesting to see if activity of these aVLS populations would also be necessary for the initiation and execution of instrumental licking. Electron microscopy studies, showed that GPe cells that receive input from VLS, project onto SNr cells that receive input from VLS as well (von Krosigk et al., 1992). The same study also showed that these SNr cells also target medullary reticular formation, that is the brainstem structure involved in orofacial movements (von Krosigk et al., 1992). Therefore they suggested that the basal ganglia orofacial motor control happens on single SNr cells that receive converging input from direct and indirect pathway VLS cells, and project to medullary reticular formation (von Krosigk et al., 1992). However, the role of striatonigral and striatopallidal pathways in instrumental licking was not known. Our corticostriatal, striatonigral and striatopallidal anatomical mapping, striatonigral and striatopallidal aVLS optogentic stimulations, and striatonigral and striatopallidal aVLS population imaging results supports the idea that aVLS is a part of basal ganglia circuit for orofacial motor control and that both aVLS pathways might be coactive during initiation and execution of instrumental licking, with indirect pathway having a permissive role

in execution (Cui et al., 2013, Tecuapetla et al., 2014, Jin et al., 2010, Jin et al., 2014, Tecuapetla et al., 2016).

MATERIAL AND METHODS

Animals

All procedures were reviewed and performed in accordance with the Champalimaud Center of the Unknown Ethics Committee guidelines and approved by the Portuguese Veterinary General Board (Direccao Geral de Veterinaria, approval 0421/000/000/2014). GENSAT Bac transgenic lines D1-Cre (FK150) and D2- Cre (Adora2a) were used to specifically target striatonigral or striatopallidal cells. Emx1-Cre line was used to map cortical projections on striatum. Animals between 3-6 months of age, that were single housed, in normal light cycle were used in these experiments. Experiments were performed during the light cycle. Animals used for mapping corticostriatal projections had free access to food and water. Water deprivation was used to motivate mice for the olfactory-guided operant task.

Surgery

Double injections of 100-150nl AAV2.2-EF1a-DIO-EYFP-WPRE (University of North Carolina, titer $1.85x10^{12}$) and AAV2.2-EF1a-DIO-tdTomato-WPRE (University of North Carolina, titer $2.7x10^{12}$) were injected in different cortical regions to map their projections on striatum. Coordinates were chosen as described in Zigg et al., 2014. Fluorescent proteins were randomly switched between injection sites. Emx1-Cre line was used to label cortical cells specifically (Gerfen et al., 2013).

Injections of 1ul AAV2.1-EF1a-DIO-Chr2(H134R)-EYFP-WPRE was performed bilaterally, using a Nanoject, Drummond Scientific, at 4,6 nl pulses with 5 second intervals in aVLS of D1-Cre (AP:+1.15, ML: 1.9, DV: 3.1mm) and D2-Cre (AP:+1.15, ML: 2.25, DV: 3.1) mice. Micropipettes with 25-35um tip size were used. 10-15 minutes after injection was completed injection pipette was pulled out slowly. GENSAT BAC transgenic lines FK150-Cre were used for labeling D1 populations and Adora2a-Cre line was used for labeling D2 populations (Gerfen et al., 2013).

230um optical fibers with zircona ferrules were prepared as explained in Sparta et al., 2012. Optical fibers were implanted bilaterally, 100um above the injection site.

Optogenetic stimulations

473 nm blue, diode laser was used for all stimulations. Stimulations were performed at 2Hz, 5Hz and 10Hz with 10ms square pulses using an acousto-optic modulator and fixed frequency drivers (AA-Optoelectronic). Master-8 stimulator was used to define precise stimulations. 2.5-2.6 mW at the tip of the fiber was used for all stimulations.

Behavioral procedures

Video recordings of locomotion using Locomouse

Mice were water deprived for two days for Locomouse experiments. Mice were placed in side-boxes and a drop of water was provided in opposite side boxes. Therefore mice crossed the Locomouse corridor to obtain water. Optogenetic stimulations were triggered in the middle of the corridor, by an IR beam break, when mice passed. 25% of the trials were stimulated in random order.

Olfactory guided operant task

Water deprivation started 2 days after surgery. In the first phase of training mice were anesthetized for 30seconds-1 minute before head fixing for the first 2-3 days during habituation. Mice were habituated for head fixing and drinking from a water port for 2-5 days depending on their performance. Go odor was introduced first. All the periods were kept fixed to 0.5-1 second during the first days of training. Training started as classical conditioning and shifted to instrumental conditioning, within variable number of trials depending on the performance of the mice. Durations of all periods were extended to the task durations within a few days. After mice reach to a go trial performance > 50% correct, no-go trials were introduced slowly without air-puff. And after no-go performance reached ≈50% correct, wait trials were introduced. Wait trials started with 1-2.5 sec waiting time depending on the performance of the mice and was extended over days depending on their performance up to 4 seconds waiting time. Mice were trained until they reach ≈ 50% wait trial performance. During wait trial training go and no-go trial performance reached to 100% and stayed 100% for 1-3 weeks depending on the performance of the mice.

2.6-4ul water per trial was delivered for go or wait trials. Water and gel food was supplemented in the home cage for some mice that dropped their weight below 80%. Air puff to the face for 100ms was delivered in incorrect no-go trials as punishment. Cuminaldehyde, octanol, carvone and limonene were used for go, no-go, wait and neutral odors respectively for optogenetic manipulations and carvone,

octanol, cuminaldehyde and limonene were used for go, no-go, wait and neutral odors respectively for population calcium imaging experiments.

Licks of head-fixed mice were detected using a custom made optical lickometer with an infrared beam. Data was acquired using B-control system as described in Matias et al., 2016.

Analysis

Trial times were aligned to either odor onset or the outcome onset/ITI beginning. The effects of stimulations on trial performance and on lick rate were calculated. Smoothed lick rate histograms were acquired, by convolution of a 34 ms Gaussian kernel function to each lick event and averaging between all trials of all mice, for each trial type and each stimulation type. Mean lick rate distributions were calculated for all trials of each trial type across all mice. To measure the effect of optogenetic stimulations on licking, mean lick rates per mouse, during the stimulation periods were compared between stimulated and non-stimulated trials of the same trial type and between trial types. All the analysis was performed using MATLAB 2014a.

Statistical analysis

All the analysis was performed using MATLAB 2014a or GraphPad Prism (GraphPad Software, Inc). All the tests were performed performances or average lick rates during stimulation periods across animals (n=4 and n=5), therefore mostly non-parametric tests were chosen. Wilcoxon rank sum test was used to compare percentage of correct trials between mice. However, 2-way ANOVA and Dunnet's multiple comparison tests were used to compare the effect of

stimulations on performance within the same trial type. 2-way ANOVA and Dunnet's multiple comparison tests were also used to compare the effect of different stimulation frequencies on all trial types. The same statistical tests were performed for 4 seconds stimulations, trace period stimulations and decision period stimulations. Friedman test and Dunnet's multiple comparison test was used to compare the effect of the one stimulation type and frequency on lick rate in stimulated trials.

ACKNOWLEDGEMENTS

A.Vaz and M.Correira for mouse colony management. This research was supported by INDP Graduate Programme, FCT fellowship, HHMI to R.M.C, ERA-NET NEURON, 7th Framework Programme.

AUTHOR CONTRIBUTIONS

All experiments were designed by S.Mutlu and R.M.Costa, loco mouse system was designed by A.Machado and M.Carey, loco mouse analysis was performed by A.Machado, head fixed olfactory guided behavioral task was designed by E.Lottem, Z.F.Mainen, R.M. Costa and S.Mutlu, population calcium imaging was performed by E.Lottem, anatomical mapping, loco mouse experiments, open field experiments and optogenetic manipulation in olfactory guided operant task experiments and their analysis were performed by S.Mutlu.

REFERENCES

Carelli, R., M., West, M., O. (1991) Representation of the body by single neurons in the dorsolateral striatum of the awake, unrestrained rat. J. Comp. Neurology 309:231-249

Cohen, J.Y., Haesler, S., Vong, L., Lowell, B.B., Uchida, N. (2012) Neuron-type specific signals for reward and punishment in the ventral tegmental area. Nature 482: 85-88

Costa, R.M., Cohen, D., Nicolelis, A.L. (2004) Differential corticostriatal plasticity during fast and slow motor skill learning in mice. Curr. Biol. 14(13): 1124-1134

Cui, G., Jun, S. B., Jin, X., Pham, M.D., Vogel, S.S., Lovinger, D.M., Costa, R.M. (2013) Concurrent activation of striatal direct and indirect pathways during action initiation. Nature 494(7436): 238-42.

Deniau, J.M., Chevalier, G. (1992) The lamellar organization of the rat substantia nigra pars reliculata: Distribution of projection neurons. Neuroscience, 46(2): 361-377

Deniau, J.M., Menetrey, A., Charpier, S. (1996) The lamellar organization of the rat substantia nigra pars reliculata: Segregated patterns of striatal afferents and relationship to topography of corticostriatal projections. Neuroscience, 73(3): 761-781

Ebrahimi, A., Pochet, R., Roger, M. (1992) Topographical organization of the projections from physiologically identified areas of the motor cortex to the striatum in the rat. Neuroscience Research 14: 39-60

Gerfen, C., R., Paletzki, R., Heintz, N., (2013) GENSAT- BAC Cre-recombinase driver lines to study the functional organization of cerebral cortical and basal ganglia circuits. Neuron 80(6):1368-1383

Grofova, I., Deniau, J. M., Kitai, S.T. (1982) Morphology of the substantia nigra pars reticulata projection neurons intracellularly labeled with HRP. J. Comp. Neurology 208:352-368

Hintiryan, H., Foster, N.F., Bowman, I., Bay, M., Song, M.Y., Guo, L., Yamashita, S., Bienkowski, M. S., Zingg, B., Zhu, M., Yang, X.W., Shih, J.C., Toga, A.W., Dong, H.W. (2016) The mouse cortico-striatal projectome. Nat. Neurosci. 19(8): 1100-14

Jicha, G., A., Salamone, J., D. (1991) Vascous jaw movements and feeding deficits in rats with ventrolateral striatal dopamine depletion: Possible relation to Parkinsonian symptoms. J. Neuroscience, 11(12): 3822-3829

Jin, X., Costa, R.M. (2010) Start/stop signal emerge in nigrostriatal circuit during sequence learning. Nature 466(7305): 457-462

Jin, X., Tecuapetla, F., Costa, R.M. (2014) Basal ganglia subcircuits distinctively encode the parsing and concatenation of action sequences. Nat. Neurosci. 17(3): 423-30

Jog, M.S., Kubota, Y., Connolly, C.I., Hillegaart, V., Graybiel, A.M. (1999) Building neural representations of habits. Science 286(5445): 1745-9

Komiyama, T., Sato, T.R., O'Connor, D., Zhang, Y. X., Huber, D., Hooks, B.M., Gabitto, M., Svoboda, K. (2010) Learning related fine scale specificity imaged in motor circuits of behaving mice. Nature 464: 1182-1186

Kravitz, A.V., Freeze, B.S., Parker, P.R., Kay, K., Thwin, M.T., Deisseroth, K., Kreitzer, A.C. (2010) Regulation of parkinsonian motor behaviors by optogenetic control of basal ganglia circuitry. Nature 466(7306): 622-6

Kravitz, A., Tye, L.D., Kreitzer, A.C. (2012) Distinct roles for direct and indirect pathway neurons in reinforcement. Nat. Neurosci. 15: 816-818

Li, N., Chen, T.W., Guo, Z.V., Gerfen, C.R., Svoboda, K. (2015) A motor cortex circuit for motor planning and movement. Nature 519: 51-59

Machado, A.S., Darmohray, D.M., Fayad, J., Marques, H.G., Carey, M. R. (2015) A quantitative framework for whole-body coordination reveals specific deficits in freely walking ataxic mice. eLife 10.7554/eLife.07892

Matias, S., Lottem, E., Dugue, G.P., Mainen, Z.F. (2016) Firing patterns of serotonin neurons underlying cognitive flexibility. http://dx.doi.org/10.1101/059758

Mallet, N., Schmidt, R., Leventhal, D., Chen, F., Amer, N., Boraud, T., Berke, J.D. (2016) Arkypallidal cells send a stop signal to striatum. Neuron 89(2): 308-16

Mallet, N., Micklem, B. R., Henny, P., Brown M.T., Williams, C., Bolam, J.P., Nakamura, K.J., Magill, P.J. (2012) Dichotomous organization of the external globus pallidus. Neuron 74(6): 1075-86

Mena-Segovia, J., Bolam, J.P., Magill, P.J. (2004) Pedunculopontine nucleus and basal ganglia: distant relatives or part of the same family? TINS 27(10): 585-588

Mink, J. (1996) The basal ganglia: Focused selection and inhibition of competing motor programs. Prog. Neurobiol. 50(4): 381-425

Mittler, T., Cho, J., Peoples, L., L., West, M., O. (1994) Representation of the body in the lateral striatum of freely moving rats: single neurons related to licking. Exp Brain Res 98: 163-167

Mogoseanu, D., Smith A.D., Bolam, A.P. (1993) Monosynaptic innervation of trigeminal motor neurons involved in mastication by neurons of parvicellular reticular formation. J. Comp. Neurology 336:53-65

Mogoseanu, D., Smith A.D., Bolam, A.P. (1994) Monosynaptic innervation of facial motor neurons by neurons of the parvicellular reticular formation. Exp. Brain Res. 101: 427-438.

Nambu, A. (2011) Somatotopic organization of primate basal ganglia. Front Neuroanat. 5:26

Pisa, M., Schranz, J. (1988) Dissociable motor roles of the rat's striatum confirm to a somatotopic model. Behavioral Neuroscience Vol. 102, No 3: 429-440

Pisa, M. (1988) Motor functions of the striatum in rat: Critical role of the lateral region in tongue and forelimb reaching. Neuroscience Vol. 24, Issue 2: 453-463

Resulaj, A., Roozbeh, K., Wolpert, D., Shedlen, M.N. (2009) Changes of mind in decision-making. Nature 461: 263-266

Resulaj, A., Rinberg, D. (2015) Novel behavioral paradigm reveals lower temporal limits on mouse olfactory decisions. J. Neurosci. 35(33): 11667-11673

Rossi, M.A., Li, H.E., Lu, D., Kim, I.H., Bartholomew, R.A., Gaidis, E., Barter, J.W., Kim, N., Cai, M.T., Soderling, S.H., Yin, H.H. (2016) A GABAergis nigrotectal pathway for coordination of drinking behavior. Nat. Neurosci. 19(5): 742-8

Sahibzada, N., Dean, P., Redgrave P. (1986) Movements resembling orientation or avoidance elicited by electrical stimulation of the superior colliculus in rats. J. Neurosci. 6(3): 723-33

Scott, G., Westberg, K.G., Vrentzos, N., Kolta, A., Lund, J.P. (2003) Effects of lidocaine and NMDA injections into the medial pontobulbar reticular

formation on mastication evoked by cortical stimulation in anesthetized rabbits. Eur. J. Neurosci. 17:2156-2162

Sippy, T., Lapray, D., Crochet, S., Petersen, C.C.H (2015) Cell type specific sensorymotor processing in striatal projection neurons during goal directed behavior. Neuron 88(2): 298-305

Smith, Y., Bolam., J (1991) Convergence of synaptic input from the striatum and the globus pallidus onto identified nigrocollicular cells in rat: A double anterograde labeling study. Neuroscience 44 (1): 45-73

Sparta, D.R., Stamatakis, A.M., Phillips, J.L., Hoveleso, N., van Zessen, R., Suber, G.D. (2013) Construction of implantable fibers for long term optogenetic manipulations of neural circuits. Nat. Protoc. 7:12-23

Stanek, E., Cheng, S., Takatoh, J., Han, B. X., Wang, F. (2014) Monosynaptic premotor circuit tracing reveals neural substates for oro-motor coordination. Elife 2014;3:e02511

Sul, J.H., Jo, S., Lee, D., Jung, M.W. (2011) Role of rodent secondary motor cortex in value-based action selection. Nat. Neurosci. **14**, 1202–1208

Tecuapetla, F., Koos, T., Tepper, J.M., Kabbani, N., Yeckel, M.F. (2009) Differential dopaminergic modulation of neostriatal synaptic connections of striatopallidal axon collaterals. J.Neurosci. 29: 8977-8990

Tecuapetla, F., Matias, S., Dugue, G. P., Mainen, Z.F., Costa, R.M. (2014) Balanced activity in basal ganglia projection pathways is critical for contraversive movements. Nat. Commun. Jul 8;5:4315.

Tecuapetla, F., Jin, X., Lima, S.Q., Costa, R.M. (2016) Complementary contributions of striatal projection pathways to action initiation and execution. Cell 166(3): 703-15

Travers, J.B., Dinardo, L.A., Karimnamazi, H. (1997) Motor and premotor mechanisms of licking. Neurosci. Biobehav. Rev. 21(5): 631-47

von Krosigk, M., Smith, Y., Bolam, J. P.& Smith, A. D. (1992) Synaptic organization of gabaergic inputs from the striatum and the globus pallidus onto neurons in the substantia nigra and retrorubral field which project to the medullary reticular formation. Neuroscience 50(3): 531-549

Uchida, N., Mainen, Z.F. (2003) Speed and accuracy of olfactory discrimination in the rat. Nat. Neurosci. 6: 1224-1229

Zigg, B., Hintiryan, H., Guo, L., Song, M.Y., Bay, M., Bienkowski, M.S., Foster, N.N., Yamashita, S., Bowman, I., Toga, A.W., Dong, H.W. (2014) Neural networks of mouse neocortex. Cell 156: 1096-1111

CHAPTER 4| DISCUSSION

DISCUSSION

The present series of studies aimed to explore the role of anterior ventrolateral striatum, and specifically striatonigral and striatopallidal populations in ventralateral striatum, in instrumental licking initiation and execution.

We began by mapping the output targets and projection patterns of specific striatal populations that were previously suggested to be involved in control of different actions (Carelli et al., 1991, Mittler et al., 1994, Yin et al., 2004, Yin et al., 2009). It was shown that different striatal populations project onto different regions of SNr (Deniau et al., 1996). However, our study aimed to extend the existing knowledge by labeling different striatal populations simultaneously and allowing comparison of projection patterns of different striatal populations in the same animal with cell type specificity. We showed that striatopallidal pathway populations directly translated their cell body position in striatum, onto their projections in GPe; i.e relative mediolateral and dorsoventral cell body position in striatum was conserved on the GPe. We also showed that patterns of direct pathway projections onto SNr were more complex. Nevertheless, the patterns still followed general rules; relative mediolateral position of cell bodies in striatum were conserved by their axon projections on SNr and the relative dorsal-ventral axis of the cell body position in striatum was inverted on SNr. We are currently conducting volume analysis of the 3D projection patterns of different populations. Such analysis should further help us relate the structural organization in basal ganglia to function.

We focused on a specific striatal region, aVLS, which develops earlier than other dorsal striatal populations, and projects onto a "core-like" part of SNr. We confirmed that this population was involved in orofacial motor control. We extended the existing knowledge by showing that both primary and secondary orofacial motor cortical regions projected to aVLS. We demonstrated that specific head movements, jaw movements, and licking were recruited in response to different levels of aVLS striatonigral pathway activations. We showed that only striatonigral aVLS activation, but not striatonigral aDLS, striatonigral aNacc or striatopallidal aVLS activations were sufficient to induce orofacial movements, specifically licking. We demonstrated that the specificity of motor output of aVLS population was conserved in naive and trained mice, but modulated by the context. In line with existing knowledge, our population imaging studies from striatonigral and striatopallidal pathway populations suggested that both pathways were active during initiation of instrumental licking. However, they suggested that striatonigral and striatopallidal pathway populations might be differentially active during execution of instrumental licking. Our optogenetic activation and population imaging results together supported the idea that balanced activity of striatonigral and striatopallidal pathway populations might be necessary for initiation and execution of instrumental actions.

We continue investigating the necessity of striatonigral and striatopallidal aVLS activity during initiation and execution of instrumental licking in different context, using optogenetic inhibitions

and identifying the functional heterogeneity of aVLS populations using cell resolution imaging techniques.

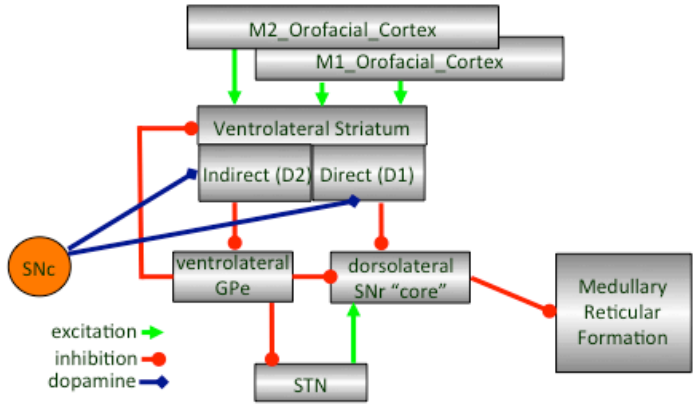

Figure 4.1| Cortico-basal ganglia-medullary reticular formation circuit that might be involved in orofacial motor control.

In this section, we will discuss the importance of our findings in relation to existing knowledge on the functions of direct and indirect populations, as well as the caveats associated with our studies.

We have shown that orofacial primary and secondary motor cortical regions project onto VLS. In the most anterior part of VLS motor input from forelimb motor cortical regions partially converged with orofacial motor cortical input, but in mid and posterior striatum forelimb and orofacial motor cortical inputs diverged into DLS and VLS, respectively. We also mapped downstream projections of DMS, DLS and VLS and showed that these regions mostly target segregated regions of GPe and SNr. VLS striatonigral projections were targeted a large core-like region in SNr that was previously suggested to be involved in orofacial movements (Deniau et al., 1996). This SNr

region was avoided by DLS and DMS direct pathway projections. Anatomical mapping of cortciostriatal projections, striatonigral and striatopallidal projections suggested that VLS might be the striatal region involved in orofacial motor control.

In freely moving mice, direct pathway stimulations at different frequencies showed different effects on movement. Different frequency stimulations induced head bobbing, jaw movements and licking. It was shown that SNr cells project to the superior colliculus (SC), thalamus, PPn, and other brainstem regions involved in many different movements (Grofova et al., 1982, Smith et al., 1991, von Krossigk et al., 1992, Mena-Segovia et al., 2004, Dautan et al., 2014). It is possible that different stimulations recruited different basal ganglia output circuits that are premotor to different motor circuits. SC was shown to be involved in head orientation, specifically medial-SC in head-up (avoidance) and lateral-SC in head-down (approach) movements and in orofacial movements (Sahibzada et al., 1986, Comoli et al., 2012, Rossi et al., 2016).

Optogenetic activations of SNr projections on lateral-SC suppressed licking but they were not sufficient to stop it (Rossi et al., 2016). It is possible that SNr to SC pathway is not the strongest basal ganglia output pathway that is premotor to orofacial brainstem CPGs, therefore its' manipulations modulate but were not sufficient to stop licking. It is also possible that optogenetic control of this pathway was not sufficient to silence SC cells due to their high firing rates and

limited kinetics of the channel rhodopsin protein (Deniau et al., 1992).

Considering the complex anatomy and dynamic function of the basal ganglia in action selection, structural and functional plasticity was expected throughout basal ganglia circuits. Changes in movement tuning properties of dopamine cells, dorsal and ventral striatal populations, GPe, SNr and motor cortex during classical and instrumental conditioning paradigms were reported (Schultz et al., 1997, Jog et al., 1999, Setlow et al, 2003, Jin et al., 2010, Jin et al., 2014, Eshel et al., 2016). In striatum, it was shown that both in naive animals, or in early stages of learning, in cue guided or self initiated instrumental conditioning paradigms, most of the cells showed movement related responses (Carelli, et al., 1991, Mittler, et al., 1994, Venkatraman, et al., 2010, Jog et al., 1999, Jin et al., 2010, Jin et al., 2014). As learning progressed, most of the cells acquired start (cue that signals the start of an instrumental action, or initiation of a self initiated instrumental action) and/or stop (reward, or stopping of an instrumental action) related activity and less cells showed movement related activity (Jog et al., 1999, Jin et al., 2010, Jin et al., 2014). However, until very late stages of learning "expert cells" showed movement related activity (Smith et al., 2014). This phenomenon of emergence of bracket-like activity, "action chunking", was suggested to be a mechanism via which striatum, and basal ganglia, codes for units of instrumental actions (Miller et al., 1956, Graybiel et al., 1989, Jog et al., 1999, Jin et al., 2010, Jin et al., 2014). It was suggested that this could also be the mechanism via which basal ganglia codes for

well-learned “natural actions” such as grooming (Meyer-Luehmann, et al., 2002). This bracket like activity in the beginning and at the end of well learned instrumental or neutral actions might be suggesting that striatum (or basal ganglia) might be involved in (exploratory stage) spontaneous actions. As the learning progresses striatum might be reducing its involvement in execution of that action and might be mostly important for the initiation and termination of these well-learned instrumental or neutral actions (Graybiel et al., 1989, Jog et al., 1999, Jin et al., 2010, Jin et al., 2014, Meyer-Luehmann, et al., 2002). Exploratory stages/early learning might require frequent initiation signal since no instrumental action sequence is formed. Therefore, striatal populations might be necessary execution of exploratory spontaneous actions, and for initiation and termination of well learned/natural actions and but they might be differentially involved in their execution (Graybiel et al., 1989, Jog et al., 1999, Jin et al., 2010, Jin et al., 2014, Meyer-Luehmann, et al., 2002, Tecuapetla et al., 2016).

Our preliminary population imaging data from striatonigral and striatopallidal aVLS during the head fixed olfactory guided operant task showed that in go trials striatonigral activity preceded licking and decayed as licking continued. Lick rates were modulated at the time of water delivery. However, this modulation was not reflected in the striatonigral population activity, as it decayed steadily after initiation of licking. Mice were trained to perform with ≈ 100% correct go trial performance for 2-3 weeks. Therefore, there was no error in the reward prediction. However, in wait trials, which were learned with ≥50% correct trial performance, we saw modulations starting with go

tone and water delivery. This signal could be a combination of reward prediction error, initiation of licking, and go tone response. We could not see lick related sustained activity within the striatonigral population. This could be due to long training as well (pretraining and 25-45 sessions training), since even the "expert cells" changed their execution related activity and acquired start-stop related activity after long training (Smith et al., 2014).

Our optogenetic stimulation results suggested that striatonigral pathway activation of aVLS was sufficient to induce licking during stimulation period, and our preliminary population imaging results suggest that its activity was necessary for the initiation of licking but might not be necessary for the execution of licking.

Interestingly, in go trials striatopallidal activity was also increased preceding licking and was sustained until the lick rate started decreasing. The decay in striatopallidal population activity seemed to precede the decay in lick rate. Water reward responses of indirect pathway aVLS population were observed in both go and wait trials. Initiation related and instrumental action execution related sustained activity of striatopallidal subpopulations was reported (Cui, et al., 2013, Xin et al., 2014) However, in DLS, lower percentage of striatopallidal cells were suggested to show execution related sustained activity and a larger percentage of striatopallidal cells were suggested to show execution related inhibited activity (Jin et al., 2014). However, our optogenetic stimulation results suggested that striatopallidal aVLS stimulation was sufficient to stop licking. It is possible that the calcium population signal is combined activity of heterogeneous populations and due to the low baseline firing rates the

inhibited activity might be masked by sustained activity. We would like to test these possibilities using cell resolution calcium imaging techniques.

Another possible explanation of the bulk calcium signal recording and optogenetic stimulation data is that the aVLS striatopallidal population comprises of at least two subpopulations. One subpopulation possibly projects onto SNr, and stops licking when it is activated, while a second subpopulation shows sustained activity during instrumental action execution until the reward is obtained (von Krosigk et al., 1992). One of the roles of striatopallidal population was suggested to be inhibiting competing actions (Mink, 1996). The bulk calcium activity observed might also be consistent with this idea and might be inhibiting competing motor programs. Alternatively, the activity might be related to complex cognitive processes related to diverging GPe output. GPe projects onto different targets in the thalamus (Pf) and SNc in addition to STN and SNr, and back to cortex and striatum (Mastro et al., 2009, Saunders et al., 2015, Mallet et al., 2012, Mallet et al., 2016).

It was suggested that anterior-striatum and posterior-striatum might be involved in different stages of instrumental learning, such that anterior-striatum might be involved in early stages (acquisition) and posterior-striatum might be involved in later stages (execution) (Graybiel, 1998, Yin et al., 2004, Yin et al., 2009). It was suggested that DMS and DLS are involved in different stages of instrumental learning (procedural learning/skill learning), such that DMS might involved in early stages and DLS is involved in late stages (Miyachi, et al., 1997, Miyachi, et al., 2002, Yin et al., 2009, Jin et al., 2010). It

is possible that change in movement tuning properties of striatal cells during training is mediated by dopamine modulations on corticostriatal plasticity (Jin et al., 2010, Jin et al., 2014).
It is not known if VLS cells will be active during learly or late stages of instrumental licking. If licking is a "neutral action sequence" it is possible that licking related striatonigral responses would be similar to grooming responses in SNr (Meyer-Luehmann, et al., 2002, Jin et al., 2010). Therefore, licking related aVLS striatonigral activities might be indicating initiation but not execution, in both early and late stages of training. By comparing striatonigral aVLS activities in early and late stages of training, one could better understand if grooming and licking are both encoded as natural action sequences initiated and modulated by basal ganglia (Aldridge et al., 1998).

Our anatomical mapping, optogenetic activation and population imaging results might help to understand the anatomical and functional organization of basal ganglia circuits involved in orofacial motor control. Therefore, understanding the role of ventrolateral striatum in orofacial motor control could help to understand the circuit mechanisms via which basal ganglia acts on specific CPG controlled actions to allow proper action selection, initiation and execution.

REFERENCES

Aldridge, J.W., Berridge, K.C. (1998) Coding of serial order by neostriatal neurons: A "Neutral action" approach to movement sequence. J. Neurosci. 18(7):2777-2787

Carelli, R., M., West, M., O. (1991) Representation of the body by single neurons in the dorsolateral striatum of the awake, unrestrained rat. J. Comp. Neurology 309:231-249

Comoli, E., Das Neves Favaro, P., Vautrelle, N., Leriche, M., Overton, P.G., Redgrave, P. (2012) Segregated anatomical input to sub-regions of the rodent superior colliculus associated with approach and defense. Front. Neuroanat. 10.3389/fnana.2012.00009

Cui, G., Jun,S. B., Jin, X., Pham, M.D., Vogel, S.S., Lovinger, D.M., Costa, R.M. (2013) Concurrent activation of striatal direct and indirect pathways during action initiation. Nature 494(7436): 238-42.

Dautan, D., Huerta-Ocampo, I., Witten, I.B., Deisseroth, K., Bolam, J.P., Gerdjikov, T., Mena-Segovia, J. (2014) A major external source of cholinergic innervation of the striatum and nucleus accumbens originates in the brainstem. J.Neurosci. 34(13): 4509-18

Deniau, J.M., Menetrey, A., Charpier, S. (1996) The lamellar organization of the rat substantia nigra pars reliculata: Segregated patterns of striatal afferents and relationship to topography of corticostriatal projections. Neuroscience, 73(3): 761-781

Eshel, N., Tian, J., Bukwich, M., Uchida, N. (2016) Dopamine neurons share common response function for reward prediction error. Nat. Neurosci. 19(3): 479-486

Grofova, I., Deniau, J. M., Kitai, S.T. (1982) Morphology of the substantia nigra pars reticulata projection neurons intracellularly labeled with HRP. J. Comp. Neurology 208:352-368

Graybiel, A. M. (1998) The basal ganglia and chunking of action repertoires. Neurobiol. Learn. Mem. 70(1/2): 119-136

Mena-Segovia, J., Bolam, J.P., Magill, P.J. (2004) Pedunculopontine nucleus and basal ganglia: distant relatives or part of the same family? TINS 27(10): 585-588

Jin, X., Costa, R.M. (2010) Start/stop signal emerge in nigrostriatal circuit during sequence learning. Nature 466(7305): 457-462

Jin, X., Tecuapetla, F., Costa, R.M. (2014) Basal ganglia subcircuits distinctively encode the parsing and concatenation of action sequences. Nat. Neurosci. 17(3): 423-30

Jog, M.S., Kubota, Y., Connolly, C.I., Hillegaart, V., Graybiel, A.M. (1999) Building neural representations of habits. Science 286(5445): 1745-9

Mallet, N., Schmidt, R., Leventhal, D., Chen, F., Amer, N., Boraud, T., Berke, J.D. (2016) Arkypallidal cells send a stop signal to striatum. Neuron 89(2): 308-16

Mallet, N., Micklem, B. R., Henny, P., Brown M.T., Williams, C., Bolam, J.P., Nakamura, K.J., Magill, P.J. (2012) Dichotomous organization of the external globus pallidus. Neuron 74(6): 1075-86

Mastro, K., Bouchard, R.S., Holt, H.A., Gittis, A.H. (2014) Transgenic mouse lines subdivide external segment of the globus pallidus (GPe) neurons and reveal distinct GPe output pathways. J Neurosci. 34(6): 2087-99.

Meyer-Luehmann, M., Thonbson, J., Berridge, K.C., Aldridge, J.W. (2002) Substantia nigra pars reticulata neurons code initiation of a serial pattern: implications for natural action sequences and sequential disorders. Eur. Journ. Neurosci. 16: 1599-1608

Miller, G.A. (1956) The magical number seven, plus or minus two: Some limits on our capacity for processing information. Psychol. Rev. 63(2): 81-97

Miyachi, S., Hikosaka, O., Lu, X. (2002) Differential activation of monkey striatal neurons in the early and late stages of procedural learning. Exp. Brain Res. 146: 122-126

Mittler, T., Cho, J., Peoples, L., L., West, M., O. (1994) Representation of the body in the lateral striatum of freely moving rats: single neurons related to licking. Exp Brain Res 98: 163-167

Miyachi, S., Hikosaka, O., Miyashita, K., Karadi, Z., Rand, M.K. (1997) Differential roles of monkey striatum in learning of sequential hand movements. Exp. Brain Res. 115: 1-5

Mink, J.W. (1996) The basal ganglia: Focused selection and inhibition of competing motor programs. Prog. Neurobiol. 50: 381:425

Rossi, M.A., Li, H.E., Lu, D., Kim, I.H., Bartholomew, R.A., Gaidis, E., Barter, J.W., Kim, N., Cai, M.T., Soderling, S.H., Yin, H.H. (2016) A GABAergis nigrotectal pathway for coordination of drinking behavior. Nat. Neurosci. 19(5): 742-8

Sahibzada, N., Dean, P., Redgrave P. (1986) Movements resembling orientation or avoidance elicited by electrical stimulation of the superior colliculus in rats. J. Neurosci. 6(3): 723-33

Saunders, A., Oldenburg, I.A., Berezovski, V.K., Johnson, C.A., Kingery, N.D., Elliot, H.L., Xie, T., Gerfen, C.R., Sabatini, B.L. (2015) A direct GABAergic input from the basal ganglia to frontal cortex. Nature 521, 85-89

Setlow, B., Schoenbaum, G., Gallagher, M. (2003) Neural encoding in ventral striatum during olfactory discrimination learning. Neuron 38: 625-636

Schultz, W., Dayan, P., Montague, P.R. (1997) A neural substrate of prediction and reward. Science 275: 1593-9

Smith, K.S., Graybiel, A.M. (2014) Investigating habits: Strategies, technologies and models. Front. Behav. Neurosci. 10.3389/fnbeh.2014.00039

Tecuapetla, F., Koos, T., Tepper, J.M., Kabbani, N., Yeckel, M.F. (2009) Differential dopaminergic modulation of neostriatal synaptic connections of striatopallidal axon collaterals. J.Neurosci. 29: 8977-8990

Tecuapetla, F., Matias, S., Dugue, G. P., Mainen, Z.F., Costa, R.M. (2014) Balanced activity in basal ganglia projection pathways is critical for contraversive movements. Nat. Commun. Jul 8;5:4315.

Tecuapetla, F., Jin, X., Lima, S.Q., Costa, R.M. (2016) Complementary contributions of striatal projection pathways to action initiation and execution. Cell 166(3): 703-15

Venkatraman, S., Jin, X., Costa, R.M., Carmena, J.M. (2010) Investigating neural correlates of freely behaving rodents using inertial sensors. J. Neurophys. 104(1): 569-575.

von Krosigk, M., Smith, Y., Bolam, J. P.& Smith, A. D. (1992) Synaptic organization of gabaergic inputs from the striatum and the globus pallidus onto neurons in the substantia nigra and retrorubral field which project to the medullary reticular formation. Neuroscience 50(3): 531-549

Yin, H.H., Knowlton, B.J. (2004) Contributions of striatal subregions to place and response learning. Learn. Mem. 11(4): 459-462

Yin, H.H., Mulcare, S.P., Hilaro, M.R., Clouse, E., Holloway, T., Davis, M.I., Hansson, A.C., Lovinger, D.M., Costa, D.M. (2009) Dynamic reorganization of striatal circuits during the acquisition and consolidation of a skill. Nat. Neurosci. 12(3): 333-41